LAWRENCE
LIVERMORE
NATIONAL
LABORATORY

LLNL-BOOK-400175

# Pulsed Power for Solid-State Lasers

W. Gagnon, G. Albrecht, J. Trenholme, M. Newton

January 2, 2008

Pulsed Power for Solid-State Lasers

This work was performed under the auspices of the U.S. Department of Energy by University of California, Lawrence Livermore National Laboratory under Contract W-7405-Eng-48.

# Pulsed Power for Solid-State Lasers

**William Gagnon**

**with**
**Georg Albrecht**
**John Trenholme**
**Mark Newton**

**Foreword by John Emmett**

# Table of Contents

**Foreword by John Emmett**

In 1960 Theodore H. Maiman demonstrated the first laser in the laboratory. In this case it was a synthetic ruby crystal ($Cr^{3+}$:$Al_2O_3$) excited by a xenon flashlamp, driven by a small capacitor bank. In the intervening years, many different types of lasers have been demonstrated and developed from electrically or optically excited gases, to electrically or optically excited semiconductors, to dyes, to a variety of lasers that depend on the nonlinear optical properties of materials. However, during the 47 years since the invention of the laser, optically pumped solid-state lasers have undergone extensive development and thus have remained one of the important laser types that find extensive application in medicine, science, and industry.

The demonstration of the ruby laser was followed rapidly by the invention of Q-switching of the laser cavity, which produced very high-power pulses of a few tens of nanoseconds in duration. The availability of high-power short pulses immediately started scientists in Russia, France, and the United States thinking about the possibility of laser induced thermonuclear fusion, and significant research programs were initiated in all three countries in the early to mid 1960s.

Laser-driven thermonuclear fusion, or inertial confinement fusion (ICF) as it is now referred to, is currently viewed to require several hundred kilojoules to a few megajoules of energy delivered to the target in times of a few to several nanoseconds. While many different types of lasers have been studied in detail for this application, the majority of experimental facilities extant in the world today employ optically pumped solid-state lasers; specifically, lasers of neodymium doped glass pumped with xenon flashlamps driven by large capacitor banks. In the case of the National Ignition Facility (NIF) laser under construction at the Lawrence Livermore National Laboratory (LLNL), the capacitor bank exceeds 400 megajoules.

The design of small capacitor banks for small solid-state lasers is a well-understood subject and is practiced commercially. However, the design of a 400-MJ system is altogether quite a different undertaking. Safety, reliability, and cost, while important at any scale, become extremely crucial issues in a 400-MJ system, a fact that can often be underappreciated. Thus a very high quality, sophisticated engineering team is required to design, manufacture, install and operate such a system.

The 400-MJ system for NIF is the largest of a series of pulsed power systems that have powered an ever larger series of solid-state lasers for ICF research at LLNL. Each of these systems is comprised of many separate individual modules. A module is comprised of capacitors, pulse-forming inductors, dump resistors, a switch, and a host of control components. As the whole pulsed power system becomes ever larger, the optimal module size becomes larger also. This is driven primarily by two factors. First, the tyranny of failure of large numbers of components argues for fewer, larger components. Second, cost drives the design to larger individual components as the cost per Joule decreases with increasing component size. While this all seems quite straightforward, what is often unappreciated is that safety issues are greatly exacerbated

by large module sizes. A catastrophic failure of a 2.2-MJ module, which will happen, is a far different matter than a failure of a 20-KJ module. In addition, huge fault currents from a failure associated with large modules (which will happen also) must be controlled. These are just two of the issues to be addressed in the design of such systems, but two that drive the critical matter of personnel safety.

LLNL was very fortunate to have an exceedingly capable engineering team to execute these pulsed power systems. In this book, they document the critical design issues they successfully addressed in the development of such systems. It is hoped that this book will provide the valuable insights to others who follow in their footsteps, whether it be in maintaining and modifying existing systems, or in the development of even larger ones.

**Acknowledgements**

Over the years, there have been so very many brilliant and talented people involved in the Livermore Laser Program. Carl Haussmann was given the charter by the Laboratory to form the backbone of the program in the early 1970s. He recruited John Emmett, Bill Krupke, Walt Sooy, Victor George, Jim Davis and many other talented people who wished to pursue Solid-State Laser Technology. At the time, the technology was in its infancy. Under John Emmett's direction, the technology has matured past laser systems with the names Cyclops, Argus, Shiva, Nova and now under the leadership of Ed Moses, to the National Ignition Facility. Every step along the way required state of the art design, materials development and engineering innovation. It was understood from the beginning that laser personnel should look outside the Laboratory to industry for help in developing and implementing the needed technologies. This has been accomplished rather well as a great many successful industrial relationships have been developed. As a result the Livermore approach has been duplicated successfully in laboratories all over the world.

It is impossible to acknowledge and thank everyone in industry and well as inside the laser program that helped bring the Pulsed Power technology to where it is today, but you know who you are and we hope this book accurately reflects your fine work.

## PREFACE

Writing a book such as this as much a labor of love as it is hard, time-consuming work. One might question the utility of such a book. There are, however, a number of compelling reasons for writing it. Imagine yourself as a young engineer attempting to become familiar with the design of pulsed power systems for solid-state lasers. Nowhere does this material exist in a single, easily accessible document. It is diffusely contained in many Laser Program Annual Reports, internal memos, conference papers and engineering notes. This book serves to fill this need, and in it, we present the details of the design method, analyses of hazards and steps to mitigate these hazards as well as numerous examples of specific designs.

There is, in addition, a second motivation for this book. When a system such as the National Ignition Facility becomes operational, often the design engineers go on to other projects, and a new team is assigned the task of maintaining the pulse power system. If, at some point, there should arise the need or desire to alter the design of the system, it is important for those making the changes to understand the potential pitfalls involved. These pulsed power systems contain both high voltage and large amounts of energy, and, if not properly managed, can create extremely hazardous situations. Before making design changes, one should first ask why a particular design was chosen. What are the potential failure modes and will a change in the design make failures more likely?

History is replete with disasters stemming from seemingly inconsequential design changes. We shall illustrate the point with two examples.

First, the collapse of the two suspended walkways at the Kansas City Hyatt Regency Hotel in 1981 in which over a hundred people lost their lives.[1] In this case, after the design was finalized, a designer changed the arrangement of the rods supporting the walkways. It was thought to be a minor change, which would make the construction easier. The original design called for a single long rod extending through and supporting both walkways. The altered design used two shorter rods in tandem. The common connecting point on the support beam was the failure point.

The second example involves fishing boats in the Alaskan king crab fishery.[2] The Americus and Altair were "state of the art" steel boats built in the Pacific Northwest in the 1980s. At the time of their construction, they were considered to be the biggest and best ever introduced into the Bering Sea fishery. Although not originally intended for the King Crab fishery, they were later converted for use in this fishery. Unfortunately, King Crab fishing involves a considerable amount of gear on or above the deck. When the changes were made, no one thought to again check the stability

[1] "To Engineer is Human, The Role of Failure in Successful Design", Henry Petroski, Vintage Books, 1992, ISBN 0-679-73416-3.
[2] "Lost at Sea", Patrick Dillon, Simon and Schuster, 2000, ISBN 0-684-6909-8

response of the vessels with the altered weight distribution. As a result, both vessels later capsized and sunk. There were no survivors.

In general, when major mistakes are made and the resulting damage is costly, it's not a pretty picture. Unfortunately today, a good fraction of what it takes to fix the problem is instead spent on assigning blame. This often results in serious career problems for those involved. Few textbook authors have had the enormous privilege to live the development of a new technology from the ground up and thus be able to share, from first-hand experience, the lessons learned from that unique point of view.

So, if just a few engineers read this book and, as a result, avoid making design changes that could result in catastrophic failures, it will have been quite worth the effort.

## INTRODUCTION

Beginning in the early 1970s, a number of research and development efforts were undertaken at U.S. National Laboratories with a goal of developing high power lasers whose characteristics were suitable for investigating the feasibility of laser-driven fusion.

A number of different laser systems were developed and tested at ever larger scale in pursuit of the optimum driver for laser fusion experiments. Each of these systems had associated with it a unique pulsed power option. A considerable amount of original and innovative engineering was carried out in support of these options. Ultimately, the Solid-state Laser approach was selected as the optimum driver for the application. Following this, the Laser Program at the Lawrence Livermore National Laboratory and the University of Rochester undertook aggressive efforts directed at developing the technology. In particular, at Lawrence Livermore National Laboratory, a series of laser systems beginning with the Cyclops laser and culminating in the present with the National Ignition Facility were developed and tested.

As a result, a large amount of design information for solid-state laser pulsed power systems has been documented. Some of it is in the form of published papers, but most of it is buried in internal memoranda, engineering reports and LLNL annual reports. One of the goals of this book is to gather this information into a single useable format, such that it is easily accessed and understood by other engineers and physicists for use with future designs. It can also serve as a primer, which when seriously studied, makes the subsequent reading of original work and follow-up references considerably easier.

While this book deals only with the solid-state laser pulsed power systems, in the bibliography we have included a representative cross section of papers and references from much of the very fine work carried out at other institutions in support of different laser approaches.

Finally, in recent years, there has been a renewed interest in high-average-power solid-state glass lasers. Much of the prime power technology developed in support of this has definite applications in the long term for fusion power plant scenarios.

# CHAPTER 1

# OVERVIEW OF SOLID-STATE LASERS[3]

## Background

As electrical engineers and pulse power specialists, the readers of this book are surely familiar with lasers. However, they might be less familiar with, but no less curious about, what happens once the flashlamp discharges and the laser "lases." This chapter attempts to provide a brief and very tutorial description of some of the most important processes at work. It is tailored towards better understanding large laser system components with the added goal of clarifying some frequently heard buzzwords and providing a feel for what typically limits large system design. True to its didactic intent, this chapter cannot and will not cover all issues, and what it does cover is intentionally limited.

A fusion laser consists mostly of ever-larger amplifiers. However, before the laser pulse can be amplified, it has to be created in a laser oscillator, the so-called master oscillator. These are specialty oscillators, since the demands on pulse shape and wavelength content are the most extreme of any field. Not only does this pulse need to have a shape that, by the time it emerges from the amplifier chain, corresponds to the hydrodynamic drive conditions the target physicists demand, it also must have a rise from "zero" that must be controllable over many decades of amplitude to avoid the so-called pre-pulse. The development of these oscillators over the decades is no less fascinating than the visually much more impressive scaling of the large amplifiers. Today, the master oscillator is based on fiber lasers, in part because the development of fiber optic communications helped generate a plethora of precision light manipulation methods. The fiber laser is pumped by a laser diode, and even the mirrors are written directly into the fiber as Bragg reflectors. By the time this "baby pulse" leaves the fiber it has an energy measured in nanojoules, but its pulse shape and spectral content are already judiciously crafted. After all, this pulse will now be amplified by some 14+ orders of magnitude before it hits the target. On the other end, the resulting MJ-level output pulse is expected to have a shape accurate to tens of picoseconds in time, again over many decades in amplitude. Unless this feeble little pulse coming out of the fiber master oscillator is precisely tuned to enable the desired output after all the nonlinearities these 14+ orders of magnitude amplification will imprint on it, the experiment in the target chamber will be a failure.

Now the amplification journey of this pulse begins.

## The Active Ion

Regardless of the size or type of the amplifier, one always has to start out with an active medium that is pumped by either flash lamps or, for small amplifiers, laser diodes. In fusion lasers, this active medium is neodymium-doped glass. When immersed in the glass matrix, the Nd atom enters as $Nd^{3+}$, which means it does not sit in the glass host as

[3] Pictures from this section have been taken from the many NIF websites and from old archival materials.

a neutral atom, but it shares three electrons with its surrounding atoms. It is the $Nd^{3+}$ that gives laser glass its distinct rose-pink color (see Figure 1), and glass experts can see just by this color which other possible ions or contaminants the glass contains. In earlier days, silicate glass was used (as compared to today's phosphate glass) and when imbedded within it, the $Nd^{3+}$ atomic levels were shifted a bit such that silicate glass had a more bluish-purple tint.

Figure 1. Laser slabs prior to integration into an amplifier (see Figure 4). The characteristic laser glass color is produced by the $Nd^{+3}$ ions.

Figure 2 illustrates what happens when flashlamp light falls on the Nd-doped amplifier glass: it gets absorbed by what we call the pump levels of the Nd ion. Of course, the lamps need to be constructed and need to be driven such that they emit most of their light at that pump wavelength. This is done by choosing the correct fill pressure, diameter, type of gas (often Xe) and the proper electrical excitation pulse. Much of this book deals with just those issues. This is labeled as Step 1 in Figure 2 and in a well-designed setup, about 10+% of the lamp light is absorbed by the $Nd^{3+}$ ion. There are many such pump levels and that's why the lamp light gets absorbed with reasonably good efficiency. Step 2 happens within the glass medium. Because the atoms always have some thermal motion (= phonons), the electrons that were elevated to the pump energy level by the lamp light will not stay there indefinitely, but rather quickly collect in the upper laser level. They stay there for a duration that is called the fluorescent lifetime, or decay time, which is roughly ½ ms. We call that state of the ion an inversion, and that's what we want: we want to "invert" the Nd ions in the amplifier. If nothing happens, random fluorescence (= spontaneous emission) will simply deplete this upper laser level over that ~ ½-ms time scale. However, if incoming photons at the lasing wavelength hit the

inverted $Nd^{3+}$ ions before that, we get "lasing" by stimulated emission (Step 3). That is the root mechanism of light amplification. This lasing does not return the Nd ion into its unexcited, quiescent ground state, but puts it in a still mildly excited state of the lower laser level. From there (Step 4), phonons return the ion back into its quiescent ground state via collisional relaxation. Note that by no means does all the lamp light absorbed in the pump level show up as laser light. The rest appears as one of many other sources of heat in the glass and is one of the reasons why the repetition rates of such large lasers are low.

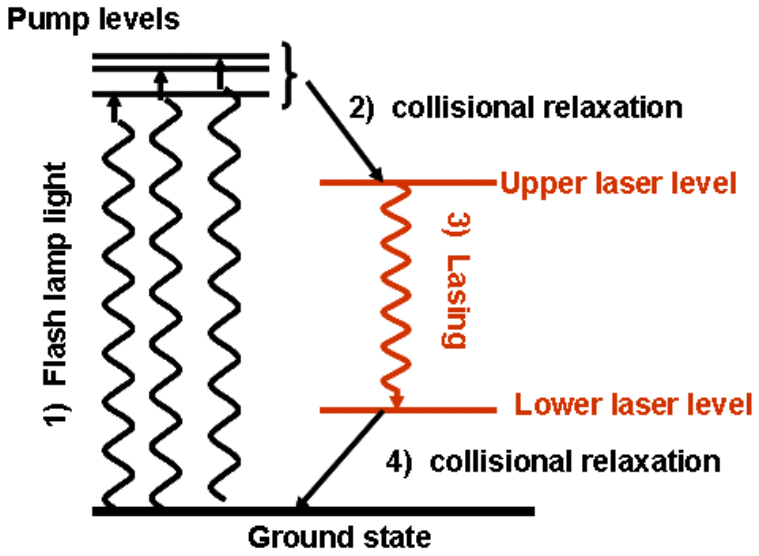


Figure 2. A sketch of pump and lasing levels of the Nd-doped amplifier glass.

The details of this entire pumping and light amplification process are actually quite complex. For example: if Step 2 or Step 4 took longer than the fluorescent decay time, we could not build up an inversion. Or, if there were only one pump level, flash lamps would not work; if the fluorescent lifetime was much shorter than the pump pulse we could make with the flash lamps, it wouldn't work either. If the lower laser level didn't exist, we would have to invert with respect to a *much* more highly populated ground state [4], and so on. It is the fact that we can store inversion in the upper laser level that makes all this work. That's why Nd:glass is also called a storage medium. Scientists have searched long and hard for possibly better atomic configurations. But for solid-state lasers, the Nd ion truly is god's gift to laser people.

So far, we have only addressed the amplification process at the atomic level. Next, we explore some of the key components and where they are located within a large laser system.

[4] In that case, we have a so-called three-level laser, whereas $Nd^{3+}$ is a four-level laser. The first laser ever built, the ruby laser, is such a three-level laser, and it takes comparatively enormous pump powers to generate an inversion.

## The Amplifier Chain

Although Figure 3 shows a laser that doesn't exist anymore (Nova), it is a good illustration of an amplifier chain since the system was built with enough open real estate to clearly see its layout. A general observation is that the individual units get bigger and longer the closer they get to the target chamber. Furthermore, not every one of these structures is an amplifier, although we shall concentrate on those first.

Figure 3. The Nova Laser System at Lawrence Livermore National Laboratory.

## Amplifier Basics

To invert the Nd ions, the Nd:glass active medium is surrounded by flashlamps, see Figure 4. The lamps inevitably are embedded in some sort of reflector structure that redirects as much of the lamp light as possible towards the active medium. However, the pump light needs to be distributed fairly uniformly across the amplifier aperture as seen by the incoming laser light. To combine lamp light illumination uniformity with efficiency is not an easy task, and in general, one can either optimize one or the other, but not both. The whole assembly is held by a mechanical structure and is enclosed. In smaller amplifiers the active medium is a rod with the flash lamps arranged radially around it. In large amplifiers, the active medium is in the form of a disk tilted at Brewster's angle for minimum transmission losses for the extracting beam, with lamps arranged to illuminate the faces of these disks. Between the flash lamps and the disk is a blast shield. If a lamp fails catastrophically, damage to the amplifier glass disk will be avoided. One needs to be aware that during flash lamp pumping, the inside of the amplifier is an exceedingly violent environment, and very few construction materials are suited to withstand it over time.

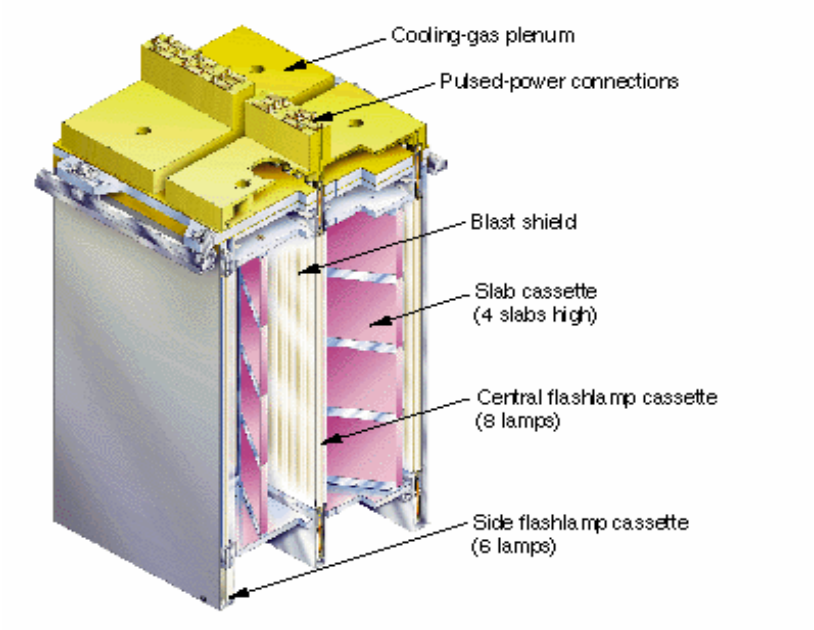


Figure 4. An integrated amplifier shown with slabs, flashlamps and blast shields.

The purpose of the smallest amplifiers is simply to increase the energy of the pulse. Compared to the large amplifiers further down the chain, such considerations as energy efficiency are not important. These are mainly rod amplifiers, and the pulse energy amplifies in the simplest possible way as $e^{g_0 \cdot L}$, where $g_0$ is the gain coefficient per cm, and L is the length of the rod in the same units. Since we can neglect efficiency considerations, we also don't have any pulse distortions: e.g., the front of a square pulse shape will be amplified just as much as the rear part of the pulse. However, even these simple amplifiers already have a restriction. After the rod amplifier has been pumped, it doesn't just "sit there and wait" for the intended laser photon to be amplified. All this population in the upper laser level creates plenty of spontaneously emitted photons at precisely the right wavelength for amplification. Since this fluorescence is emitted into $4\pi$, some of these photons will naturally be emitted right down the length of the highly inverted amplifier, and thus be amplified. The situation gets much worse if we have several highly inverted amplifiers lined up in a row. This effect is called, logically enough, amplified spontaneous emission (ASE). It will deplete the gain in a sufficiently long, highly inverted amplifier much faster than spontaneous decay alone. It is this effect that ultimately limits the length of a rod amplifier or, more generally, the $g_0 L$ of every large amplifier, no matter what the configuration. ASE tends to become noticeable for $g_0 L$ above ~ 3. Viewed the other way, a good amplifier is designed such that in the direction along which the beam is extracted, ASE considerations limit its extend. It is particularly important that none of the ASE somehow gets redirected back into the amplifier for a second or several more passes, and the ultimate dread is if an ASE photon finds a closed loop within the active medium. In this worst of all scenarios, the

amplifier has developed a parasitic self-oscillation, and gain in the amplifier will simply disappear,[5] no matter how hard we pump it.

Two measures serve to minimize or suppress this ASE gain depletion effect. The first is applying what is called an edge cladding. The name comes from large disk amplifiers where the edge (the perimeter) of the disk is the only place left where one can put such a cladding. It absorbs all spontaneously emitted light and makes sure none of it gets re-emitted back into the active medium. For rods, it is often enough to sand blast the barrel surfaces; after all, the flash lamp light needs to be able to enter these as well. For this edge cladding to absorb any ASE that comes its way, it is obviously necessary that the application of the edge cladding itself does not create reflective surfaces due to a possible refractive index mismatch. In decades past, much effort was spent on this issue, and today this problem has been solved through adhesive polymers that transmit the ASE to the edge cladding, have a precisely matched refractive index, and can tolerate the violent UV exposure that comes with flash lamp pumping of the active medium. The edge cladding itself has a greenish tint from the copper-doped glass, which is an excellent absorber at the laser wavelength.

The second measure to suppress ASE gain depletion is to isolate the amplifiers from each other, so that the ASE from one amplifier cannot enter into the next. This requires an isolator, of which there are three kinds.

**Isolators**

For smaller apertures, one uses a Pockels[6] cell. There, a fast high-voltage pulse changes the birefringence of a suitable crystalline material (KD*P) so that during the time the electric field is applied, the polarization of a transmitted beam is rotated by a specified amount. Together with polarizers, this allows an extremely fast (~ns) shutter for polarized light. As a result, it is now possible to isolate all amplifiers from each other. A series of Pockels cells, located between successive amplifiers, open sequentially just for the brief moment the light pulse passes through.

Another most useful isolating element is a Faraday rotator. Here, in a glass with a high Verdet[7] constant, a longitudinal magnetic field also rotates the polarization of the beam passing through. A big distinction from a Pockels cell, as well as from wave plates, which also rotate the beam polarization, is that the sense of polarization rotation does not reverse ("undo") itself if a photon travels backwards through the Faraday rotator. Envision a Faraday-active long glass rod, imbedded in an energized solenoid. Imagine the beam traveling along the axis of the glass rod parallel to and in the direction of the magnetic field lines. As the beam travels as described, its direction of polarization is rotated counter clockwise (right hand rule for electrons) with respect to its direction of

[5] Especially so-called zigzag lasers need to be designed with great care to avoid this problem.

[6] Named after F.C. A. Pockels, 1865-1913, who discovered electric field-induced birefringence. His sister, A. Pockels, corresponded with Lord Rayleigh on issues of surface tension of water. The often-found genitive "Pockel's cell" is wrong.

[7] The effect of polarization rotation in certain materials of a beam traveling along a magnetic field is named after Emile Verdet, French physicist (1824-1866).

travel. If we now reverse the direction of the light beam and leave everything else the same, that beam now obviously travels *against* the direction of the magnetic field lines, hence its polarization will now rotate clockwise with respect to its direction of travel. In other words, the direction of polarization rotation is dictated by the direction of the magnetic field, not by the propagation direction of the beam. Together with wave plates and polarizers, this is a great way to allow beam propagation in one direction only, and the arrangement is sometimes called an optical diode. Hence, Faraday rotators are a favorite way to isolate against back-reflected light. Since the Verdet constant is not large (~ tens of rad/Tesla/m), Faraday rotators are by necessity long and require a hefty current pulse to get the required magnetic field strengths. This, in turn, results in some similarities in the drivers for Faraday rotators and for flash lamps.

The third type of isolator introduces the last key component, the spatial filter. In principle, a spatial filter is deceptively simple, since it consists just of two lenses and a pinhole at the common focus. The collimated beam enters one lens, gets focused through the pinhole and gets re-collimated by the second lens. Since only a well-collimated beam makes it through the pinhole in the middle, any light not being highly directional, like ASE, will effectively get blocked. Although spatial filters tend to be quite long, they are passive devices with no power or cables required, but there is a vacuum pump. As simple as this might sound, a spatial filter actually has two functions in addition to being an isolator (imaging and spatial filtering), which are well worth understanding.

**Spatial Filtering and Fill Factor**

The second function (imaging) and third function (actual spatial filtering) of a spatial filter maybe a bit harder to understand for those who do not have some background in wave optics, but the following picture might help.

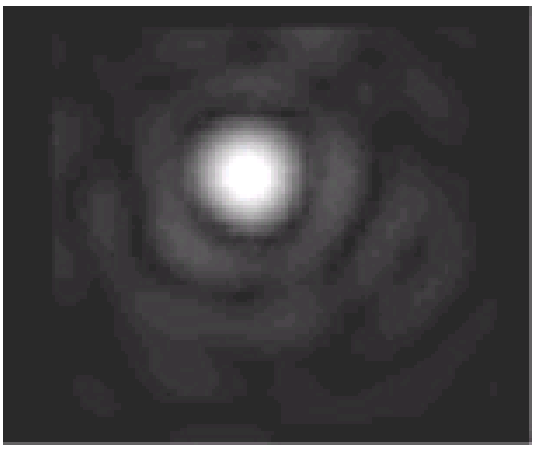

Figure 5. The faint rings around the central spot are the diffraction rings. The limited print contrast makes them hard to see here, but in a MJ laser, they contain a considerable amount of energy.

Even though the entrance and exit beams are collimated, the two-lens arrangement of a spatial filter has imaging properties, as we would expect from any other sort of lens arrangement. In fact, a spatial filter with two lenses of the same focal length $f$ will transport an object plane into an image plane, separated by $4 \cdot f$.

This is an important characteristic for several reasons. A typical polarized laser beam with a very narrow spectrum will increasingly show diffraction rings as it propagates along. These are the faint outer rings in Figure 5. In a helium neon laser, these are almost too faint to see well. In the beam of a ns, MJ laser, however, these can pack a considerable punch and need to be avoided unless the beam travels in vacuum. Therefore, and this is the

crux of the imaging capability of spatial filters, the amplifiers are normally arranged such that the spatial filter located between them images one amplifier into the next.

The other reason this is important is that in the image plane, diffraction has been reset to being essentially absent. Hence, through this relay imaging technique from one amplifier into the next, one also gets a greatly improved fill factor, which simply is a measure of how well the cross-sectional beam area of an amplifier is actually utilized by the cross-sectional beam area that extracts its inversion. Clearly, we want to make this fill factor as large as possible, but without the beam hitting any edge structures due to overfilling the amplifier. The fill factor is one of those system performance parameters that is less important in small amplifiers, but is crucial in the largest amplifiers in the system that provide the beam with most of its energy.

This leaves the last function of the spatial filter, namely spatial filtering. In essence, as the beam travels down the amplifier chain, it also travels through many meters of glass with many surfaces in between. This causes a variety of effects that turn an originally very smooth beam profile (that is the beam power uniformity across the aperture) into a more and more ragged one, much like an electrical signal being amplified acquires noise. As the ragged beam gets focused onto the pinhole by the entrance spatial filter lens, it turns out that only the smooth part of the transverse beam profile makes it through the spatial filter pinhole. The ragged part is not focusable to the same degree, so it will miss the pinhole and hit the solid parts of the structure. In this way, the spatial filter "cleans up" the beam profile and resets the beam quality, albeit at the cost of losing the energy in the non-focusable part of the beam. Suffice it to say, that even this effect is more complicated than it looks at first glance. Just envision that the first spatial filter lens brings a beam that already packs, say, a MJ, to a rather tight focus. Therefore, the ragged parts of the beam can pack enough power so that, when focused, they might destroy the pinhole. Even the edges of the "clean" part of the beam grazing the edges of the pinhole create a plasma which can lead to so called pinhole closure so that only part of a longer pulse even makes it through. The only way out of this is to make the pinhole focus larger by making the spatial filter longer. This is the main reason why the spatial filters are by far the longest components of the laser system. It pays to optimize them carefully, since their length eats up a considerable fraction of the overall length of the building, thus impacting its cost.

In summary, the fundamental layout of an amplifier chain, in principle, is simple enough: amplifier, isolator, and spatial filter. Then the beam flows into the next set of amplifier, isolator, and spatial filter, with all components getting progressively larger, and the spatial filters progressively longer. This is what we see as we look down an amplifier chain, and this is how all fusion lasers are by necessity configured.

**Noise Sources and Nonlinear Effects**

Let's briefly return to the spatial filter. Having discussed the function that gave it its name, we should look a bit closer at some salient causes of beam quality degradation as the beam travels down the amplifier chain, i.e., what are the sources of noise that the spatial filter cleans up?

Obvious noise sources are imperfections in the glass itself, in the form of unavoidable micro scratches and other such imperfections. These imperfections cause diffraction in the beam as it travels on, with diffraction from different sources eventually overlapping within the beam profile, causing further ripples across the beam. This is a major driver for the exceedingly expensive quest of ever-purer glass and ever purer surface polishes. There are, however, additional effects. The beam can be powerful enough so that the electric field strength of its light wave can change the refractive index of the very medium through which it travels. This manifests itself in a plethora of ways that go, for obvious reasons, by the name of non-linear effects. Here, we shall concentrate on only the most important one for the operation of large, high-fluence lasers, namely small scale self-focusing.

Above, we described how the beam can acquire "ripples" on its beam profile, e.g., through diffraction and interference between diffracting parts of the beam within the beam profile itself. Hence, we have a local beam perturbation, in which the local ripple in irradiance[8] can exceed the threshold at which the non-linear effect of the beam influencing its own local refractive index sets in. This is due to an electric field-depended part of the total index of refraction, which is given by:

$$n = n_0 + n_2 E^2$$

where $n$ is the refractive index, $n_0$ is the low irradiance part that is quoted in any text book, and $n_2$ is the electric field dependent non-linear part. $E$ is the electric field of the light wave in the laser beam. It is important to understand the units of $n_2$ that are used, because sometimes they are in the [gcs] system, and sometimes they do and sometimes they don't include the dielectric constant of the vacuum, $\varepsilon_0$. This nonlinearity means that where the beam irradiance $\sim E^2$ is higher, the propagating beam changes its own medium refractive index, $n$, to be higher as well. Hence, a ripple in the beam profile, subject to this effect, will begin to focus down on itself, thus amplifying the very effect that caused it to collapse in the first place. This effect will continue until the local beam irradiance gets high enough to destroy the very medium it propagates through. What we've just described is called small-scale self-focusing.[9] It causes tiny but lethal "bubble tracks" in the laser glass and is to be avoided at all cost. They can be seen as exceedingly fine lines, which sometimes start in the middle of the amplifier glass disk and track through at an increasing diameter towards the rest of the amplifier glass. If not noticed, the destruction gets worse shot after shot, and additional components get destroyed. The onset criterion for this phenomenon, described by an accumulated phase retardation called the B-integral, is to be avoided at all cost, and it forms one of the key limiting criteria for high-power laser design, be that fusion lasers, petawatt lasers, or any other high-peak-power system. In the test laboratory, other aspects of such nonlinear effects can actually be quite picturesque: even though only $1.05\mu m$ infrared light is sent

[8] The units of irradiance are W/m$^2$. Almost everywhere this is incorrectly called intensity. The actual units of intensity are W/sterad. See OSA Handbook of Optics, Radiometry and Photometry, or Hecht Zajak: "Optics".

[9] An excellent treatment of this effect is given in an article by J. Trenholme, 1974 Laser Program Annual Report.

into the amplifier, beautiful rainbow colors can result due to such additional effects as multiple Raman shifting. Alas, by the time one sees these colors, the active medium is effectively destroyed.

There are also other non-linear effects. Imagine sending a perfectly square top-hat pulse profile into an amplifier, out of which most of the energy will be extracted. Since the front part of that square input pulse gets there first, it will "see" the full inversion of the amplifier. The rear end of the square pulse, by comparison, only gets to see what the extraction of the front part of the pulse left behind. Hence, this mechanism will distort the temporal shape of the input pulse. The only way to counteract it was addressed at the very outset of this chapter: we need to pre-compensate the input pulse accordingly. This brings us to the last salient feature of this chapter.

**Energy Scaling of Large Laser Systems**

Let us start with a Gedanken experiment that will introduce the governing scaling parameter, the saturation fluence,[10] or $E_{sat}$. $E_{sat} = \frac{h\nu}{\sigma_{em}}$ = where h is Planck's constant, $\nu$ is the frequency of the laser photon, and $\sigma_{em}$ is the stimulated emission cross section. Typical values for laser glasses are between 4 and 5 J/cm$^2$.

Now imagine we have an amplifier inverted at several $g_0 \cdot L$, and we now vary the amount of laser energy that we put in to extract the inversion of that amplifier. As we look into that amplifier with a beam cross section area A and a stored energy E, we see a stored energy density of $E_{sto} = \frac{E}{A}$. In fact, the amplifier is typically characterized by how many $E_{sat}$ it stores, since $\frac{E_{sto}}{E_{sat}} = g_0 L$.

For very small input fluences, very much smaller than the $E_{sto}$ in the inversion of the amplifier, the input will be amplified exponentially like $e^{g_0 \cdot L}$. The energy stored in the amplifier will essentially be unaffected or, put differently; the energy extraction efficiency will be very low. Next imagine the other extreme, where we provide an input signal with a fluence that is very much larger than the $E_{sto}$ in the amplifier. Now, we clearly cannot possibly expect exponential signal amplification. The most we can expect is that we extract the amplifier completely, and thus at best add the energy stored in the amplifier to that in our beam.

It is clear that somewhere between these two extremes is a regime where we begin to trade off high amplification and low amplifier extracted energy, versus low amplification and high energy-extraction efficiency.

[10] Note its dimension is Joules/m$^2$. This is an aerial energy density, also called fluence.

Quantitatively, this scaling law is known as the Frantz Nodvik equation, and the scale parameter that describes at what input fluence we change from one regime to the other is the saturation fluence $E_{sat}$.

The saturation fluence, then, is a measure of the fluence at which the exponential amplification of the input beam begins to saturate, hence the name. The Frantz Nodvik equation is given by:

$$\frac{E_{out}}{E_{sat}} = \ln\left\{1 + \left[e^{\frac{E_{in}}{E_{sat}}} - 1\right] \times \frac{E_{sto}}{E_{sat}}\right\}$$

The importance of $E_{sat}$ as the scale parameter is obvious; input $E_{in}$, output $E_{out}$, and amplifier stored energy $E_{sto}$ all normalize to $E_{sat}$.

It now also should become clear how to scale amplifiers in large amplifier chain: at the front, where the amplifiers are small (and cheap), we will emphasize amplification. Towards the end, where the amplifiers are very large, we will emphasize efficient energy extraction. There is no sense to try to extract an amplifier with more than maybe two to three times $E_{sat}$ of input fluence (see the $\frac{E_{in}}{E_{sat}}$ in the Frantz Nodvik equation), since we need to provide an increasingly higher input fluence for an ever smaller increase in energy extraction efficiency. Also, the non-linear effects we mentioned above will set a limit to the irradiance than can be propagated. Remember that the pinhole closure effect in the spatial filter sets a similar sort of limit.

Obviously, a lot of money and stored energy sits in the largest amplifiers. Therefore, people have thought hard about how to provide for better energy extraction. Multi-pass amplifiers have been scoped out to various degrees over the decades, and this evolution can be followed in the Laser Program Annual Reports of the seventies and eighties. As the name says, in a multi-pass amplifier the extraction pulse travels through the same amplifier twice or more. A simple double pass can be arranged with passive components like a mirror, wave plates, and a polarizer. Passive arrangements with more than two passes, e.g., slightly angle-misaligned between passes with the input and output near a central focus, become very tricky. If we keep the extraction pulse in an amplifier for more passes than that, we need some sort of electro-optic switching element that first captures the extracting beam inside the multi-pass configuration and releases it after a specified number of passes. A testbed called Beamlet first demonstrated a large amplifier multi-pass subsystem based on a very large aperture Pockels cell, which finally has found its way into NIF. Again, especially for amplifiers as large as required for a fusion laser, the cost of this electro-optic switching subsystem figures greatly in where in the overall amplifier chain will be placed and how many passes through any one amplifier will be made.

**Frequency Conversion**

Finally, we have arrived at the point in which the pulse has been sufficiently amplified and reached the desired level of energy. For reasons that have to do with the laser–

plasma interaction at the target, the pulse is now frequency converted from the fundamental wavelength at 1.054 micron that got amplified, to one-third of that at .35 micron. That's three times the frequency of the fundamental laser light; hence, it's called "3 omega" ($3\omega$) light. This frequency conversion process happens passively in a non-linear frequency conversion crystal. For very large-aperture systems, KD*P[11] is the best choice, and the development of a rapid, ultrahigh-quality crystal growth technique to make them has spanned decades.

Now let's discuss the process by which this frequency conversion occurs. At low powers, electromagnetic radiation is emitted at a given frequency because electrons move at that frequency. If this electron resides in a homogeneous, isotropic medium, an electromagnetic wave at frequency ω will simply cause this electron to reemit at that same frequency. This explanation is often provided for electromagnetic wave propagation through a medium like glass, and we call $\omega$ the fundamental frequency. Imagine an electron in a highly anisotropic crystal that we drive hard enough that it acquires a non-linear response. Like in any other non-linear circuit, this means that higher harmonics are being excited. It is, in essence, this sort of non-linearity that causes an "overdriven" electron to emit at the higher harmonics of the incoming wave frequency.

The crystal orientation in this process is also important. In a randomly oriented crystal, the refractive index for the fundamental frequency at $\omega$ and the second harmonic at $2\omega$ is likely to be different. There are, however, crystals with the remarkable property that not only is their non-linear refractive index high (i.e., it is "easy" to overdrive the electron into a non-linear response), but they also can be oriented in such a way that the refractive index at $\omega$ and the generated $2\omega$ are the same. This means that at a certain crystal orientation, the fundamental frequency at $\omega$ continually and phase coherently adds/ converts to the second harmonic. Under optimized conditions rather high fractions (85+ %) of light at the fundamental frequency can indeed be converted to light at twice that frequency.

The generation of $3\omega$, which is in the UV well beyond what is visible to the eye, is a bit more involved and takes two crystals in tandem, but the concept remains the same. The first crystal converts 2/3 of the fundamental beam energy to $2\omega$ and leaves 1/3 of the energy at the fundamental frequency. A different way of looking at this energy split is that we now have redistributed the beam energy at the fundamental frequency to an equal number of photons at $\omega$ and at $2\omega$. These now enter a second KD*P crystal, oriented differently from the first, to generate light at $3\omega$. Based on the description supplied above, it is clear that the photons at $\omega$ and $2\omega$ need to have a strict phase relationship with respect to each other or the frequency conversion process will be less than optimum.

[11] The KDP in KD*P stands for potassium (=**K** in the periodic table) **D**i-hydrogen **P**hosphate. The star stands for the hydrogen having been largely replaced by deuterium. This shifts an absorption feature in the pure KDP crystal out of the 1.05-μm band and thus make the crystal more transparent to laser light.

Even though the frequency conversion process is passive, there is far more to it than to simply place large KD*P crystals in the beam and let frequency conversion take care of itself. A number of effects complicate things. Since frequency conversion is non-linear, it means that for efficient conversion, sending a linear ramp pulse in does not provide a linear ramp pulse out. After conversion efficiencies reach a maximum, reconversion occurs where, within the crystal, $2\omega$ light reconverts to $1\omega$ light before it exits the crystal. Finally, and this is a most difficult design constraint, the damage threshold for $3\omega$ light is far less than the damage threshold for $1\omega$ light. The fluence loading (Joules/m$^2$) of a $3\omega$ crystal has to be carefully optimized or the exit face of the crystal will get damaged by the very $3\omega$ light that it generates. In fact, as far as laser plasma interactions at the target are concerned, many plasma physicists would rather have $4\omega$ light, and it can, in principle, be generated by a conceptually straightforward extension of what we described above. However, many media simply are not sufficiently transparent at $4\omega$, and that makes their damage threshold too low to be seriously considered.

**Conclusion**

All of this seems a simple enough recipe on how to design a large, reliable laser. But what tends to push designers and decision makers[12] into the danger zone is cost. Clearly, a smaller laser is cheaper than a bigger one. And equally clearly, driving the laser design closer to its limits will give the same output power in a smaller laser than a more conservative design that stays farther away from critical powers and fluences. In different manifestations this holds true for the amplifiers, the spatial filters, the frequency converters and just about any component where one strives to get the most "bang for the buck". At those limits, especially non-linear effects are a statistical phenomenon whose deleterious consequences accumulate over time. Hence, a more conservative design will result in a laser that works for a longer time before optical parts need to be replaced. For lasers that cost billions, the question of where to draw this line, at which compromise between cost and performance one freezes the design, is a truly agonizing one, and never entirely free of criticism.

[12] Blessed the professional who works within a team in which the decision maker is also an experienced designer. The inverse is true as well, and the consequences are disastrous for almost everyone.

# CHAPTER 2

# FUNDAMENTAL CONSIDERATIONS

## Overview

The basic function of the pulsed power system in a glass laser is to extract energy from the power grid and time compress and format it for delivery to the flashlamps that pump the laser disks. This is delivered in the most effective way to the upper states in the glass laser host. The pulse durations are generally about twice the fluorescent decay time (~.5 milliseconds) of the laser host.

## Pulse Compression

The desired goal of a fusion research laser is to put on target a very large amount of energy sufficient for fusion burn[13] in a very short pulse.[14]. The shape of the laser pulse and its energy specifications derive from how the laser plasma interactions at the target subsequently drive the hydro dynamics of the radial implosion. In essence, the laser pulse on the target is a result of a series of pulse compressions beginning at the power grid and ending at the target. Presently, this is accomplished by;

- Charging a large capacitor bank over minutes.
- Discharging this into the flashlamps in a sub-millisecond time frame.
- Extracting the energy from the laser system in a ~ nanosecond-scale pulse.

A simplified block diagram of such a pulsed power system is shown in Figure 6.

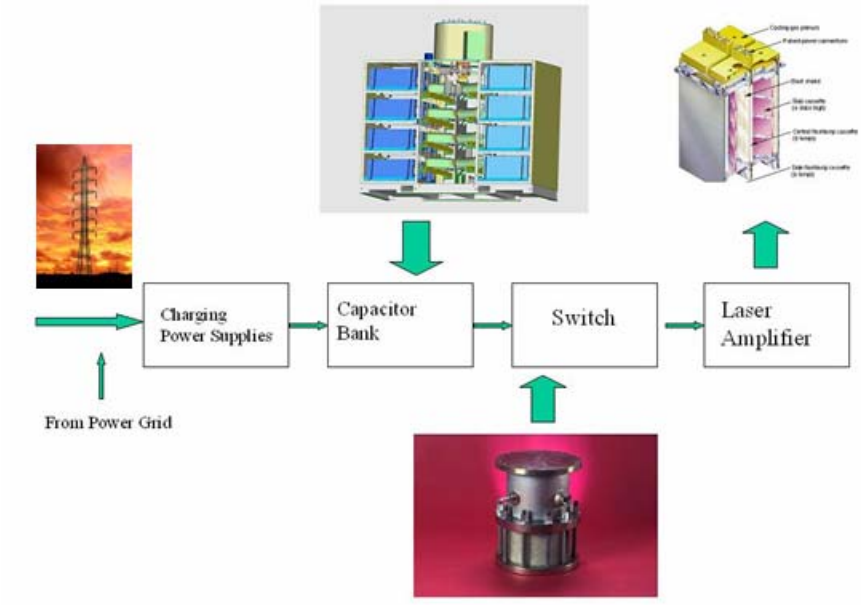


Figure 6. Simplified block diagram of pulsed power system for a group of flashlamps pumping a solid-state laser.

[13] S. Atzeni, J. Meyer-Ter-Vehn, "The Physics of Inertial Fusion," Clarendon, 2004
[14] G. Albrecht, S. Payne, "Solid-state Lasers," Electro-Optics Handbook, Waynant Ediger, Editor.

**Time Scale of Pulse Compression**

As shown, the energy is extracted from the power grid over a period approaching 60 to 120 seconds and converted to the proper capacitor voltage (~ 20 kV) by the charging supplies. Once the capacitors are fully charged, the switch is closed, and the capacitor bank discharges into the flashlamps in approximately 500 μsec. In the final phase of the process, the extracted energy from the laser is in a pulse with a width in the order of nanoseconds. This pulse compression process is shown in Figure 7.

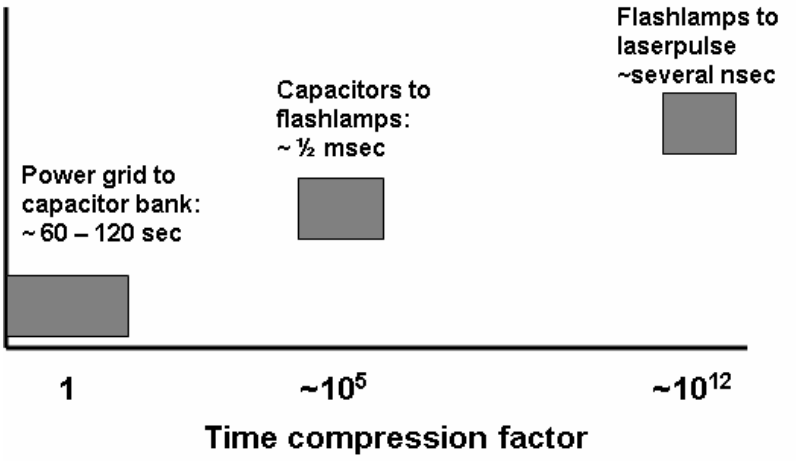


Figure 7. An illustration of the pulse compression taking place from the input power grid to the output laser pulse. Note that the pertinent time scales span some 12 orders of magnitude.

The transfer of energy from the capacitors to the flashlamps is accomplished using nearly critically damped LRC[15] circuits. A simple example is shown in Figure 8. There are a number of possible circuit geometries that apply for larger systems, and these are discussed in the following sections.

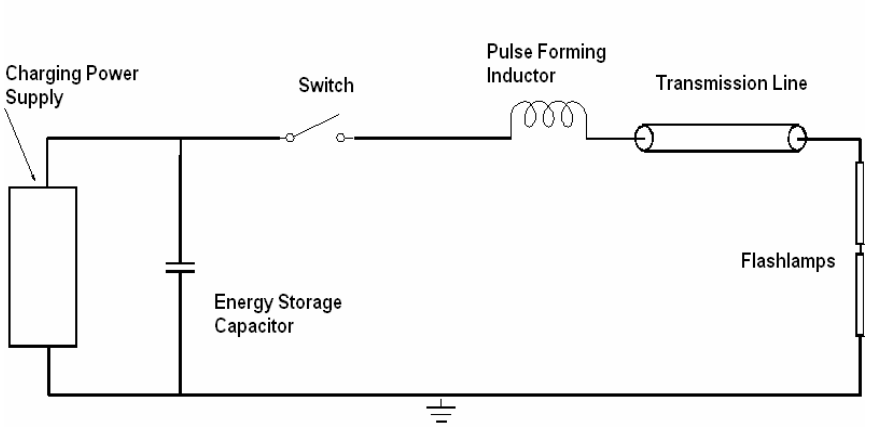


Figure 8. A single mesh LRC circuit driving a flashlamp pair.

[15] LRC stands for the inductance (L), resistance (R) and capacitance (C) of the circuit.

# CHAPTER 3

# CIRCUIT GEOMETRIES

## Introduction

In large solid-state laser systems, many hundreds of lamps must be supplied with the proper energy and pulse shape. There are a considerable number of possible circuit geometries for driving flashlamps. However, as systems become larger and more complex, the choices narrow because the requirements for cost and reliability override other considerations. In the following section, these circuit options are outlined and their limitations explained.

## Basic Single Mesh Circuit

A "stand alone" basic single mesh LRC circuit arrangement such as that shown in Figure 9, although suitable for a small number of lamp circuits, is not practical for larger systems. This is because in a large system, it would be necessary to replicate the components many times resulting in substantial compromises in the areas of reliability and cost. This is principally driven by the switching requirements and the circuit geometry.

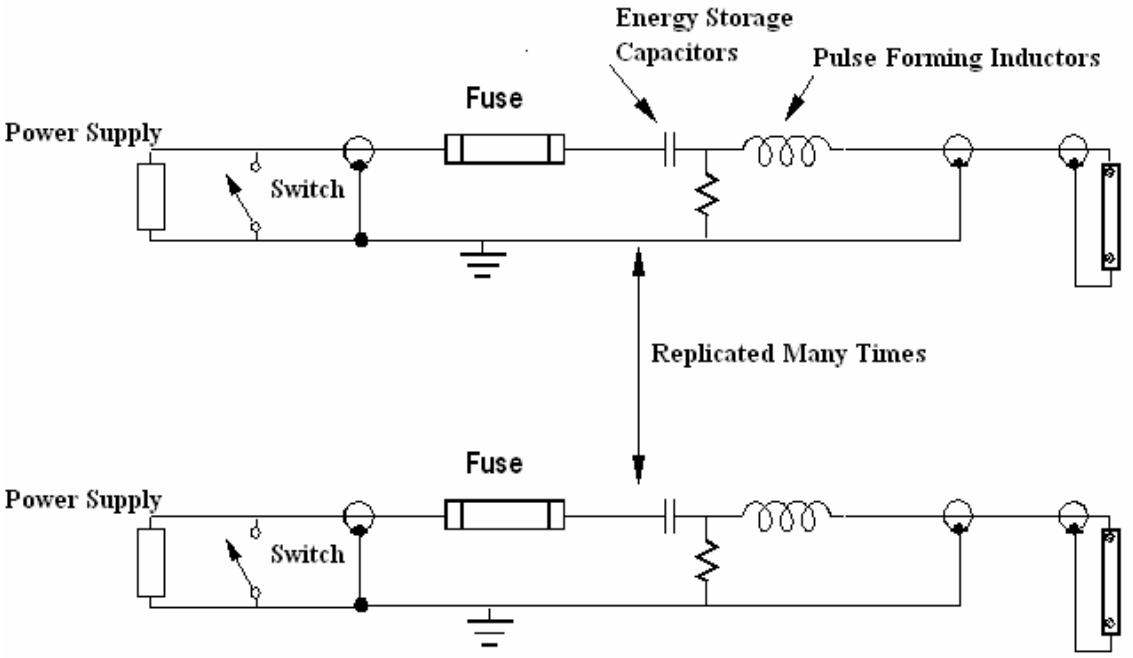


Figure 9. A design approach that replicates a large number of single mesh circuits each with an individual power supply and switch. This is not practical for large systems with many flashlamps because reliability and cost are not optimum.

**Single Mesh Circuits with a Common Power Supply and Switch**

Another approach taken with large solid-state laser systems is generally to group a number of lamp loads together, such that the number of switches and other circuit components are minimized. When this approach is taken, particular attention must be given to the following:

- Fault protection in the circuit.
- Distribution of inductance.

These very important design issues are covered in detail in later sections. Examples of such circuit approaches are shown below.

This approach, shown in Figure 10, connects a number of parallel LRC circuits to a common switch and power supply.

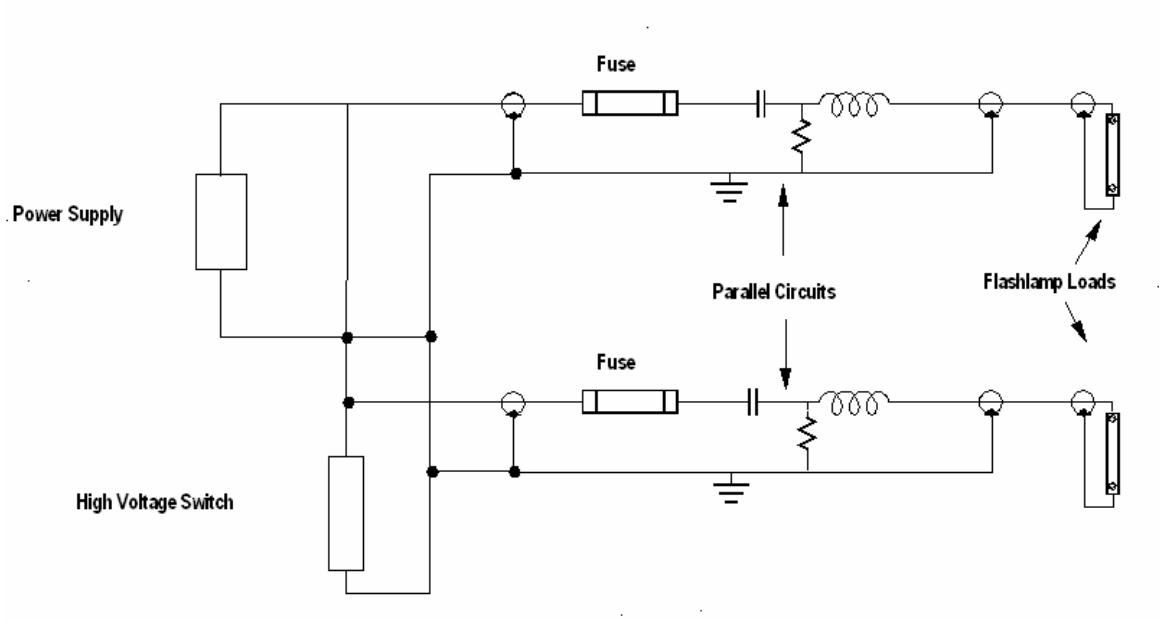


Figure 10. Design approach that parallels a large number of single mesh circuits common to a single power supply and switch. This works well for small systems, but is not ideal for very large systems with many flashlamps because reliability and cost are not optimum. Using high-voltage fuses are one option to protect against faults.

The limit to the maximum number of parallel circuits is generally set by the coulomb transfer capability of the switch. As an example, the Lawrence Livermore National Laboratory laser systems built in the late 1970s and early 1980s used National NL-1059 ignitrons [16] [17] [18]. They were configured with two ignitrons in series because a single

[16] Bruce Carder, Bill Gagnon, "Energy Storage Options for SHIVA Upgrade," IIB-91st IEEE International Pulsed Power Conference, Lubbock, Texas, 1976, T. R. Burkes and M. Kristiansen, Editors, IEEE Catalog Number 76CH1147-8.

[17] E. L. Kemp: "Principal Considerations in Large Energy-Storage Capacitor Banks," IIC-11st IEEE International Pulsed Power Conference, Lubbock, Texas, 1976, T. R. Burkes and M. Kristiansen, Editors, IEEE Catalog Number 76CH1147-8.

ignitron was prone to triggering by fast voltage transients across anode to cathode. In this series geometry, they operated reliably at the 60-Coulomb level. This is equivalent to switching 3000 $\mu$F at 20 kV or 32 parallel branches of 87 $\mu$F each. Figure 11 shows a typical example as implemented in the Argus and Shiva lasers. Another example is the pulsed power system at the University of Rochester[19] Laboratory for Laser Energetics. This system uses Richardson Electronics size D ignitrons operating at 15 kV and 50 coulombs per shot. In most cases, the design uses two ignitrons in series for reliable voltage hold-off.

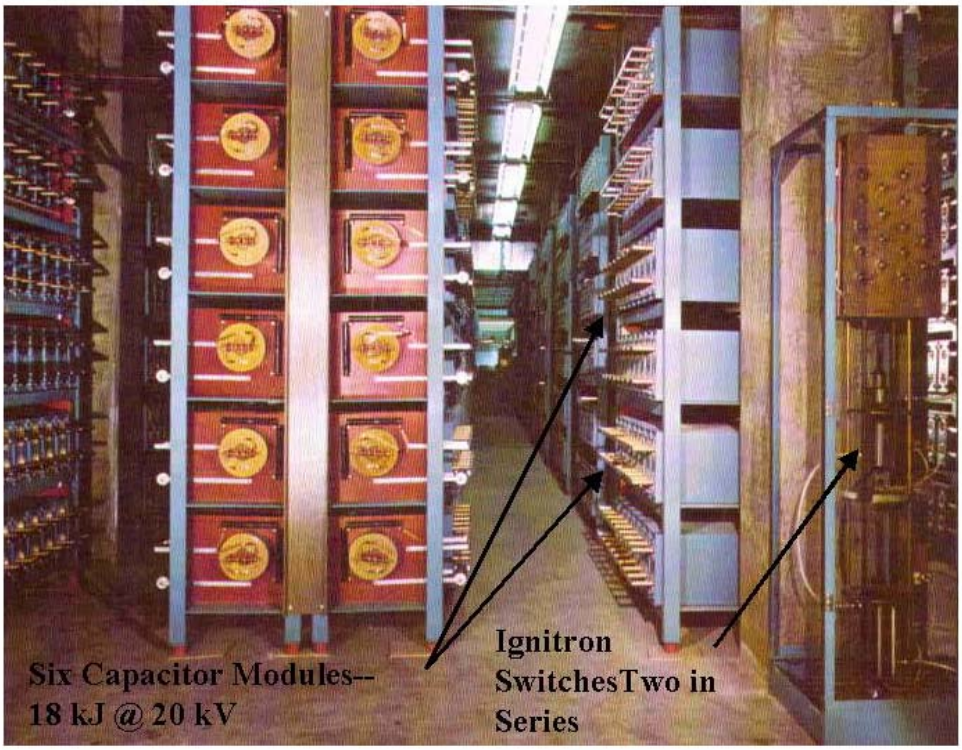


Figure 11. An example of parallel capacitor modules sharing a common switch in the LLNL Argus laser system. Each energy storage segment consists of six capacitors and stores 18 kJ at 20 kV.

There are some important design issues to be taken into account when using this approach. First and foremost is fault protection. Because the circuits are all in parallel, a fault in one circuit is driven by the energy from the other parallel circuits. An example is shown in Figure 12. Here, a high-voltage fuse is inserted into each of the parallel circuits

---

[18] W.L. Gagnon, G. Allen, A. Pemberton, R. Holloway, J. Vieira, H. Lane, K. Snyder, S, Hawlery, D. Matoon, C. Nelson, D. Padilla, R. Parker, T. Pelley, "Glass Laser Power Conditioning," Lawrence Livermore National Laboratory, 1975.

[19] "Design of the 40 MJ Turnkey Power Conditioning System for 60 Beam Omega Laser E-Stage and F-Stage Single Segmented Amplifiers." N.C. Jaitly et al., Maxwell Laboratories and L. Folnsbee et al., Laboratory for Laser Energetics, U of Rochester. 1994 Pulsed Power Conference, pp. 164-169.

for protection. This type of fuse[20] will open in times approaching 10 to 30 $\mu$ sec, thus limiting the amount of energy deposited into the fault. Figure 13 shows a fuse of this type. These consist of a number of parallel conductors embedded in a filler. During a fault, adiabatic heating of the conductors causes them to vaporize and present a permanent high-resistance path. They are enclosed in a fiberglass outer shell to prevent rupturing from internal forces.

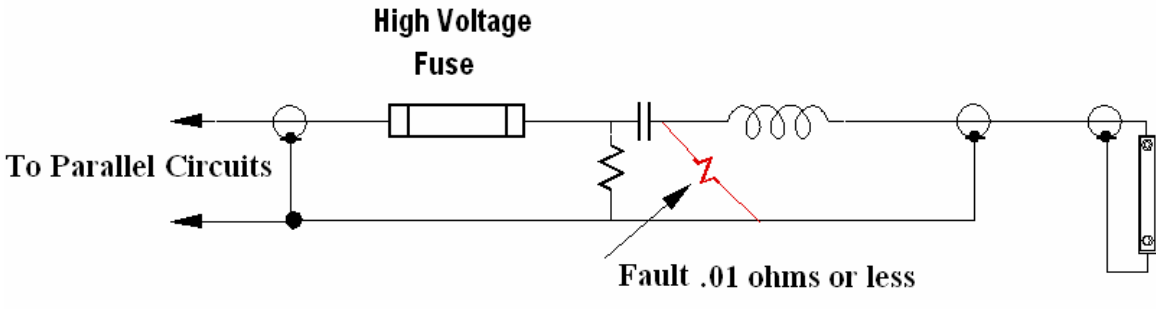


Figure 12. A high-voltage fuse is used to fault isolate parallel capacitor bank sections. These fuses will open under fault conditions in 30 to 50 $\mu$ sec and limit fault damage.

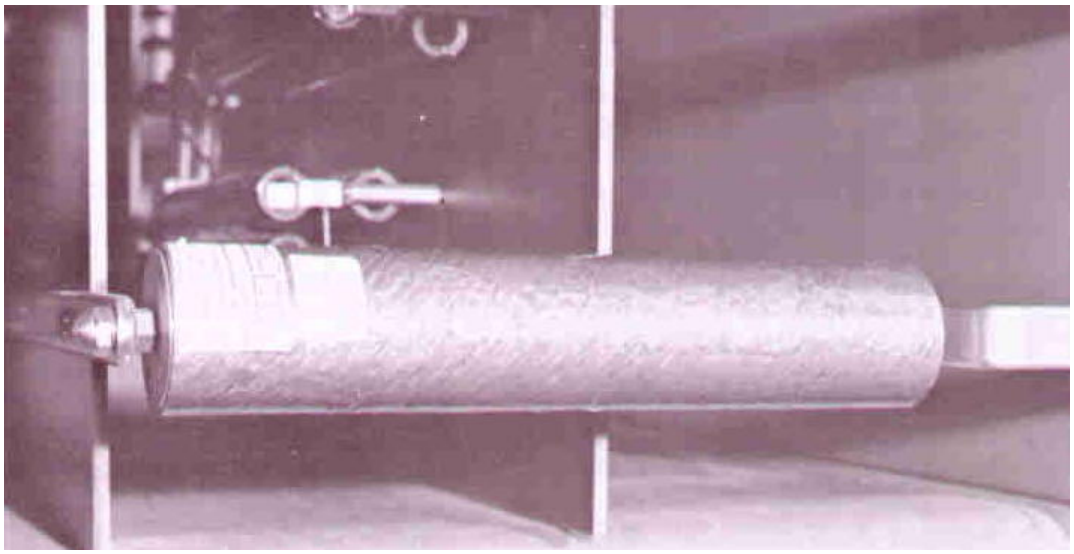

Figure 13. A high-voltage fuse limits the energy transfer from parallel bank segments in the event of a fault. These consist of a number of parallel conductors embedded in a filler. During a fault, adiabatic heating of the conductors causes them to vaporize and present a permanent high-resistance path. They are enclosed in a fiberglass outer shell to prevent rupturing from internal forces.

[20] N. C. Jaitly et al., "Pulsed Discharge Fuses for Capacitor Bank Protection" Maxwell Laboratories.

## Grouping of Circuits and Evolution to NIF 1.6-MJ Modules

As systems become larger and larger, at some point the number of additional components, reliability considerations, and cost factors dictate a different approach to capacitor banks. The Shiva Laser required about 20 MJ, the Nova Laser about 60 MJ and the National Ignition Facility about 300 MJ.

A design such as that shown in Figure 10, in which a number of energy storage units share a common switch and power supply worked well at this level. Figure 14 shows the evolution of these circuit choices. However, given that the National Ignition Facility required almost 400 MJ of energy storage, it was necessary to re-examine the design approach. A design centered about a grouping of identical, self-contained, high-density-energy storage modules with a common switch was developed [21]. This circuit is shown in Figure 15, and the actual module is shown in Figure 16.

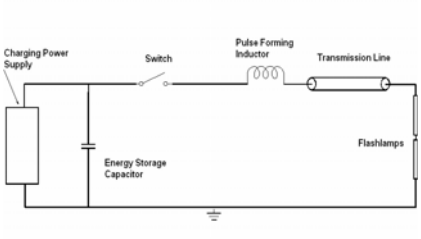


**A simple LRC circuit driving flashlamps.**

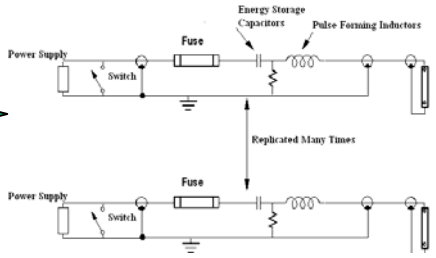


**Multiple numbers of single mesh circuits each with an individual power supply and switch. High voltage fuses are one choice to control faults.**

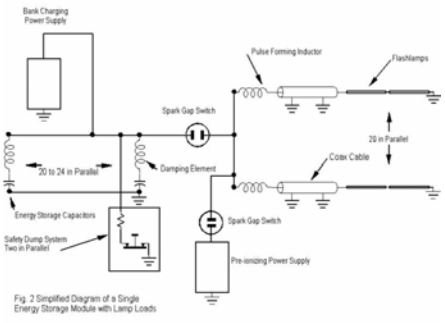


**A better circuit for large systems. A large group of capacitors share a common power supply and switch. In the design for the National Ignition Facility, these modules stored 1.6 MJ each**.

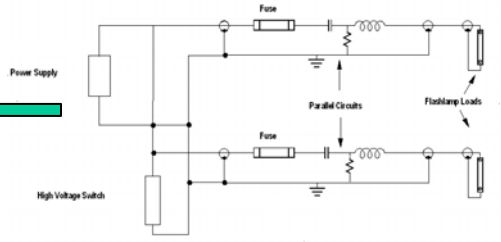


**A large number of single mesh circuits tied to a common power supply and switch. This is not always ideal for very large systems with many flashlamps because reliability and cost are not optimum.**

Figure 14. Circuit configurations for flashlamp driving. Only the configuration shown in the lower left is optimum for large systems because of the large number of components and the problems of fault mitigation.

[21] American Control Engineering, "Final Report for fabrication and testing of a 2-MJ capacitor bank," LLNL Subcontract BC 39943.

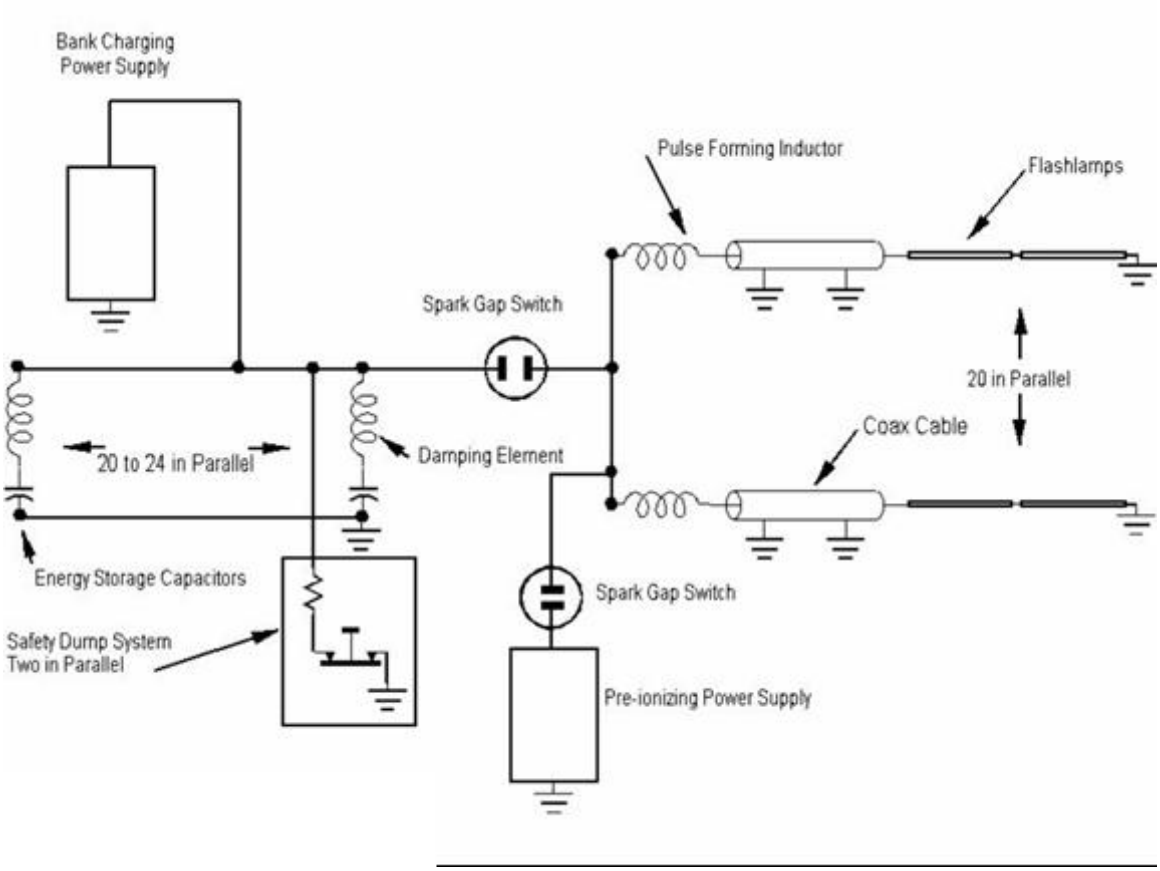


Figure 15. The prime power circuit developed for the National Ignition Facility. This configuration has 20, 315-$\mu$Fd, 24-kV capacitors in parallel. The damping elements (9 $\mu$Hy) are included to limit the rate of rise of the current in the event of a fault. Note the pre-ionizing power supply and associated switch used both to trigger the lamps and act as a diagnostic for the lamps.

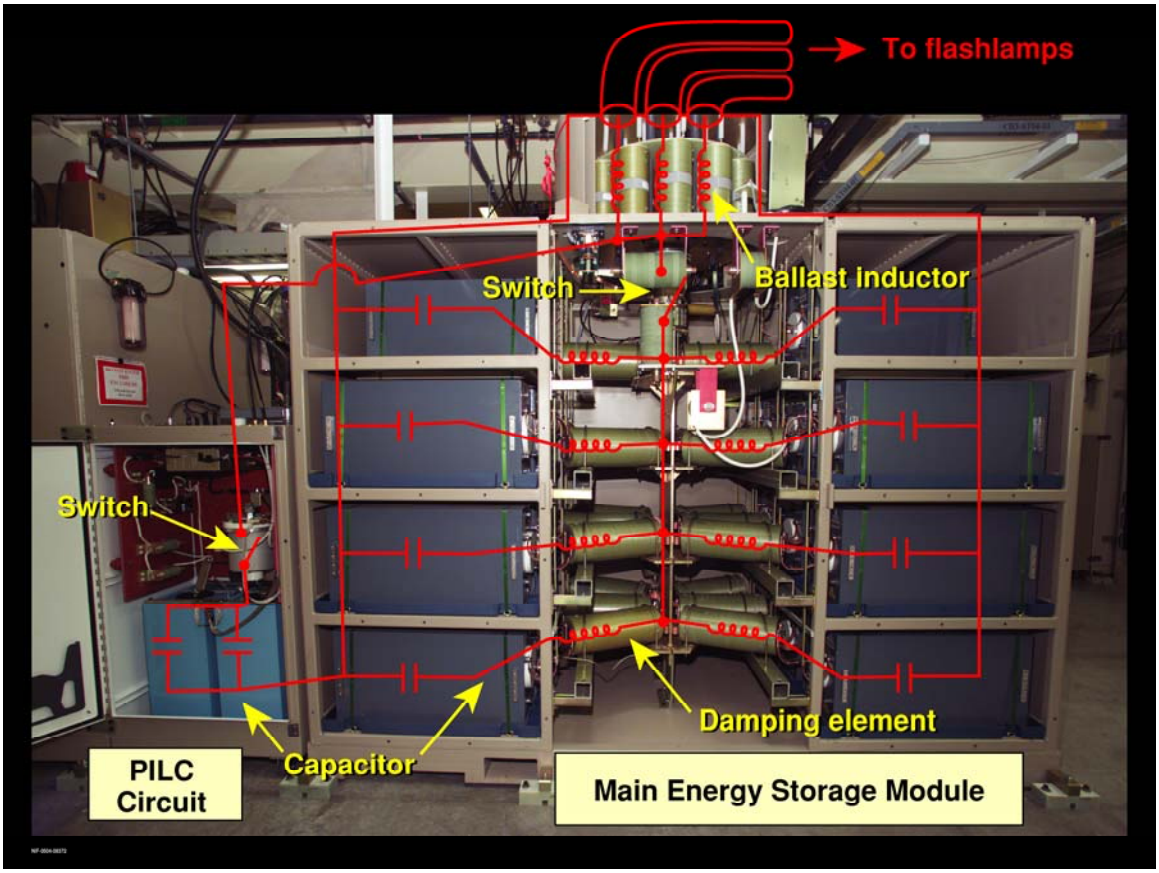


Figure 16. Energy storage module as designed and implemented for the National Ignition Facility at the Lawrence Livermore National Laboratory. This stores and switches up to 2 MJ at 24 kV.

This module stores and switches up to 2 MJ at 24 kV. Each module is self-contained with a single spark gap switch and charging power supply.[22] There are 192 modules in the prime power system. An interior view is shown in Figure 17, and a row of modules as installed in the National Ignition Facility is shown in Figure 18. This configuration requires a high-coulomb capacity switch and special damping inductors to limit fault currents. The details of this design are covered in later sections.

[22] M.A. Newton, R.E. Kamm, E.S. Fulkerson, S.D. Hulsey, D.L. Pendleton, D.E. Petersen, M. Polk, M. Tuck, G.T. Ullery,M3-2 Initial Activation and Operation of the Power Conditioning System for the National Ignition Facility, Lawrence Livermore National Laboratory, W.B. Moore, Sandia National Laboratory.

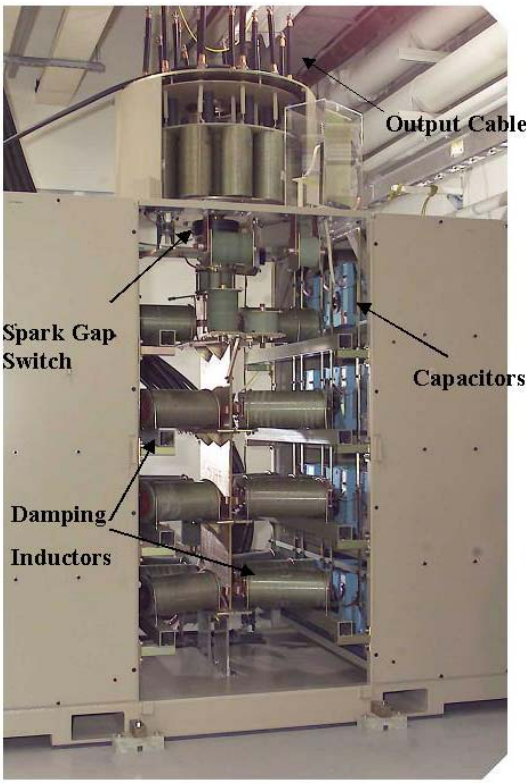


Figure 17. Interior view of the 2-MJ module showing the capacitors, damping inductors, spark gap switch and output cables. Approximately 192 such modules are installed in the National Ignition Facility.

Another example of this approach is the OMEGA Laser[23] at the University of Rochester. There, two different sized modules were developed. A 386-kJ module powers the 20-cm amplifiers and the 276-kJ module powers the 15-cm amplifiers. These are shown in Figures 18 and 19.

Figure 18. NIF energy storage modules. The system contains 192 modules storing 2MJ at 24 kV each.

[23] N.C. Jaitly et al., Maxwell Laboratories and L. Folnsbee et al., "Design of the 40 MJ Turnkey Power Conditioning System for 60 Beam Omega Laser E-Stage and F-Stage Single Segmented Amplifiers," Laboratory for Laser Energetics, University of Rochester, 1994, Pulsed Power Conference, Pgs. 164 to 169.


Figure 19. A Power Conditioning Unit at the University of Rochester OMEGA Laser. This delivers 272 kJ at 14.8 kV. (Courtesy of Larry Folnsbee, University of Rochester.)

Figure 20. OMEGA Laser—Power Conditioning Modules.

# CHAPTER 4

# FLASHLAMP EQUATIONS

## Introduction

To design pulsed power circuitry for flashlamps, it is necessary to understand the lamp parameters and the effect these have on the peak current, the delivered energy, and the temporal shape of the pulse. Other factors such as explosion limits and lamp life also must be taken into consideration.

Flashlamps currently used in today's large solid-state laser systems have diameters of several centimeters and lengths approaching 2 meters. The design and scaling information in this chapter are limited to lamps filled with xenon gas with diameters of 1 cm or greater and operating at pressures in the range of 100 Torr. There are other excellent sources of information available directed at flashlamps in general [24] [25] .

A typical large bore lamp is shown in Figure 21, and an array of lamps being prepared for mounting into a large laser amplifier is shown in Figure 22.

Figure 21. Large-bore xenon flashlamp used in the National Ignition Facility at Lawrence Livermore National Laboratory.

[24] EG&G Electro-Optics, "Flashlamp Application Manual."
[25] W. Koechner, "Solid-State Laser Engineering," Springer Series in Optical Sciences, 5th edition, 1999.

Figure 22. A flashlamp cassette assembly before insertion into a laser amplifier.

**Pulse Length and Energy Considerations**

Flashlamps are arranged spatially and driven electrically to optimize the transfer of energy to the laser media and thus result in the highest population of the upper states. There are fundamental limits with regard to energy, pulse length, voltage and maximum current that must be observed. In general, these are:

1. Too short a pulse length can cause the lamps to turn opaque and reabsorb a significant percentage of the light energy.
2. Too long a pulse is inefficient because the stored energy in the disk decays faster than the lamps can replace it.
3. Too much energy in a single pulse or on a repetitive basis can significantly reduce the life of the lamp or in extreme situations, destroy it. This last limit is quantified as follows:

**Single Shot Explosion Energy**

The approximate single shot explosion energy $E_{\exp}$ is given as;

$$E_{exp}=2\cdot 10^{4}\, l\cdot d\cdot \tau^{1/2} \qquad [1]$$

Where:

$E_{\exp}$ = Single Shot Explosion Energy

$l$=*Lamp Length*

$d$ = *Lamp Diameter*

$\tau = \sqrt{LC}$

The approximate number of shots before failure is given as:

$$N = \left( \frac{E \exp}{Eo} \right)^{8.8} \qquad [2]$$

Where n is the approximate number of shots before failure.

$E_{epx}$ = Single shot explosion energy limit

$Eo$ = Energy at which the lamp is actually being operated.

A plot of this relationship is shown in Figure 23 below.

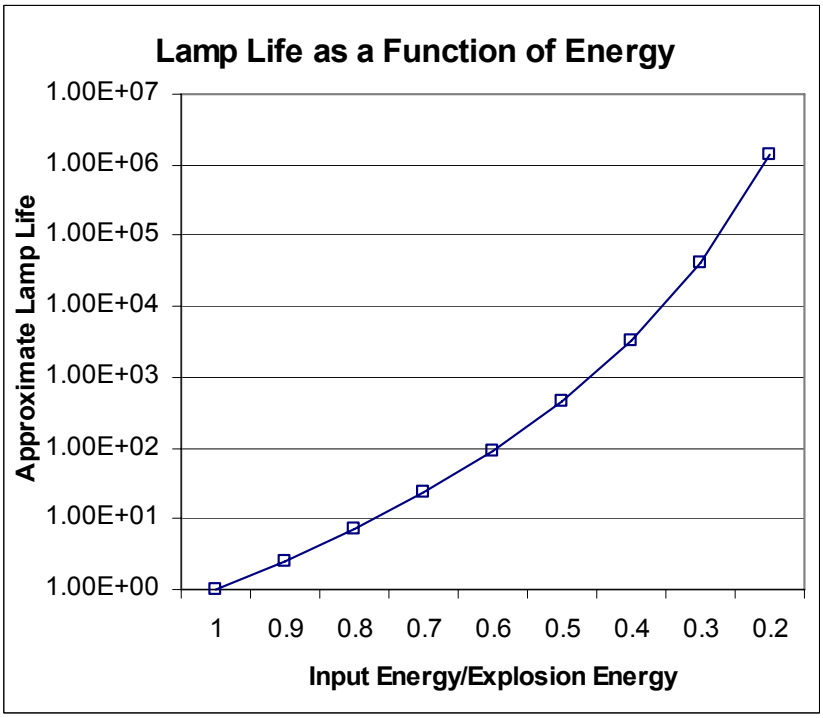


Figure 23. Expected number of lamp Shots as a Function of lamp energy versus explosion energy.

Note the steep curve resulting from the function $N = \left( \frac{E \exp}{Eo} \right)^{8.8}$.

These factors are important and cannot be ignored, because flashlamp failure can result in catastrophic consequences to the laser disks in an amplifier, as well as cause system downtime and serious credibility issues for the responsible engineers. An example from an early developmental amplifier is shown below in Figure 24.

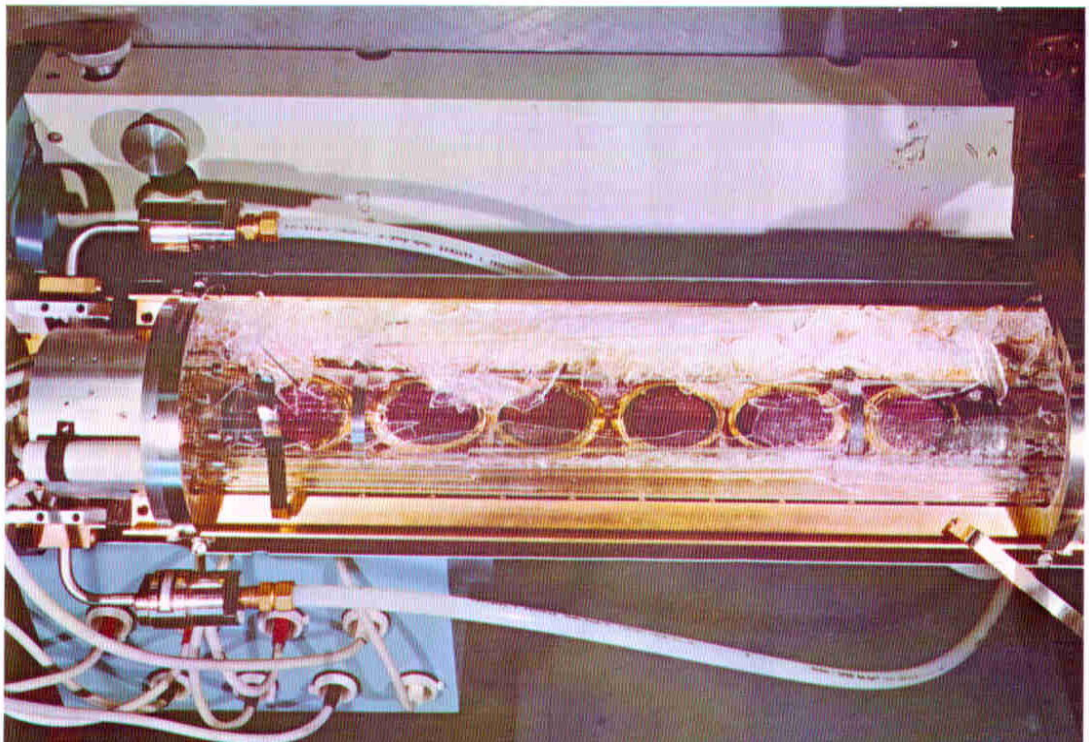

Figure 24. Catastrophic damage to an early developmental laser amplifier as a result of flashlamp failure.

### Equivalent Flashlamp Resistance $K_0$

Flashlamps behave as nonlinear resistors, and the differential equations describing the circuit behavior of lamps are linear in time but nonlinear in current. This was addressed, and a solution to the nonlinear equations was developed by J.L. Emmett and J.P. Markiewicz in 1966.[26] From this work, a set of design equations was established.

In these design equations, it will be shown that there are two loss terms to be considered. The first is $\alpha$, the nonlinear term associated with the flashlamp. The second is the linear resistive term β. Examples of circuits with and without resistive loss are developed in the sections that follow. It has been shown that the resistance of flashlamps with diameters approaching several centimeters, when operated in the fully ionized region can be approximated by the relationship:[27]

$$V \sim K_0 I^m \quad \text{or} \quad K_0 = V/I^m, \quad \text{where:} \qquad [3]$$

V = Voltage across the lamp,
I = Current through the lamp
m = is a function of lamp characteristics

[26] J.P. Markiewicz and J.L. Emmett, "Design of Flashlamp Driving Circuits Journal of Quantum Electronics," Vol. QE2, No. 11, 1966.

[27] See Appendix C, Internal LLNL Note, John Trenholme, July 2004.

**$K_0$ for flashlamps in series and in parallel**[28]

Suppose we have a flashlamp that approximately relates the voltage V across it, to the current I through it, by the formula:

$$V = K_{1,1} I^P$$

Here, P is a power that is traditionally taken to be 0.5, although careful experiments in the 1983 Annual Report show it to be near 0.41 for NIF-style lamps. $K_{1,1}$ is a constant that depends on the diameter and length of the lamp, and on the composition and pressure of the gas fill. In everyday practice it is usually called $K_0$, but we for now want to use the detailed subscripts to indicate the number of series and parallel lamps. If the current is negative, we take the absolute value when calculating $I^P$, and then apply the sign:

$$V = K_{1,1} sign(I)\left[abs(I)\right]^P$$

We will use the positive-current form from now on, to simplify the formulae.

Suppose that we put M of these lamps in series. The current through each lamp is the same (call it I, again), and so the voltage of each lamp is given by the formula above. The total voltage of all the lamps is the sum of the individual voltages, so the V-I relation is

$$V = MK_{1,1} I^P$$

The series string gives the same V-I behavior as a single lamp with a $K_0$ value of:

$$K_{M,1} = M\ K_{1,1}$$

Now suppose that we instead put N of the flashlamps in parallel. Since the lamps are assumed identical, the current through each lamp will be I/N (the natural variation in real-world lamps makes this hard to do in practice). The voltage across each lamp is the voltage applied to the parallel array and is given by:

$$V = K_{1,1}\left(\frac{I}{N}\right)^P = \frac{K_{1,1}}{N^P} I^P$$

The parallel array gives the same V-I behavior as a single lamp with a K value of:

$$K_{1,N} = \frac{K_{1,1}}{N^P}$$

[28] John Trenholme, LLNL Internal Note, 26 Jan. 2005.

We can now consider the general case of N parallel strings of M lamps in each series. Again, assuming perfect current division, the current in each string is I/N, and the voltage across any string (and therefore across all the strings) is M times the voltage across one lamp with current I/N. Thus the series-parallel group of lamps has the V-I relation:

$$V = MK_{1,1}\left(\frac{I}{N}\right)^{P} = \frac{MK_{1,1}}{N_p} I_p$$

The series-parallel group thus has a K value corresponding to a single lamp with a K of:

$$K_{M,N} = \frac{MK_{1,1}}{N^{p}} \qquad [4]$$

This is the expression that explicitly keeps track of series and parallel lamp combinations.

$K_0$ can also be measured directly by simply observing the voltage across the lamp and the current through the lamp at a point in the pulse where the lamp is fully ionized.

From the lamp characteristics themselves, $K_0$ is calculated as follows:

$$K_0 = \frac{4}{3} \times \frac{l}{d} \times \left[\frac{p}{450}\right]^{.2} \sqrt{V \times Ohms} \qquad [5]$$

Where

$d$ = Lamp diameter [cm]

$l$ = Lamp length [cm]

$p$ = lamp gas pressure [Torr]

$K_0$ = Lamp constant [(V ohms)$^{0.5}$ ]

As an example, consider a 180cm x 4.3-cm flashlamp filled with xenon gas at a pressure of 100 Torr. Assume the current exponent is .5.

$K_0$ for this lamp is calculated as follows, using [5]:

$$K_0 = \frac{4}{3} \times \frac{l}{d}\left(\frac{p}{450}\right)^{.2} = \frac{4}{3} \times \frac{180}{4.3} \times \left(\frac{100}{450}\right)^{.2} = 40.3\ \left(Volts \times Ohms\right)^{.5}$$

If the circuit consists of two lamps in series, $K_0$ for the combination is 2x 40.3 = 80.6. If the circuit consists of a parallel combination of two series lamps and two parallel strings,

$$K_0\ combination = K_{(0)} \times \frac{n_{(series)}}{\left(n_{parallel)}\right)^{(m)}} \text{ where } K_0 = K\ for\ a \text{ single lamp,}$$

$n_{(series)}$ = number of lamps in series and

$n_{(parallel)}$ = number of lamps in parallel

$m$ = the exponent the current is raised to in order to fit a particular lamp

( See Appendix C)

Later studies refined this to take into account transient and hysteresis effects, which produce a time lag between the power input to the lamp and radiated power from the lamp.[29] From this study, it was shown that electrical characteristics of lamps were different during the current rise as opposed to the current fall. It was concluded from these experiments that the internal flashlamp energy simply tracks the input power with a time lag.

To demonstrate this, numerical values were extracted from the measured waveforms of flashlamp current and voltage as shown in Figure 25 and 26.[30] The voltage values were then delayed by 50 μsec to take into account the above-mentioned hysteresis effects. These are compared in Figure 27 with the calculated value of the voltage using equation [3]: $V = \sqrt{I} \times K_0$, where $K_0 = 79$. There is good agreement between measured and calculated values at the peak of the current pulse (650 to 750 μsec). Note in Figure 25 the rapid voltage spike at the beginning of the pulse. This is the lamp trigger pulse.

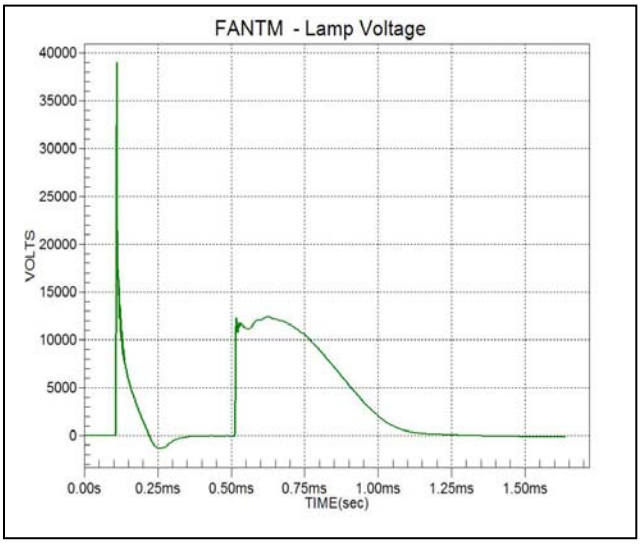


Figure 25. Measured voltage for two 180 x 4.3 cm lamps in series. The initial spike is produced by the pulsed ionized lamp check circuit, which acts as a trigger for the lamps.

[29] A. E. Orel and H.T. Powell, "Transient Response of Flashlamps". LLNL Laser Program Annual Report, 1983.

[30] John Trenholme, LLNL Laser Program Internal Memo, July 2003.

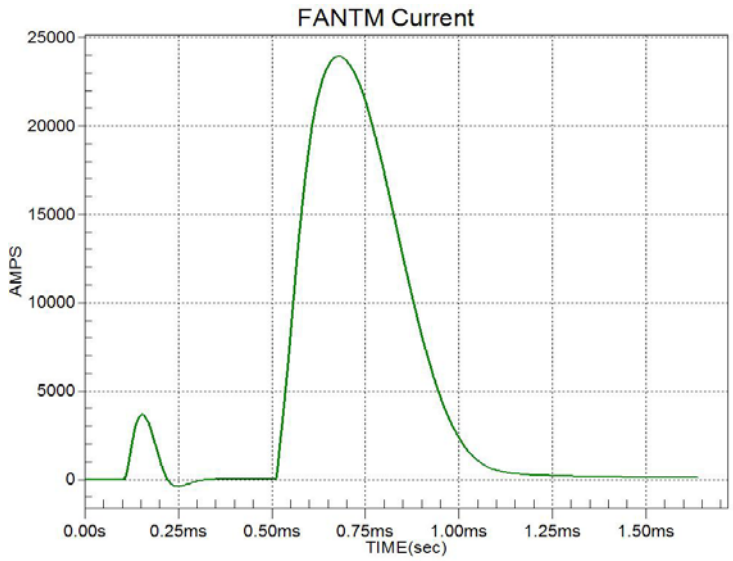


Figure 26. Measured current for two 180- x 4.3-cm lamps in series. The initial smaller current pulse is produced by the pre-ionization (pulsed ionized lamp pulse) circuit.

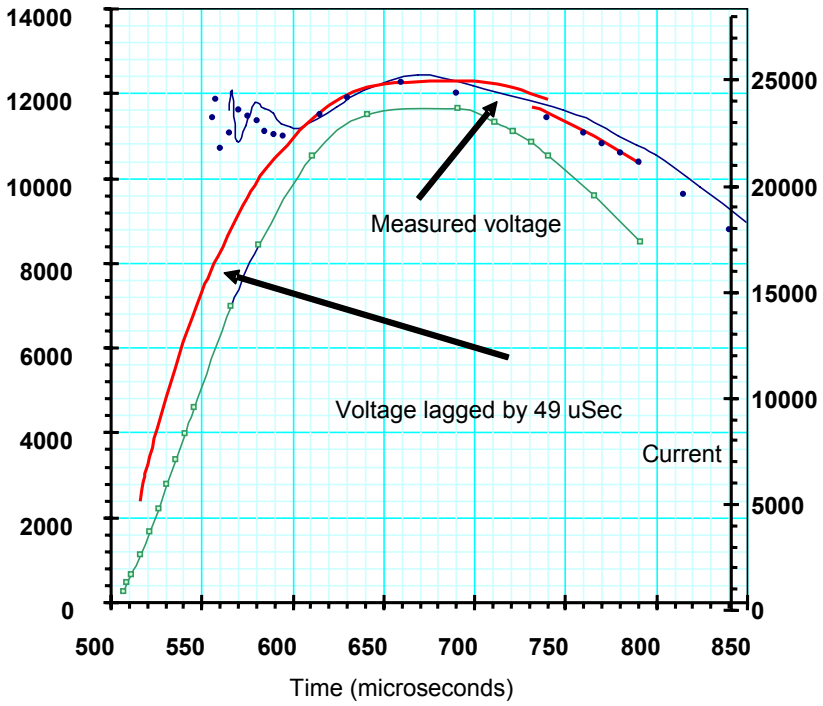


Figure 27. Comparison of measured versus calculated voltage with $K_0$ set at 79 and the voltage delayed by 50 μsec. The red curve is the calculated voltage (left axis). The blue curve is the measured voltage lagged by 50 μsec. There is good agreement after the plasma is established in the lamp.

# CHAPTER 5

# FLASHLAMP DRIVING CIRCUITS

Flashlamps are most commonly driven using critically damped LRC circuits. Critical damping isn't necessarily optimum, but reflects the best technology presently available[31]. In the following sections, two design examples are developed in order to clarify the design method. The first assumes only flashlamp (non-linear) resistance. The second example includes linear circuit resistance. These are necessarily simplified examples intended to illustrate the basic principles involved. Later sections will show complete designs that include all circuit components.

## Design Equations for Circuits with Flashlamp Resistance Only

### Example – Single Mesh Circuit

A simple single mesh flashlamp driving circuit is shown in Figure 28. In this example, circuit resistance losses other than the flashlamp are ignored.

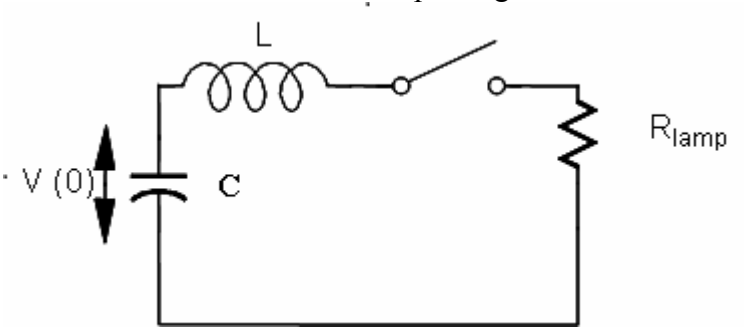


Figure 28. A typical single mesh LRC circuit used to drive a flashlamp. Circuit losses are ignored.

The nonlinear differential equation for this circuit is;

$$L\frac{di}{dt} + K_0\sqrt{i} + \frac{1}{C}\int i\,dt = V_0 \qquad [6]$$

If the following normalizations are made (assume no circuit losses other than the flashlamp):

[31] A better approach would be to shape the drive pulse such that it is terminated shortly after the energy is extracted from the laser media. This would result in more efficient energy use by saving the energy supplied to the lamp following the laser pulse extraction. This would also result in less energy absorption in the laser disks and therefore less optical distortion.

$$Z_0 = \sqrt{\frac{L}{C}} \quad i = I\frac{V_0}{Z_0} \quad \tau = \frac{t}{T} \quad T = \sqrt{LC} \qquad [7]$$

$$\alpha = \frac{K_0}{\sqrt{V_0 Z_0}} \quad = \text{Nonlinear Damping Factor} \qquad [8]$$

Equation [6] becomes:[32]

$$\frac{dI}{dt} \pm \alpha\sqrt{I} + \int_0^{\tau} I dt = 1 \qquad [9]$$

The solution to this equation yields relationships, which, after specifying $K_0$, α, and τ and the required input energy $E_0$, allow one to calculate $C, V_0$, and $L$. These relationships are as follows:

$$E_0 = \frac{CV^2}{2} = \textit{Input Energy} \qquad [10]$$

$$C = \left[\frac{2E_0\alpha^4\tau^2}{K_0{}^4}\right]^{1/3} = \text{Circuit Capacitance} \qquad [11]$$

$$\tau = \sqrt{LC} = \text{ Pulse Width } \approx \text{ 10\% to 80\%}$$

$$V_0 = \sqrt{\frac{2E_0}{C}} = \text{ Circuit Voltage} \qquad [12]$$

$$L = \frac{\tau^2}{C} = \text{ Circuit Inductance}$$

**Example – Flashlamp Resistance Only**

Assume we wish to drive a flashlamp with the following specifications:

$l = 180$ cm  d = 4.3 cm and Pressure = 100 Torr

Then, from [5]

$$K_0 = 1.3\frac{l}{d} \times \left(\frac{p}{450}\right)^{.2} = 1.3 \times \frac{180}{4.3} \times \left(\frac{100}{450}\right)^{.2} = 40.3$$

[32] See Appendix A for derivation. G. Albrecht, LLNL Internal Memo, July 2003.

The lamp is to be driven with an energy that is 20% of its explosion energy and with a pulse length of 120 μsec.

Calculating the explosion energy from [1]:

$$E_{\exp} = 2\times10^4 ld\tau^{1/2} = 2\times10^4\times180\times4.3\times\left(120\times10^{-6}\right)^{1/2} = 169.6\,kJ$$

Calculating 20% of the explosion energy:

$$.2\times169600 = 33914\,J$$

Calculating C from [5.6]:

$$C = \left[\frac{2E_0\alpha^4\tau^2}{K_0{}^4}\right]^{1/3} = \left[\frac{2\times33920\times.75^4\times\left(120\times10^{-6}\right)^2}{\left(40.3\right)^4}\right]^{1/3} = 493\,\mu Fd$$

Calculating $V_0$ from [12]:

$$V_0 = \sqrt{\frac{2E_0}{C}} = \sqrt{\frac{2\times33290}{493\times10^{-6}}} = 11.73kV$$

And finally, determining the value of L from equation [12]:

$$L = \frac{\tau^2}{C} = \frac{\left(120\times10^{-6}\right)^2}{493\times10^{-6}} = 29.2\mu Hy$$

The circuit diagram for this case is shown in Figure 29.

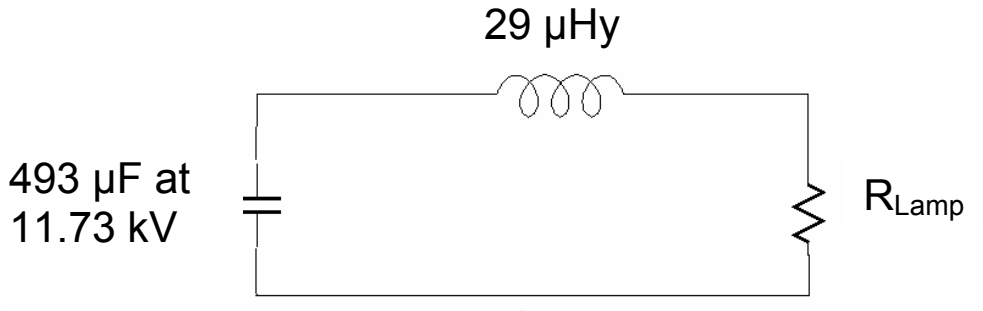


Figure 29. Circuit values for a 180- x 4.3-cm amp with 3τ = 360 μsec. Circuit resistance other than the flashlamp is assumed to be zero.

Because there are no resistive losses other than the flashlamp in the circuit, it is under-damped. A critically damped circuit would have an $\alpha$ value of about .75 for β equal to zero (no resistance in the circuit). However, for this example, $\alpha = \frac{K_0}{\sqrt{V_0 Z_0}} = .55$ and the circuit rings. The current minimum is –3700 amps.

A plot of the calculated current waveform is shown below in Figure 30.

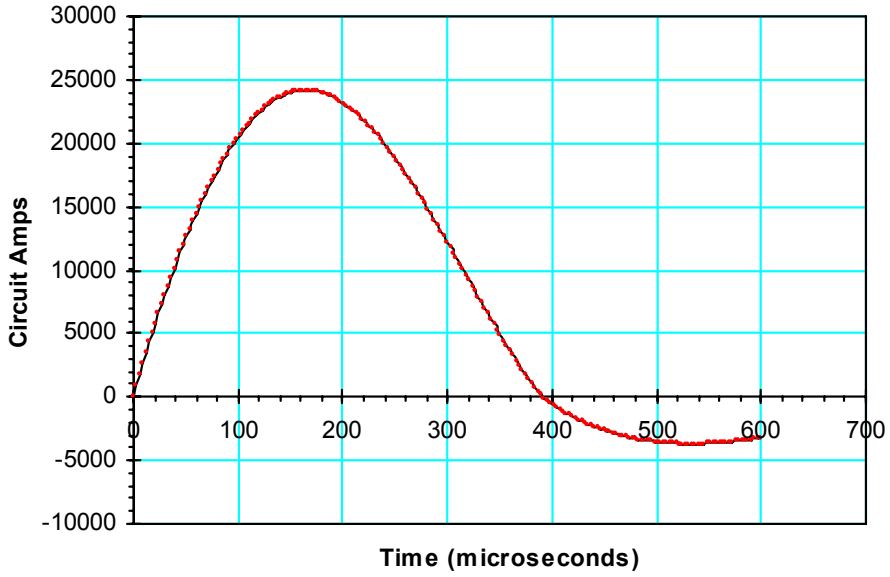


Figure 30. Plot of the current waveform for the 180cm x 4.3cm lamp example.

## Circuits with Resistive Losses

In real applications, flashlamp driving circuits contain components that are used to pulse shape and limit the peak currents in the event of a major fault or short in the circuit. In addition, coaxial cable is generally used to transport energy from the energy storage module to the lamps. These elements introduce linear resistive losses as well as additional inductance and capacitance to the circuit. Designs that take into account all of the above factors are illustrated in later sections. Simple circuits with both linear and nonlinear resistance losses are described below.

## Design Equations Accounting for Linear Losses

To account for the resistive losses in the design, a linear loss term, $\beta = \frac{R}{Z_0}$ is introduced in equation [9]:

$$\frac{di}{d\tau} \pm \alpha\sqrt{I} + \beta I + \int_0^{\tau} I d\tau = 1$$

There are now two loss terms in the equation. The first is the nonlinear loss term $\alpha = \frac{K_0}{\sqrt{V_0 Z_0}}$ and the second, the linear loss term $\beta = \frac{R}{Z_0}$.

The design equations then become:

$$E_0 = \frac{CV_0^2}{2} = \text{ Input Energy} \qquad \text{(same as [10])}$$

$$C = \left[\frac{2E_0\alpha^4\tau^2}{K_0^4}\right]^{1/3} = \quad \text{Circuit capacitance} \qquad \text{(same as [11])}$$

$$\tau = \sqrt{LC} \approx \text{ Pulse Rise Time to 80 \%} \qquad \text{(same as [12])}$$

$$\beta = \frac{R}{Z_0} = \text{ Linear Loss Factor} \qquad [13]$$

$$\alpha = \frac{K_0}{\sqrt{V_0 Z_0}} = \text{ Nonlinear Loss Factor} \qquad [14]$$

**Relationship of α versus β for Critical Damping**

Generally, flashlamp driving circuits are designed to be critically damped or very close to critically damped. This results in the most efficient transfer of energy from the capacitors to the lamps as well as, in most cases, extending the life of the high-voltage capacitors in the driving circuit. It is necessary, then, to quantify the relationship between $\alpha$ (nonlinear loss factor) and $\beta$ (linear loss factor) under conditions of critical damping. Figure 31 shows this relationship. When α and β fall on the curve, the circuit will be critically damped.

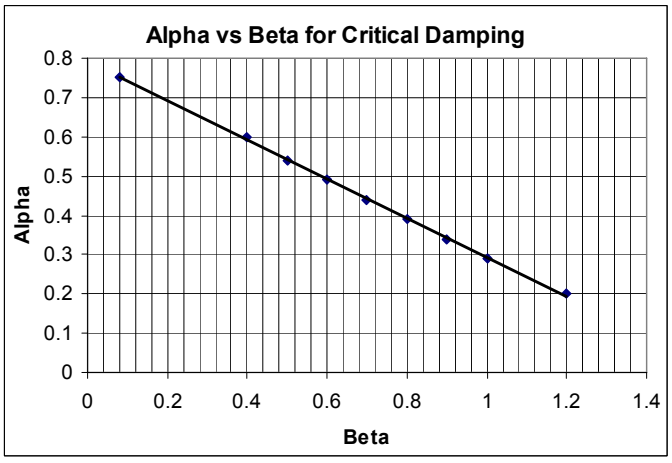


Figure 31. Values of α and β for a near critically damped circuit. For critical damping, α =.75 and β =.5. This curve, when taken over a broad range is not linear. We have extracted a narrow area of interest as an engineering aid.

**Circuit Example with Both Flashlamps and Circuit Losses**

When designing a flashlamp driving circuit containing both the non-linear resistance of the lamp plus added linear circuit resistance, both must be taken into account.
Assume we must to drive a xenon lamp with the following specifications:

Lamp length = 50 cm
Lamp diameter = 2.0 cm
Pressure = 100 Torr

Further assume that a pulse length 3t = T = 3 √(LC) = 360 μsec is required and the lamp will be driven with approximately 20% of explosion energy. We estimate the linear resistance added to the circuit will be .02 ohms.

We will also stipulate that the circuit be near or at critical damping. Therefore, we will fix the non-linear damping factor α at .75 and develop the design such that the α and β values satisfy the criteria in Figure 31 for critical damping.

Calculate explosion energy from [1]: $E_{\exp} = 2\times10^4 ld\tau^{1/2}$

$$E_{\exp} = 2\times10^4 \times 50 \times 2 \times \sqrt{120\times10^{-6}} = 21900\,J$$

Calculate 20 % of explosion energy: $.2\times21900 = 4380\,J$

Calculate $K_0$ for the lamp from [5]: $K_0 = 1.3\times\frac{50}{2}\times\left[\frac{100}{450}\right]^{.2} = 24$

Calculate circuit capacitance from [11]:

$$C = \left[\frac{2E_0\alpha^4\tau^2}{K_0{}^4}\right] = \left[\frac{2\times4380\times.75^4\times\left(120\times10^{-6}\right)^2}{24^4}\right]^{1/3} = 495\mu Fd$$

Calculate the voltage from [12]: $V = \sqrt{\frac{2E_0}{C}} = \sqrt{\frac{2\times4380}{.000495}} = 4203V$

Calculate the inductance from [12]: $L = \frac{\tau^2}{C} = \frac{\left(.000120\right)^2}{.000495} = 29\mu Hy$

Calculate β from [13]: $\beta = \frac{R}{Z_0} = \frac{.02}{\sqrt{\frac{.000298}{.000483}}} = .08$

A plot of the calculated current waveform is shown in Figure 32. Note that the values for $\tau = \sqrt{LC}$ *and* $T = 3\sqrt{LC}$ *are shown.*

$3\sqrt{\mathrm{LC}}$ is the time measured from 15% on the rise to 15% on the fall of the current pulse. Note that these are approximate values and assume the pulse is near critical damping.

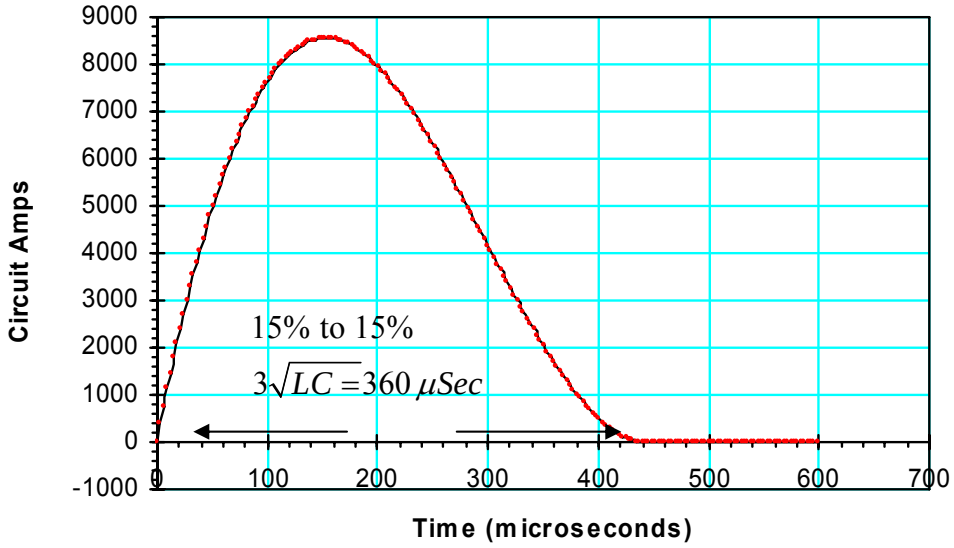


Figure 32. Plot of calculated current for the 50- x 2-cm flashlamp example with the values for $T = 3\sqrt{LC}$ shown.

For the above example, a value of linear resistance was selected such that the values of α (0.75) and β (0.08) resulted in a near critically damped circuit. If a different value had been picked, the circuit would have been either over-damped or under-damped. It would have been necessary then to recalculate, trying different values of the variables until the desired result was achieved. Generally, it is necessary to iterate the design a number of times to optimize the result. An example of a Microsoft Excel spreadsheet designed for this purpose is included in Appendix B.[33] In addition, the CD included with the book contains this spreadsheet.

**Calculating $K_0$ for multiple lamp loads**

In large laser systems, flashlamps are most often driven in series or series/parallel arrays. In this configuration the lamp constant $K_0$ for the series/parallel configuration is calculated according to [4] and the preceding development as follows:

$$K_{M,N} = \frac{M\ K_{1,1}}{N^{(P)}}\ I^{(P)} \quad \text{Where } K_{M,N} = K_{(combination)}$$

$M$ = number of lamps in series

N = number of lamps in parallel

I = current in a single lamp

p = current exponent

[33] John Trenholme, LLNL Laser Program Internal Note, Aug. 2003.

Assume the following;

1. The load consists of 2 series lamps with 20 groups in parallel.
2. Lamp length is 180 cm, diameter is 4.3 cm, and pressure is 100 Torr.
3. The measured current exponent is .5.

Then, $M = 1, N = 20\ P = .5$

$$K_{\text{(Single Lamp)}} = 1.3 \times \frac{180}{4.3} \times \frac{100}{450}^{(.2)} = 40.3$$

$$K_0 \text{ of the combination } = 40.3 \times \frac{2}{20^{(.5)}} = 18.02$$

An illustration of this circuit is shown in Figure 33.

Examples of designs with series/parallel arrangements are covered in some detail in later chapters.

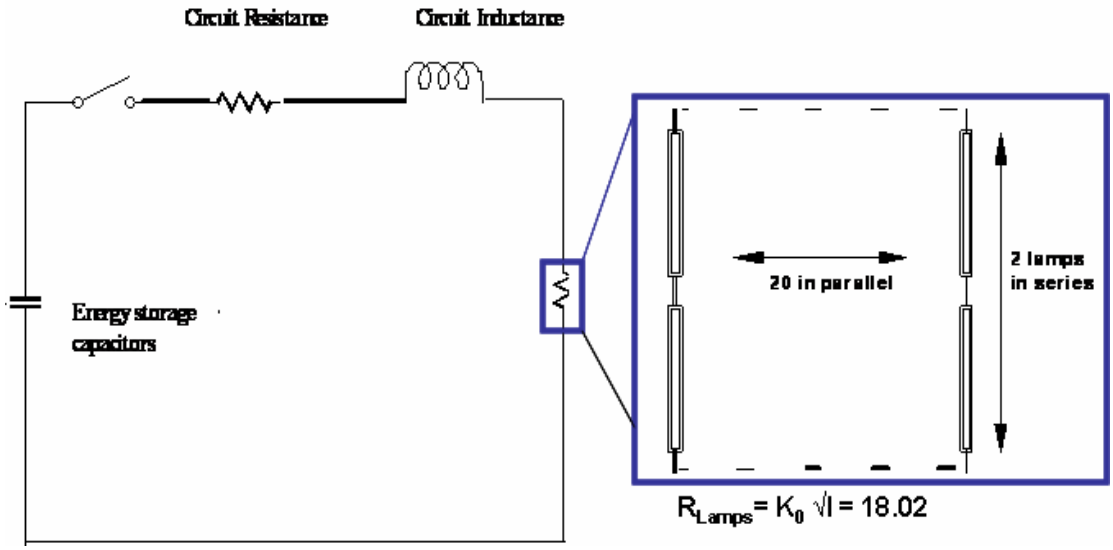


Figure 33. A common flashlamp configuration for large solid-state lasers. The flashlamps are generally arranged in series/parallel arrays and driven by single or multiple mesh LRC circuits.

**Design Example – Multiple Lamp Loads**

When designing circuits with multiple lamp loads, it is generally convenient to utilize a modeling program. This enables the designer to quickly iterate through the many variables and optimize the solution. An Excel spreadsheet designed to do this is included with this book. However, in order to make clear to the reader the design process, examples of multiple lamp designs are presented in this section using just the design equations.

**Design Example—Two Series Lamps**

Assume a load consisting of two series lamps, each 50 cm in length and 2 cm in diameter as shown in the circuit diagram of Figure 34. We are given that the lamps are filled with Xenon at a pressure of 100 Torr. We will design for $\tau = \sqrt{\mathrm{LC}} = 120 \times 10^{-6}$ sec and $\alpha$, the nonlinear loss term = .75.

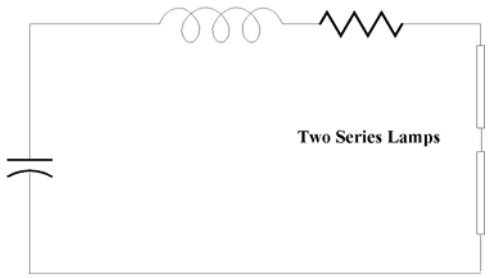


Figure 34. Two series lamps in a typical driving circuit.

By now we assume familiarity with the equations developed in this chapter and applied previously. They are also again summarized in Appendix C. We again start with the explosion energy:

$$E_{\exp} = 2 \times 10^4 ld\tau^{1/2} = 2 \times 10^4 \times 50 \times 2 \times \sqrt{102 \times 10^{-6}} = 21908 J$$

We will run the lamps at 20% of the single shot explosion energy.

Therefore the single lamp energy is:

$$E_{(\text{single lamp})} = .2 \times 21908 = 4382\ J$$

*The circuit energy is then* $2 \times 4282 = 8764\ J$

Calculating $K_0$ for a single lamp:

$$K_0 = \frac{4}{3} \times \frac{l}{d} \times \left( \frac{p}{450} \right)^{.2} = \frac{4}{3} \times \frac{50}{2} \times \left[ \frac{100}{450} \right]^{.2} = 24.05$$

For the series combination, $K_0 = 2 \times 24.05 = 48.1$

We have now defined the circuit as a single lamp load that consists of two lamps in series. We have:

- Calculated the explosion energy for a single lamp, and stipulated operation at 20% of this energy. The total energy required for two series lamps is twice this amount.
- Calculated $K_0$ for the two-lamp combination.

- Defined α as .75, near critical damping.

Calculating the circuit capacitance:

$$C = \left[\frac{2E_0\alpha^4\tau^2}{K_0{}^4}\right]^{1/3} = \left[\frac{2\times 8764\times(.75)^4\times\left(120\times10^{-6}\right)^{.5}}{(48.1)^4}\right]^{1/3} = 246\mu Fd$$

Calculating the circuit Inductance:

$$L = \frac{\tau^2}{C} = \frac{\left(120\times10^{-6}\right)^2}{246\times10^{-6}} = 58.5\mu Hy$$

Calculating the circuit driving voltage:

$$V_0 = \sqrt{\frac{2E_0}{C}} = \sqrt{\frac{2\times8764}{246\times10^{-6}}} = 8441\,\mathrm{V}$$

Calculating Zo:

$$Z_0 = \sqrt{\frac{L}{C}} = \sqrt{\frac{58.5\times10^{-6}}{246\times10^{-6}}} = .49$$

Estimate the linear circuit resistance to be .02 ohms.

Then β, the linear loss factor is:

$$\beta = \frac{\mathrm{R}}{\mathrm{Z}_0} = \frac{.02}{.49} = .04$$

As shown in Figure 31, this is reasonably close to the optimum value for critical damping.

**Spreadsheet Example – Two Series Lamps**

The spreadsheet is shown below, and a plot of the calculated wave form is shown in Figure 35.

| **Input Parameters:** | | | |
|---|---|---|---|
| | | | |
| **Initial voltage $V_0$** | **8.5** | **kilovolts** | |
| **Capacitance** | **246** | **microfarads** | |
| **Inductance** | **58.5** | **micro henries** | |
| **Resistance** | **20** | **milliohms** | |
| **Lamp K factor** | **48** | **volts per amp$^p$** | |
| **Lamp V-I exponent P** | **0.5** | | |
| | | | |
| **Calculated quantities:** | | | |
| | | | |
| **Impedance Z** | **487.65** | **milliohms** | |
| **3*√(L*C)** | **359.88** | **μsec** | |
| **Stored energy** | **8.88** | **kilojoules** | |
| | | | |
| **α** | **0.74** | **[nonlinear damping]** | |
| **β** | **0.04** | **[linear damping: R / Z]** | |
| | | | |
| **Peak current** | **8845.2** | **amps** | |
| **Peak time** | **155.95** | **μsec** | |
| **Lowest current** | **-69.7** | **amps** | |
| | | | |
| **Maximum time** | **599.81** | **μsec** | |
| **Reference current** | **17.43** | **kiloamps** | |
| | | | |
| **Energy=8.7 kJ Eff.= 97.1%** | | | |

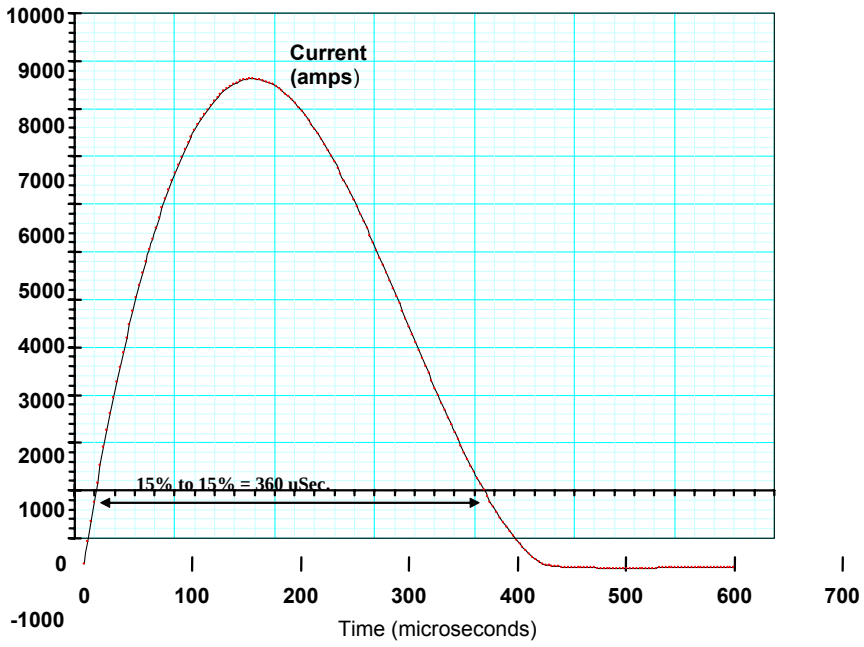


Figure 35. A plot of the calculated current for the two series lamp design.

**Example – Series /Parallel Lamps**

As a second design example, consider a circuit that consists of two parallel strings of two lamps each as shown in Figure 36.

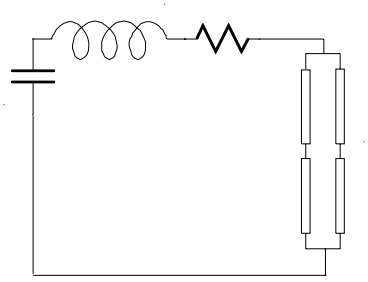

Figure 36. A circuit consisting of two parallel strings of two flashlamps each.

Once again we will use 50cm- x 2-cm lamps for this example and use the formulas from Appendix C. We will reduce the lamp load to an equivalent single resistance and calculate the circuit values for this resistance. Again, we will assume a circuit resistive loss of .02 ohms.

$K_0$ for a single lamp is:

$$K_0 = \frac{4}{3} \times \frac{l}{d} \times \left( \frac{p}{450} \right)^{.2} = \frac{4}{3} \times \frac{50}{2} \times \left( \frac{100}{450} \right)^{.2} = 24.05$$

$K_0\ combination = K_{(0)} \times \dfrac{n_{(series)}}{\left(n(_{parallel})\right)^{(m)}}$ where $K_0 = K\ for\ a$ single lamp,

$n_{(series)}$ = number of lamps in series

$n_{(parallel)}$ = number of lamps in parallel

and $m$ = the exponent the current is raised to in order to fit a particular lamp

Therefore, given the lamp constant $m = .5$

$K_0$ For the series / parallel combination is:

$$K_{0(\text{Combination})} = 24.05 \times \frac{2}{2^{.5}} = 34$$

The single shot explosion energy for a single lamp is:

$$E_{\exp} = 2 \times 10^4 ld\tau^{1/2} = 2 \times 10^4 \times 50 \times 2 \times \sqrt{120 \times 10^{-6}} = 21908J$$

Again using the lamps at 20% of explosion energy:

$$E_{(\text{single lamp})} = .2 \times 21908 = 4382\ J$$

The combination of four lamps will require 17528 Joules.

Calculating C:

$$C = \left[\frac{2E_0\alpha^4\tau^2}{K_0{}^4}\right]^{1/3} = \left[\frac{2 \times 17528 \times (.75)^4 \left(120 \times 10^{-6}\right)^{.5}}{(33.94)^4}\right]^{1/3} = 497\mu Fd$$

Calculating L:

$$L = \frac{\tau^2}{C} = \frac{\left(120 \times 10^{-6}\right)^2}{497 \times 10^{-6}} = 29\mu Hy$$

Calculating Circuit Voltage $V_0$:

$$V_0 = \sqrt{\frac{2E_0}{C}} = \sqrt{\frac{2 \times 17528}{497 \times 10^{-6}}} = 8400V$$

The spreadsheet solution is shown below and a plot of the current is shown in Figure 37.

| Input Parameters: | | |
|---|---|---|
| | | |
| Initial voltage $V_0$ | 8.4 | kilovolts |
| Capacitance | 497 | microfarads |
| Inductance | 29 | microhenries |
| Resistance | 20 | milliohms |
| Lamp K factor | 34 | volts per amp$^p$ |
| Lamp V-I exponent P | 0.5 | |
| | | |
| Calculated quantities: | | |
| | | |
| Impedance Z | 241.5 | milliohms |
| 3*√(L*C) | 360 | microseconds |
| Stored energy | 17.5 | kilojoules |
| | | |
| $\alpha$ | 0.75 | |
| $\beta$ | 0.087 | |
| | | |
| Peak current | 17104 | amps |
| Peak time | 153 | microseconds |
| Lowest current | -33 | amps |
| | | |
| Maximum time | 600 | microseconds |
| Reference current | 34.7 | kiloamps |
| | | |

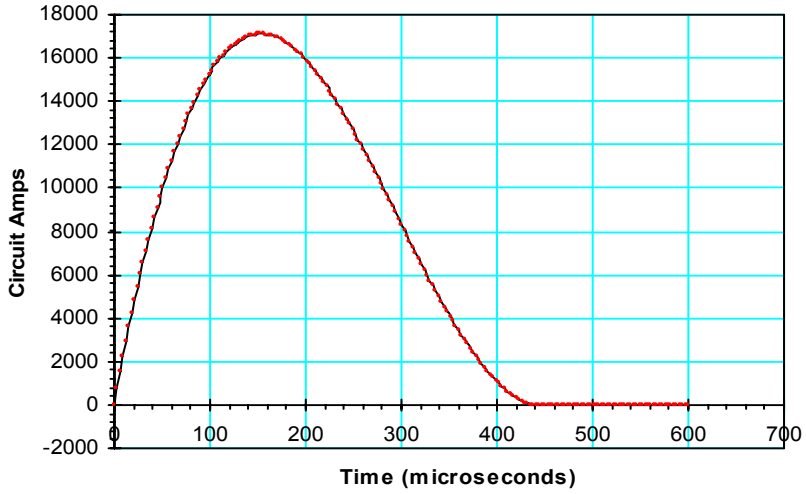


Figure 37. A plot of the calculated current for the series / parallel lamp example.

Note that in all these designs it will be necessary to iterate some of the parameters slightly to optimize the result.

# CHAPTER 6

# FLASHLAMP TRIGGER AND PULSED IONIZED LAMP CHECK (PILC) DIAGNOSTIC

## Flashlamp Diagnostics

A significant precursor for a lamp failure that has been observed in previous systems, generally occurs at the end of a system shot and appears as small cracks in the lamp glass envelope. This phenomenon is called "crazing" and results from an increasingly fatigued lamp envelope due to UV loading of the envelope material. This is an indication of incipient envelope rupture, the lamp in question is likely to fail during the next shot. If this is detected before the next firing, a catastrophic lamp explosion can be avoided.

In a large laser system with many hundreds of flashlamps, it is necessary to provide a diagnostic tool that determines the condition of the lamps prior to and following a system shot. The Pulsed Ionized Lamp Check (PILC) circuit fills this need as well as providing a reliable pre-ionizing pulse for the lamps in advance of the main trigger.[34] One method of providing this diagnostic is to pulse the lamps with an energy that is 10 to 15 % of the main pulse. This is sufficient energy to ionize the lamps. Diagnostics can then examine the current and voltage waveforms, compare them with the established norm and flag the lamp for examination and replacement. Although this will not intercept 100% of lamp failures, it will intercept a good number of them.

## Flashlamp Triggering

Lamp triggering is accomplished by allowing the cable feeding the lamps to ring up and cause an arc between the trigger electrode and the grounded reflector. Figure 38 shows a series pair of lamps connected to the bank module with a coaxial cable. When the **P**ulsed **I**onized **L**amp **C**heck (PILC) circuit is triggered, a transient of approximately 40 to 50 kV occurs at the lamp. This is because the cable is not terminated in its characteristic impedance and voltage doubling takes place. This transient voltage divides between the two series capacitances that exist from the trigger electrode to the lamp wall and the lamp wall to the reflector. The essential circuit diagram is shown in Figure 39.
The PILC and lamp trigger module as installed on NIF is shown in Figure 40, and the voltage and current waveforms are shown in Figure 41.[35]

[34] American Control Engineering, "Preliminary Pre-ionization Circuit Notes," LLNL Subcontract B313903, Sept. 20, 1996.
[35] American Control Engineering, "Trigger Latitude Testing of NIF Production Flashlamps," April 6, 2000, LLNL Subcontract B348073.

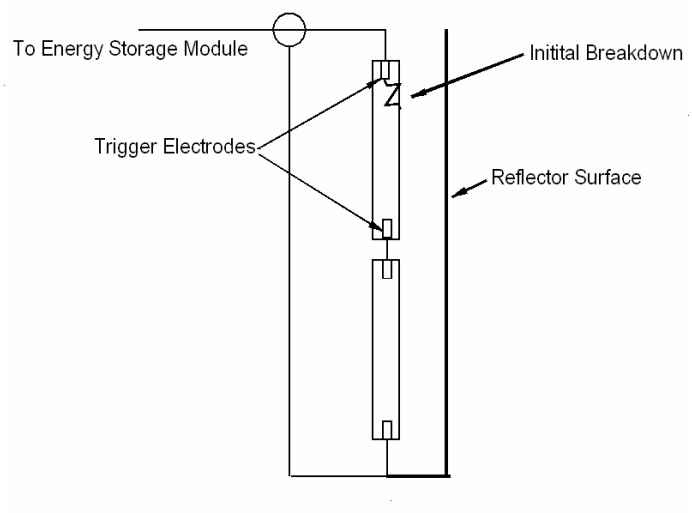


Figure 38. Initial breakdown of the lamps is caused by the transient ring-up of the coaxial cable. This is in the range of 50 kV. There is a capacitive voltage division between the trigger electrode, lamp wall and the reflector. An arc is then established along the wall of the lamp and then grows to fill the entire volume.

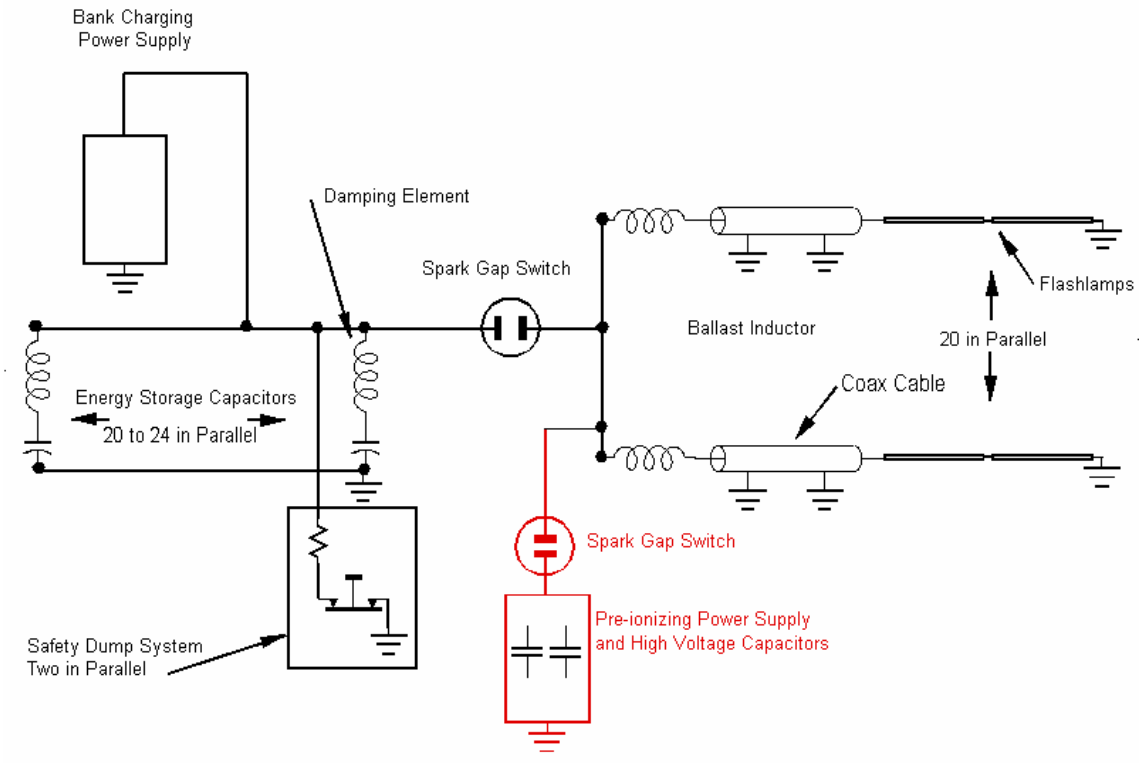


Figure 39. The flashlamp trigger pulsed ionized lamp circuit (PILC). This circuit is both a flashlamp diagnostic and trigger.

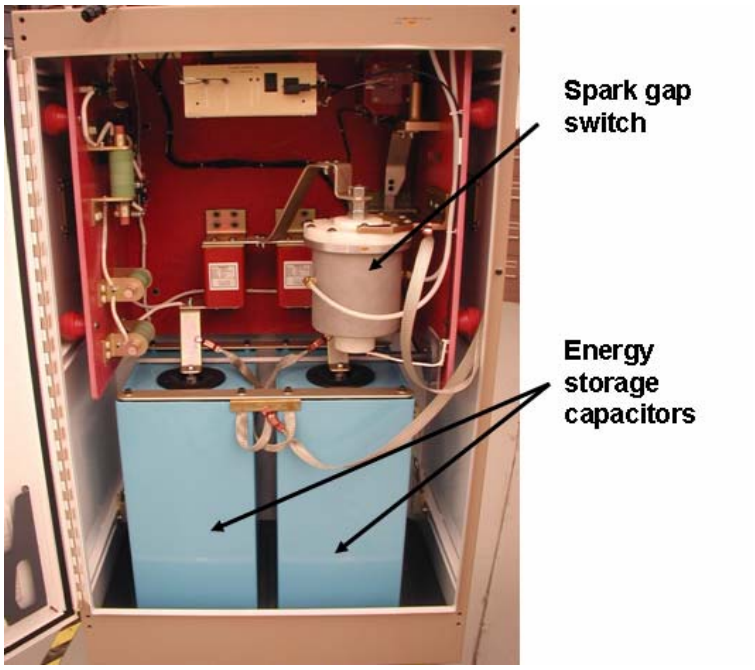


Figure 40. The Pulsed Ionized Lamp Check (PILC) and flashlamp trigger circuit for NIF. The capacitors are charged to 26 kV and switched with a spark gap.

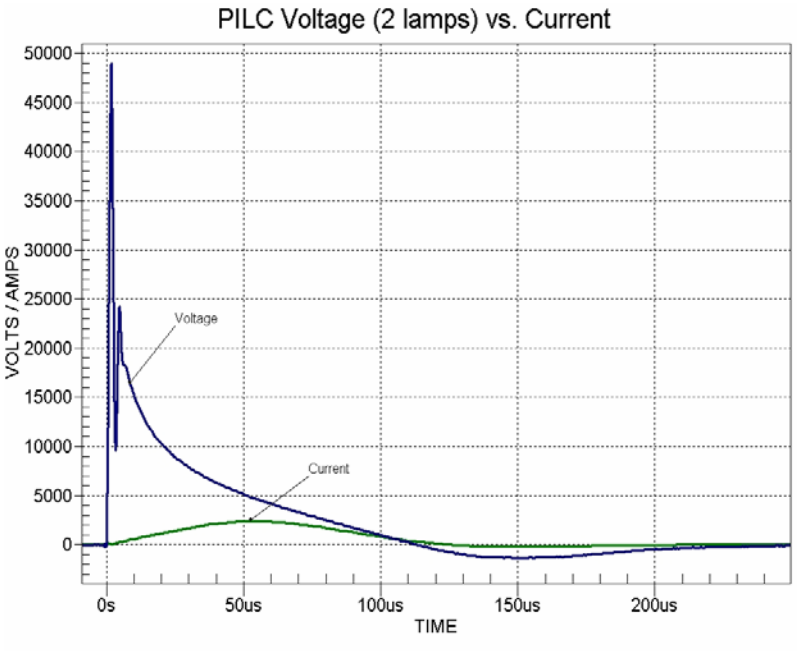


Figure 41. Transient voltage waveform at the flashlamps due to cable ringing following the PILC trigger. This circuit ionizes the flashlamps a few hundred microseconds before the main pulse. The initial voltage transient is in the range of 50 kV and causes the initial breakdown within the lamps. It is used as a diagnostic to detect lamp failures.

As shown in the voltage waveform in Figure 41, the initial peak of the voltage is close to 50 kV and this is sufficient to ionize the lamps. Figure 41 shows both the voltage and current waveforms. A few hundred microseconds following the pre-ionization pulse, the main switch is fired discharging the capacitors into the lamps.

# CHAPTER 7

## FAULTS AND FAULT MITIGATION

Generally leading edge technical professionals prefer to present papers and talks dealing with the results of successful designs. However, a great deal more can be learned from the analyses of failures. For this reason, a number of faults encountered during the development and testing of the National Ignition Facility pulsed power system are included in the following sections.

In spite of the best planning and design, there will be, on occasion, faults in a very large pulsed power system. Generally, these are the result of components such as flashlamps or capacitors failing. Faults of this type can and will be very energetic resulting in arcs and over-pressure in high-voltage modules. In addition, very energetic faults will cause debris to be created and accelerated away from the fault site. It is important to understand the potential physical damage and personnel hazards these types of faults can produce.

Experience has shown that large systems are particularly prone to failure when operating outside of the "normal" mode. This can occur because

1. Components are stressed beyond their design limits.
2. The built-in limiting actions in the control system are not designed to intercept this particular failure mode.
3. The operations personnel fail to recognize a problem because it is outside the normal operating mode.

Another situation in which faults are likely to occur is after modifications have been made to the system. These can take the form of an upgrade of a component or a reconfiguration of the existing system. When it is necessary to make such changes, it is best to review them very carefully and, in some cases, institute "off-line" testing to ensure failures are not introduced into the system.

One important factor in the overall design of the system is to anticipate and identify the fault modes.[36] Having identified these, one can build into the design approaches that either eliminate the cause of the fault or mitigate the effects.

In the design of the National Ignition Facility energy storage module, it was recognized that having on the order of 1.6 MJ tied to a common bus could result in very energetic faults. To mitigate the effects of high-energy faults, the design included a specially designed inductor in series with each capacitor. These are called "damping elements" or "damping inductors" and are shown in the schematic in Figure 42.

[36] Mark A Newton, LLNL, and William Gagnon, Brookings Engineering, NIF Amplifier Power Conditioning System Hazard Analysis and Safety Implementation Plan, UCRL-MA-150514, Oct. 2002.

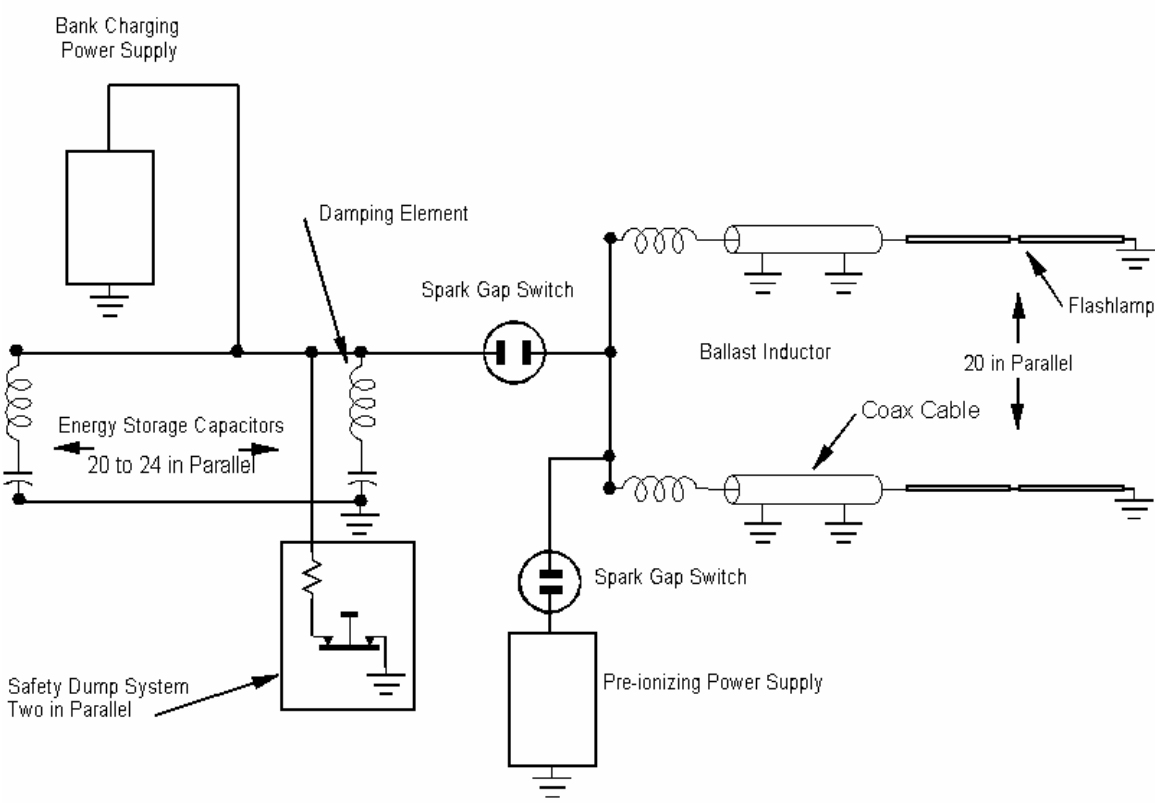


Figure 42. Shown is the circuit diagram of the energy storage module for the National Ignition Facility. Damping inductors attached to each capacitor limit the rate of rise and the magnitude of fault currents.

To illustrate these issues, some examples of faults that were uncovered during the prototype development of the National Ignition Facility modules and the steps taken to either eliminate them or mitigate their effects are included in the following sections.

## Fault Examples

### Dump Resistor Fault

The original prototype contained redundant "dump" resistors (see Safety Dump System in the above figure). The function of these is to discharge the capacitors and insure the safety of personnel who enter the module for troubleshooting and repairs. Each dump assembly consisted of a single resistor sized to absorb the full module energy. There is, in addition, a ground hook and diagnostics to ensure the bank is grounded and safe. During prototype testing, one dump resistor shorted end to end. This essentially shorted the capacitor bank to ground and produced a very high-energy fault inside the module.

Figures 43 and 44 show examples of damage resulting from a fault in this unit. As shown, there was extensive damage to the inside of the module. In addition, as a result of the internal arc, a large over-pressure was created inside the module, which then caused the doors to be blown off.

Figure 43. Damage resulting from a fault in a dump resistor. This occurred in an early prototype module.

Figure 44. Damage from the prototype fault. The arc caused an over-pressure condition inside the module which then blew off the doors. Later designs included an over-pressure vent in the module enclosure.

Following an analysis of these events, it was clear that the design had to be improved. Several changes were made. First, the dump resistor assembly was modified to include two resistors in series. Each resistor is capable of absorbing the full module energy.

In addition, the second dump resistor assembly was relocated. One assembly is located at the top and the second at the bottom of the module, minimizing the possibility of fratricide. The top resistor is shown in Figure 45.

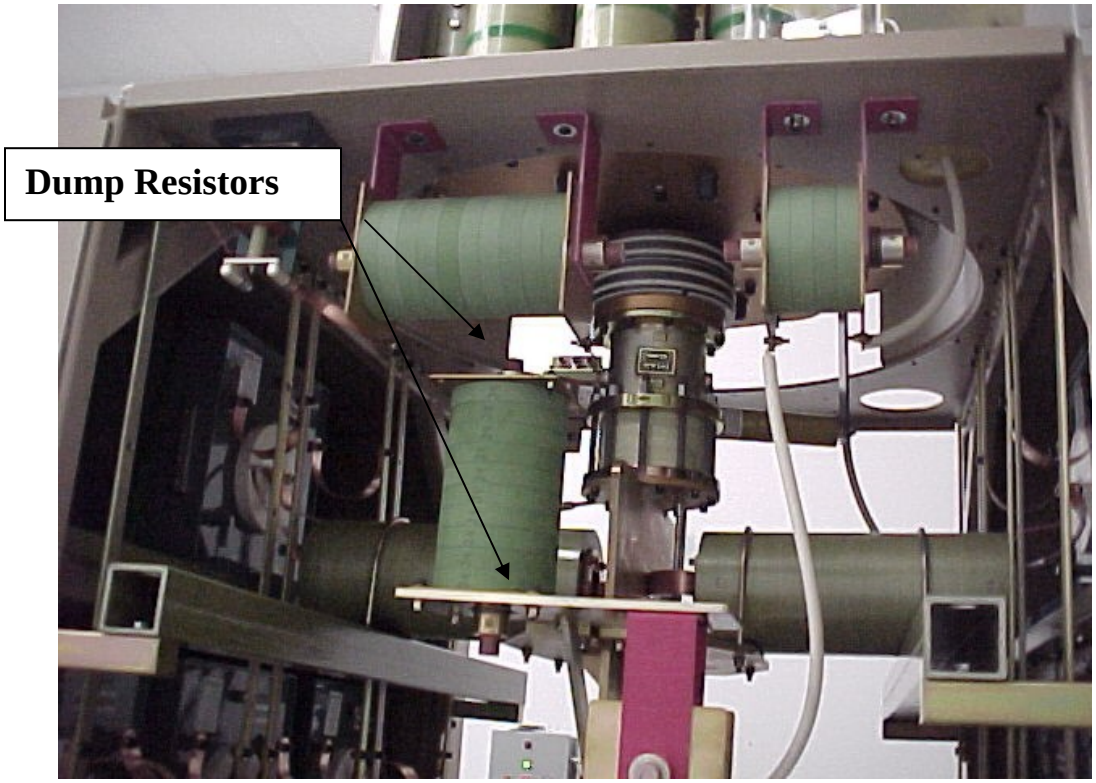


Figure 45. The module was redesigned to include two dump resistor assemblies. Each has two resistors capable of absorbing the full module energy. The top resistors are shown.

To avoid an over-pressure situation inside the module, the enclosure was modified to include vents[37] and shrapnel traps.[38] These are shown in Figure 46.

Using "ray-tracing codes" the module enclosure, vents and shrapnel traps were designed to contain any shrapnel that could be generated during an internal failure. To provide an extra layer of safety, it was decided to line the capacitor bays walls with 1-1/4-inch plywood that could prevent any shrapnel from escaping the capacitor bay.

[37] Russel Greenlaw, Revised Draft Report, Jan. 2001, Lawrence Livermore National Laboratory Structural and Applied Mechanics Group.
[38] Sandra Brereton et al., LLNL Mechanical Engineering Safety Note MESN99-066-0A. "Analysis and Control of Hazards Associated with NIF Capacitor Module Events," Sept. 1999.


Figure 46. As a result of a prototype fault, an over-pressure condition was produced inside the module. Subsequently, the door was redesigned to include vents and shrapnel traps. These are shown above.

**Flashlamp Fault Example**

Flashlamp failures are potentially destructive because the most likely failure is an explosion followed by an arc to the reflector. If not limited, fault currents can approach 100 kA. Should this occur, there is a possibility of breaking the shield glass (between the lamps and the laser glass) and damaging the laser glass. An example of this failure from an early prototype amplifier is shown in Figure 47.

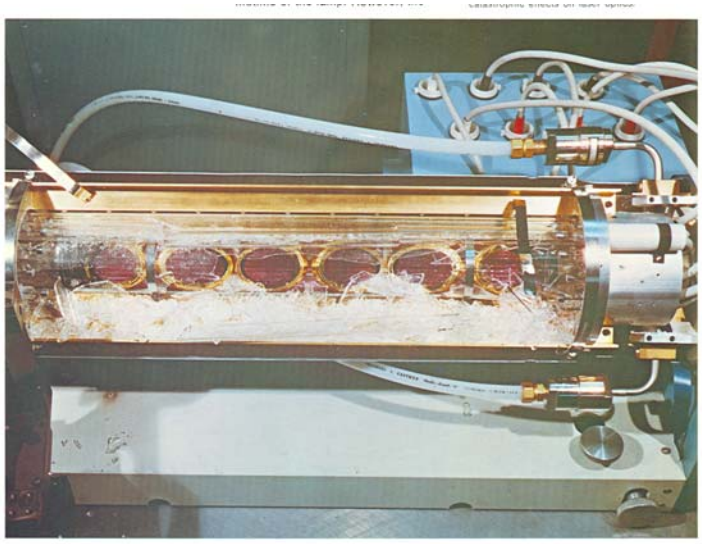

Figure 47. An exploding flashlamp will cause severe damage in a laser amplifier if the fault current is not limited. Shown above is a failure example from an early LLNL amplifier.

To develop a method of limiting this damage, tests were carried out at American Control Engineering in San Diego, California. In these tests, flashlamps were installed in a test fixture and covered with a blast shield equivalent to that used in the laser amplifiers. Figure 48 shows the result of a lamp explosion with no limits on the fault current. The damage is extreme.

*American Control Engineering " Flashlamp Explosion Tests"*

Figure 48. Damage caused by flashlamp explosion with no limits on the fault current. In this test, the shield glass was shattered. This would have badly damaged the disks in a laser amplifier.

This failure mode was mitigated by inserting a resistor between the reflector and ground. This limits the fault current to an acceptable value and prevents major damage to the laser disks. A second test was carried out after inserting a current limiting resistor in the return path from the reflector to ground. This is shown in Figure 49. The damage is minimal.

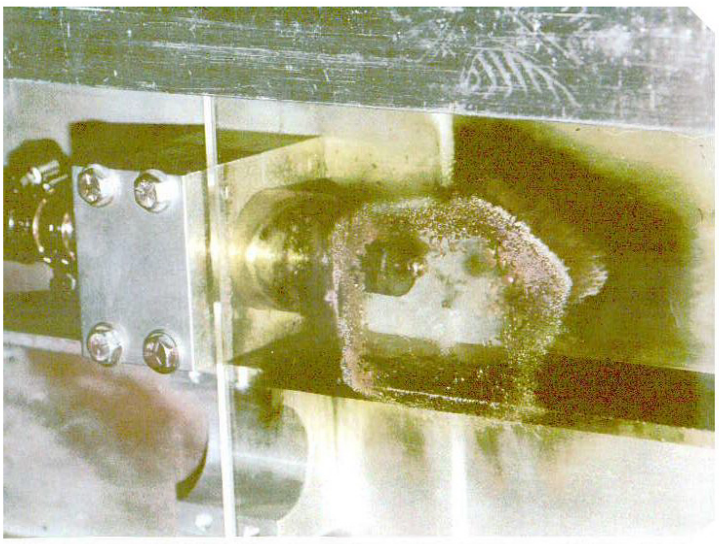

Figure 49. A second flashlamp fault test. A current limiting resistor was inserted into the ground return path. The shield glass is damaged, but not broken.

An example of this limiting circuit is shown in Figure 50.

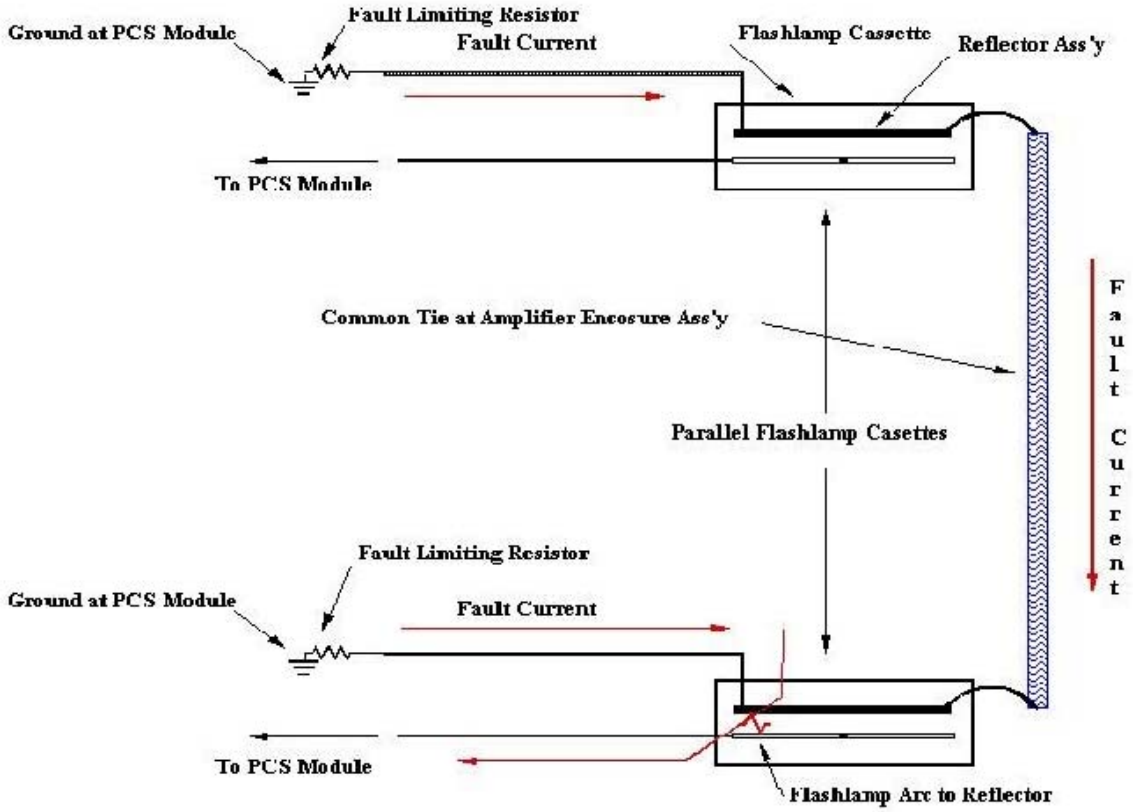


Figure 50. An example of a fault-limiting circuit for flashlamp faults. If the lamps arcs to the reflector, the current is returned to ground through a limiting resistor.

## Tool Fault

During the design of the National Ignition Facility Laser, a prototype energy storage module was constructed and run for many thousands of shots. This was done so that the module could be life tested, and new components tested at full voltage and current. During the testing of this prototype unit, it was necessary to carry tools into the test module to implement repairs or replace components. On one such occasion, a socket wrench handle was accidentally left behind in the module. The location of the tool in the module is shown in Figure 51. It was left, as shown, in the support strut for damping inductor number 13. This caused a high-energy fault, and the image was captured on the monitor system. This is shown in Figure 52. According to the incident notes, "The

failure[39] occurred in the following manner: on damping element 13, a dowel pin which penetrates the outer sleeve (one of four which retains the coil terminal inside the outer sleeve) arced to the u-bolt used to clamp the damping element to the support tube, the u-bolt arced to the wrench handle inside the tube, which in turn arced to the bolt connected to the unistrut support. This shorted the Module high voltage bus to ground through damping element 13, at the same time capacitor 13 is shorted directly to ground."

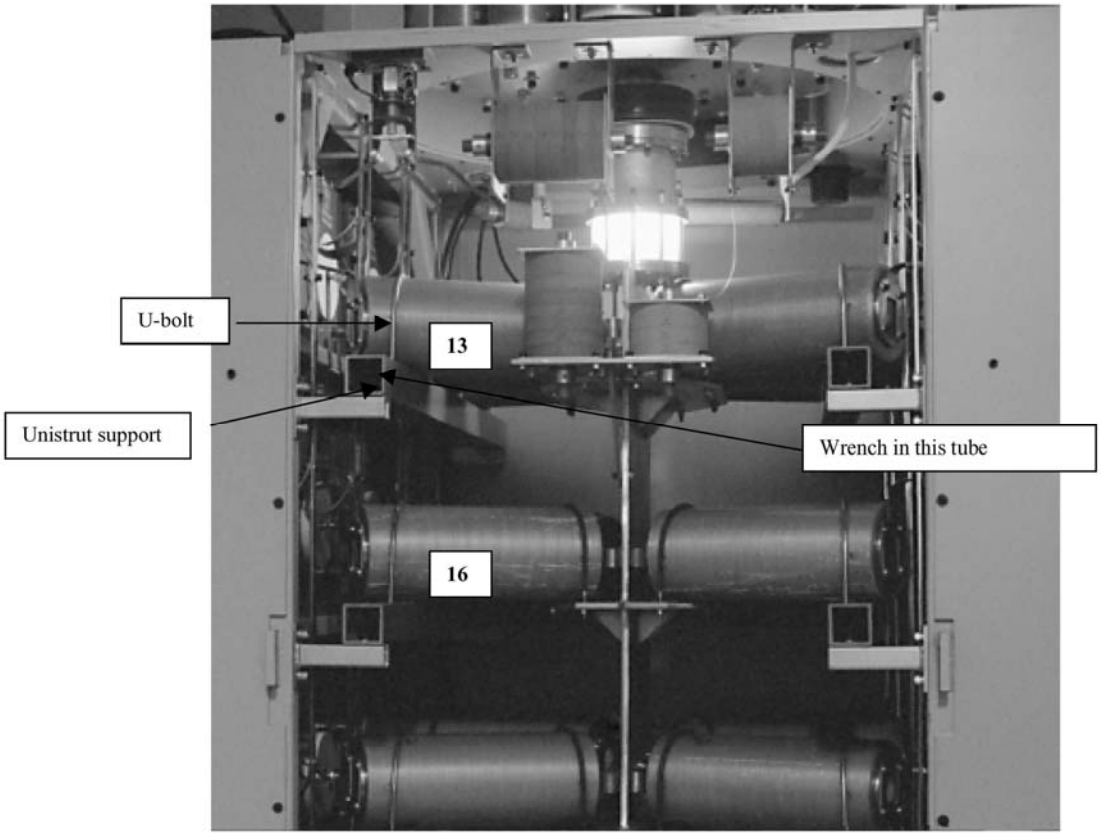


Figure 51. Location of the wrench that caused a fault in the prototype test module.

[39] William B. Moore, "Wrench Incident In the Prototype Module Test Facility," Internal Note, NIF Power Conditioning (SNL).

Figure 52. Arcs caused by a socket wrench accidentally left inside the prototype test module.

Figure 53 shows the simulated currents in the damping element and capacitor involved in the fault. This is shown in order to point out how energetic these kinds of faults can be.

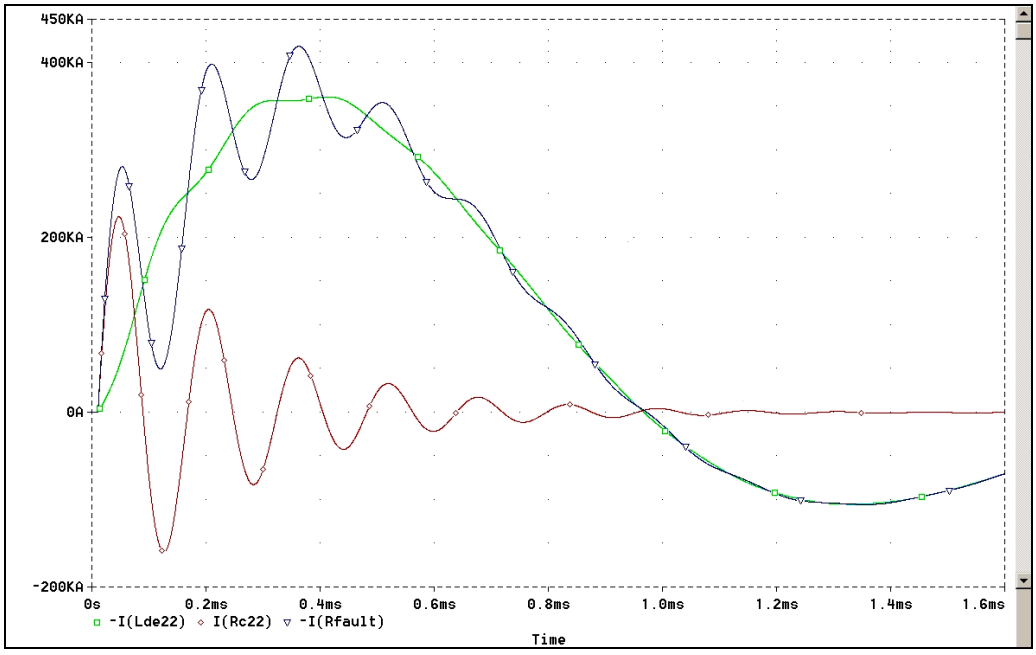


Figure 53. Simulated current waveforms for the wrench fault. Note that the magnitude of the fault currents exceed 400 kA.

# CHAPTER 8

# COMPONENT DEVELOPMENT

"The path from small to larger and larger solid-state lasers hinges upon developing components which can safely handle higher energy levels. This includes both optical and electrical energy. On the one hand, bigger components address the problems of too many parts and the associated costs and the risk of higher failure rates. On the other hand, larger components handling higher power and energies, while less expensive per joule, can produce highly energetic failures. The impact of such failures results in increased safety risk, system downtime, expense and aborted experiments," said John Emmett, Lawrence Livermore National Laboratory Associate Director from 1975–1989.[40]
The absolute worst time to do component testing is after the laser has begun operation. Failures at this stage are extremely destructive and difficult to sort out in the midst of tight schedules and limited maintenance windows.

These risks can be minimized by well thought out design, detailed component specifications and extensive testing. This testing should be carried out well in advance of construction, and continue as long as it takes to refine the design and verify the lifetime of all the components in the pulsed power system. In the case of the National Ignition Facility, numerous test facilities were constructed and operated for several years. The testing included energy storage capacitors, flashlamps, inductors, switches and complete energy storage modules.

Since such failures almost inevitably have their origin in a component failure that in turn led to the system failure, *testing of that component under appropriate conditions* would obviously have been highly advisable. But since a full-up system consists of many components, themselves integrated within subsystems, thinking through a cost effective test program requires a deep understanding of how each component functions and how components influence each other as the level of system integration increases. Such planning should seek to identify the most critical failure modes that subsequently require the most attention. A huge amount of literature on reliability engineering in general and on testing in particular has been generated, mostly very specific to a given technical specialty, and often found in conference proceedings.

Some examples of component development and testing are included in the following sections.

## Energy Storage Capacitors

In the early days of solid-state laser development, the then best available capacitor technology was used. This took the form of units that stored 3 kJ at approximately 20 kV and cost approximately 58 cents/joule in today's dollars. As systems increased in

[40] John Emmett, July 2006. Note to Bill Gagnon.

size and energy, a joint development effort was undertaken with vendors to increase the energy storage density, reduce cost and tailor the lifetime and reliability to the specific needs of the solid-state lasers. Beginning in the 1970's and extending to the present, vendors have developed energy storage capacitors with much higher energy density, lower cost per joule, and reliability specifically tailored to the operating life of the lasers.

The first of these innovations was a 29 $\mu Fd$ capacitor that stored approximately 5.8 kJ at 20 kV. This was accomplished by allowing the dielectric stress to rise from 2100 volts/mil[41] to 2600 volts/mil. However, the life of an energy storage capacitor is a function of dielectric stress, voltage reversal and ringing frequency. Taking all of this into consideration, it was estimated that the 14.5- $\mu Fd$ capacitor would have a mean life of $10^6$ pulses when used in solid-state laser applications, and the 29 $\mu Fd$ could be expected to operate for $.3\times10^6$ pulses. Intensive testing of these units showed this to be true.

This was well within the bounds of the expected operating life of the facility. An example of this design is shown in Figure 54. As shown, metal foil is sandwiched between dielectric impregnated kraft paper and the top and bottom of the bundles are swaged to make connections.

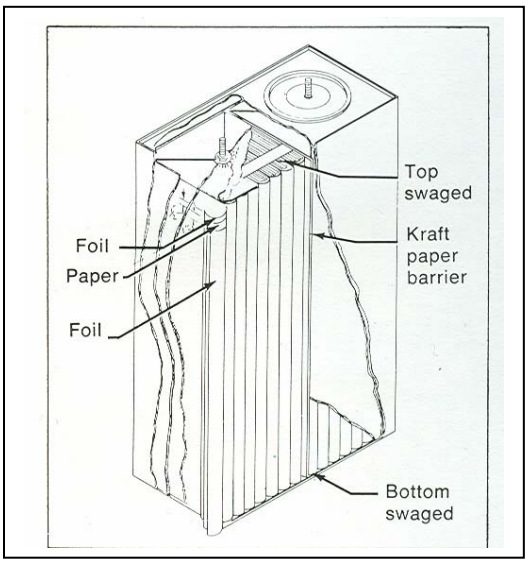


Figure 54. A view of the 3-kJ, 20-kV capacitor used in the laser program in the early 1970s. These used foil separated by kraft paper impregnated with a dielectric.

In the late 1990s, the National Ignition Facility was able to take advantage of an advanced concept in energy storage capacitor design. In this design, a thin metalized layer is deposited on the surface of the dielectric. This has several very important advantages.

- The energy density is much higher
- The cost is much lower

[41] mil = 1/1000 inch.

- The failure mode is most generally non-catastrophic because the failure occurs gradually by arcing away small sections of the metalized layer. This will reduce the value of the capacitance, but will generally not produce an explosive failure.

These units as used in the National Ignition Facility are rated at 290 $\mu Fd$ at 24 kV and store 83.5 kJ. Because of the proprietary nature of the design, details of the interior can't be shown. Pictures of the completed units are shown in Figure 55.

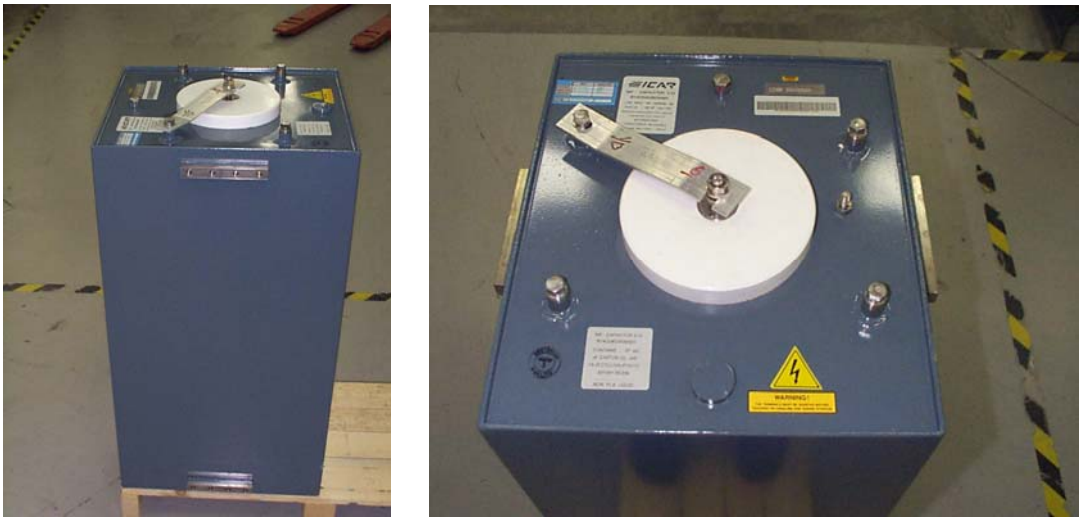

Figure 55. Shown are two views of the 290-$\mu Fd$ capacitors used in the National Ignition Facility. Two vendors, ICAR and Sorrento, supplied the units.

A summary of the improvements in energy storage, cost and estimated lifetime is shown in Figure 56. Note that nothing is for free: the improvement in energy storage per unit, hence, Cost/Joule, comes at the expense of lifetime. Consequently, it is important to understand the lifetime requirements of the laser. It is less cost effective to build a system with a lifetime much longer than the projected shot life of the laser. The maximum cost efficiency for this component is reached when the tradeoff between lower Cost/Joule versus life time has reached the lifetime specifications of the laser system as a whole.

| **Capacitance** | **Stored Energy** | **Cost / Joule Cents (2006)** | **Estimated Lifetime Pulses** |
|---|---|---|---|
| **15 $\mu Fd$ Shiva** | **3 kJ @20 kV** | **58** | $10^6$ |
| **29 $\mu Fd$ Nova** | **5.8 kJ @20 kV** | **13** | $.3\times10^6$ |
| **290 $\mu Fd$ NIF** | **85.5 kJ @24kV** | **4.9** | **30,000** |

Figure 56. Results of vendor development of energy storage capacitors from the 1970s to the present. The stored energy is higher, the cost lower and the lifetime tailored to meet the specific requirements of the lasers.

**Testing of Energy Storage Capacitors**

The capacitors used in the National Ignition Facility are metalized film capacitors, developed by vendors to meet a particular specification. These capacitors are actually a series and parallel network of hundreds of smaller individual capacitor windings. They are nominally 290 μF and can store up to 85 kJ at their nominal operating voltage of 24 kV. There are numerous possible failure modes internal to this design, but they usually manifest themselves as either a shorted capacitor or a capacitor that has lost capacitance, i.e., sections are open circuit.

The capacitors can short internally due to a failed insulator or possibly dielectric winding breakdown. The insulator breakdown can occur across the inner surface of the high-voltage terminal insulator. This breakdown may be caused by impurities in the impregnation oil, air bubbles in the oil or over-voltage of the capacitor. Shorts may also occur due to catastrophic failure of a section of dielectric windings. While possible, this scenario is unlikely due to the "self-healing" nature of this capacitor design.

Sections, ranging in size from a single winding to all of the windings, may become disconnected due to failures of interconnections between winding, resulting in sections loosing capacitance. Each winding is connected to the other windings by soldering a conductor onto the end of the windings, which has been sprayed with an Al or AlZn end spray. The bonding between the end spray and the winding may fail due to over current, excessive mechanical stress on the end spray connection, such as may occur during shipping, or incorrect manufacturing processes. Quality control is crucial.

The development occurred over several years with extensive testing. During early phases, many capacitor failures were experienced both during individual capacitor testing and during module testing. The following is a summary of efforts in developing high-energy-density capacitors and the relationship of this effort to the production capacitors that are used on the National Ignition Facility.

**Pre-Production Capacitors**

- There were six capacitor failures on the "First Article NIF Test Module" at Sandia National Laboratory in New Mexico.
- All capacitors used in the original prototype were pre-qualification units.
- One of the vendors supplying capacitors for this prototype was eliminated from the bid list because of failures during qualification testing.

**Qualification Capacitors**

- Qualification tests were conducted to "qualify" capacitor designs and manufacturing processes.
- Extensive testing was performed on units from four vendors to qualify each vendor to be on the bid list ---- 17 units were tested for a minimum of 25,000 shots each.
- Total qualification shots on production units --- 1,500,000 shots with zero failures.

**Production Capacitors**

- 100% of production capacitors are tested for 500 shots before acceptance.

- One capacitor in every 1 - 2 shipments is life tested (.5% sample).
- Acceptance testing to date (January 2002) -- 157,000 shots with zero failures.

Analysis of the qualification test data indicates that the mean time to failure, averaged over the life of the facility, would be on the order of 35,000 shots. This is believed to be a very conservative number based on life test data. The sample of capacitors that have been tested have individual life times in excess of 65,000 – 100,000 shots. The extrapolation of this test data to the National Ignition Facility is shown in Figure 57. As seen in the figure, most of the failures are predicted to occur in the later years of operation.

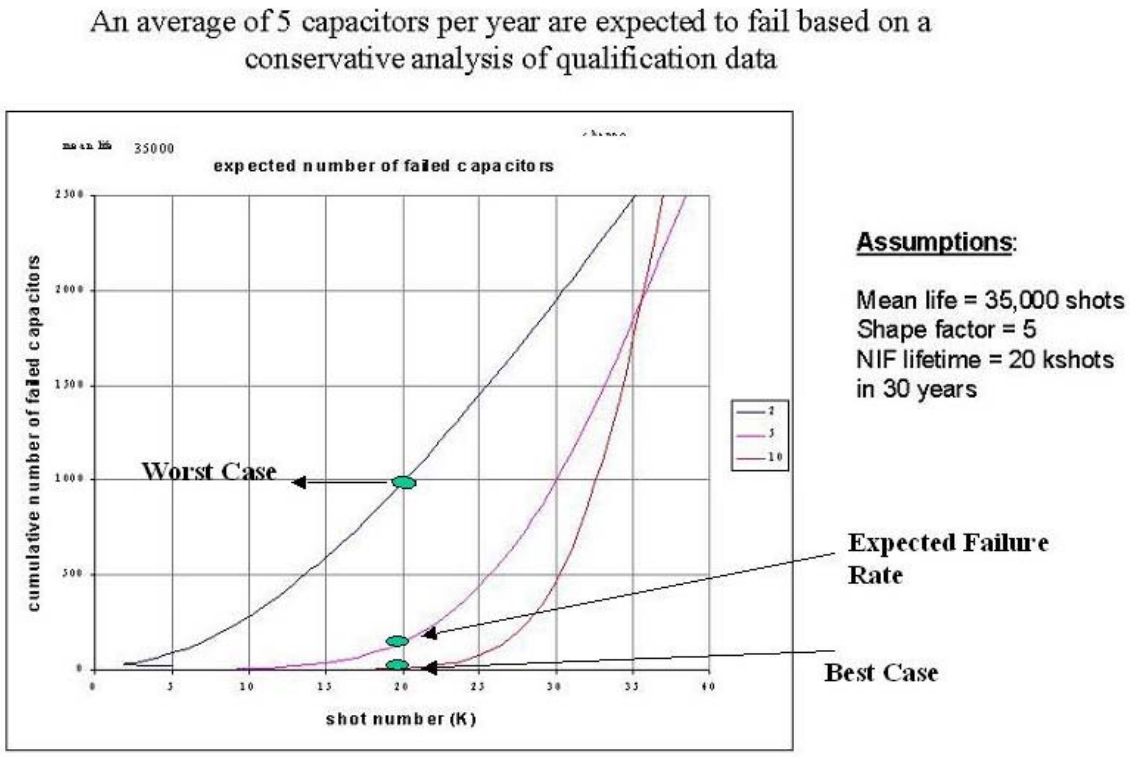


Figure 57. Results of lifetime testing of the National Ignition Facility energy storage capacitors.

As mentioned above, component testing should not only occur before the purchase of large number of components, but should continue through the construction phase and perhaps beyond. It is obvious that an "off-line" facility is the most efficient way to sort out and identify component reliability problems. In the case of the National Ignition Facility, a prototype of the energy storage module (one of the 192 units powering NIF) was set up in a separate test laboratory. The original facility was first located at Sandia National Laboratory. Following extensive prototype testing at SNL, the module design was modified, built and tested at the Livermore National Laboratory. During many thousands of test shots numerous problems were uncovered and corrected. This facility with some of the crew of engineers and technicians responsible for it is shown in Figure 58, and the flashlamp cassette load is shown in Figure 59.

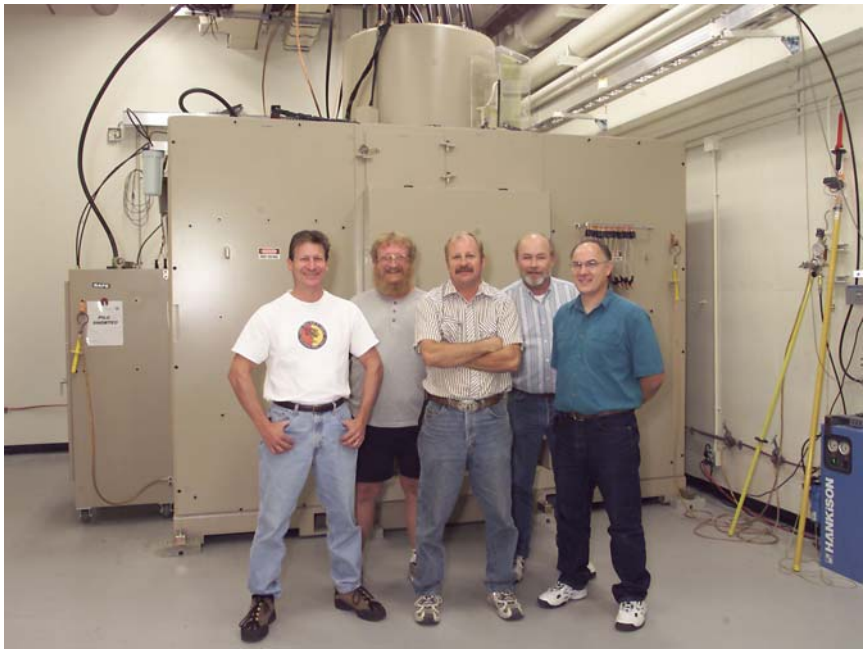


Figure 58. The National Ignition Test Facility for the energy storage module and the team responsible for operating it. From left to right, Dave Pendleton (LLNL), Gary Ullery (LLNL), Scott Hulsey (LLNL), Bill Moore (Sandia National Laboratory) and Dave Petersen (LLNL). Not shown is Steve Fulkerson (LLNL).

Figure 59. Flashlamp Cassette load for the Test Facility.

**Development and Testing of Fault Limiting Inductors (Damping Element)**

One of the disadvantages of lumping large amounts of energy into a single module is that faults will be very energetic. As an example, consider the circuit model shown in Figure 60, the energy storage module for the National Ignition Facility. As shown, there are 24 capacitors in parallel charged to 24 kV.

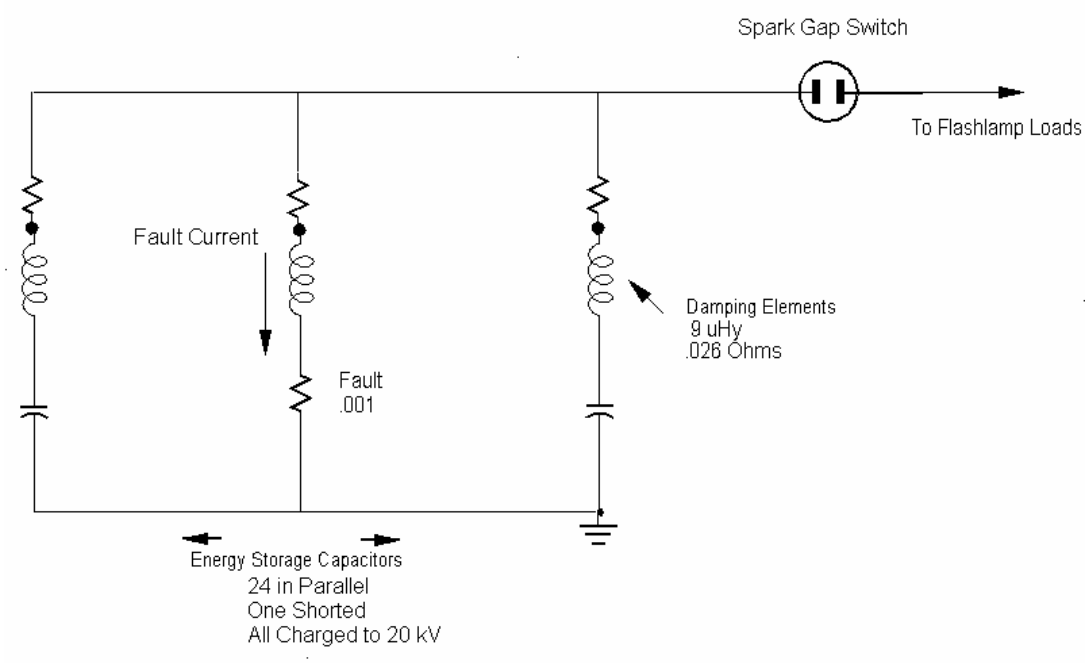


Figure 60. An equivalent circuit demonstrating a worst case hard fault in an energy storage module. It is assumed the capacitors are charged and main switch has not yet fired. A bushing to ground fault occurs in one capacitor. The damping inductor limits the fault current, and must be replaced following the fault.

Assume one of the capacitors develops a hard short to ground. An example would be an arc to ground across the bushing insulator. To mitigate this fault, each capacitor has in series with it a damping inductor. The damping inductors are designed to limit this fault current without disassembling.[42] A simulation of this fault is shown in Figure 61. As shown, the peak current is in the order of 400,000 Amps. A failure of the damping element or ballast inductor would be catastrophic and cause damage to many of the internal components of the module. Figures 62 and 63 show examples of a ballast inductor failure.

An effort was undertaken to improve the design and construction of both inductors so that it could survive faults of this nature and not disassemble.

[42] American Control Engineering, "Capacitor Fault Damping Element Status," LLNL Subcontract B313903, Oct, 1996.

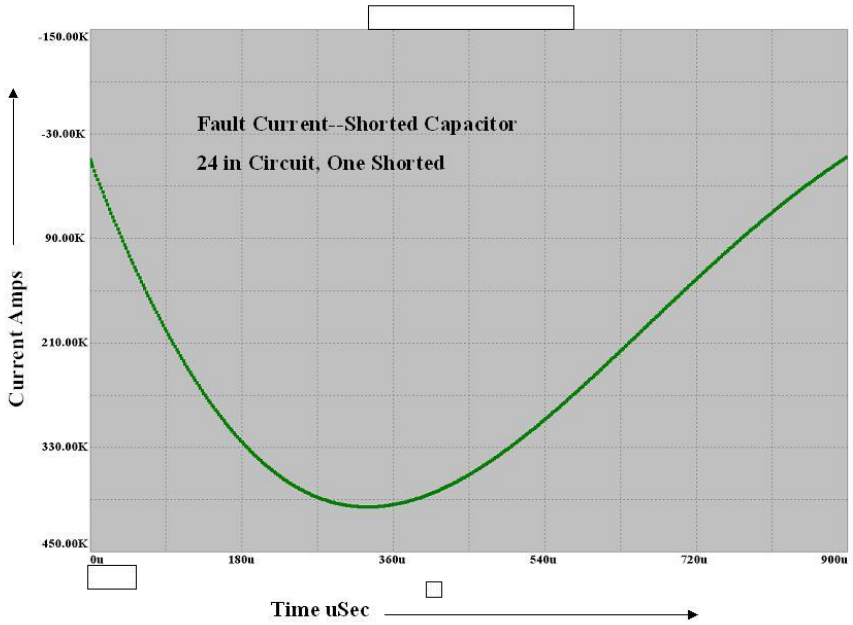


Figure 61. A simulation of the capacitor fault shown in Figure 60. The peak current through the damping inductor is in the order of 400,000 Amps.

Figure 62. Example of a failure of an early design of a ballast inductor. The fault current caused the inductor to disassemble and create high velocity debris inside the energy storage module. Some of the collected pieces are shown.

Figure 63. Damage to the interior of the energy storage module as a result of a ballast inductor failure. The ballast inductor failed, and shrapnel was distributed over the interior of the module.

Following failures in the prototype module and off-line testing, a concerted effort was made to improve both inductor designs. This work was carried out at American Control Engineering in San Diego.[43]

As an example, the improved design of the damping element involved the following; (see Figure 65)

- Metal sleeves were welded to the ends of the coil.
- Pins at each end of the coil were used to lock the end sleeves to the outer shell.
- Threaded fiberglass rods were placed inside the stainless steel coil winding to maintain the length of the coil.

Pinning ensures that the metal sleeves won't come out of the coil under fault current conditions. The threaded fiberglass rods inside the coil winding ensure that the change in the length of the coil is minimal during a fault. Fiberglass spacers were added between coil turns in order to avoid turn-to-turn shorts. The threaded fiberglass rods are shown in Figure 64 and 65.

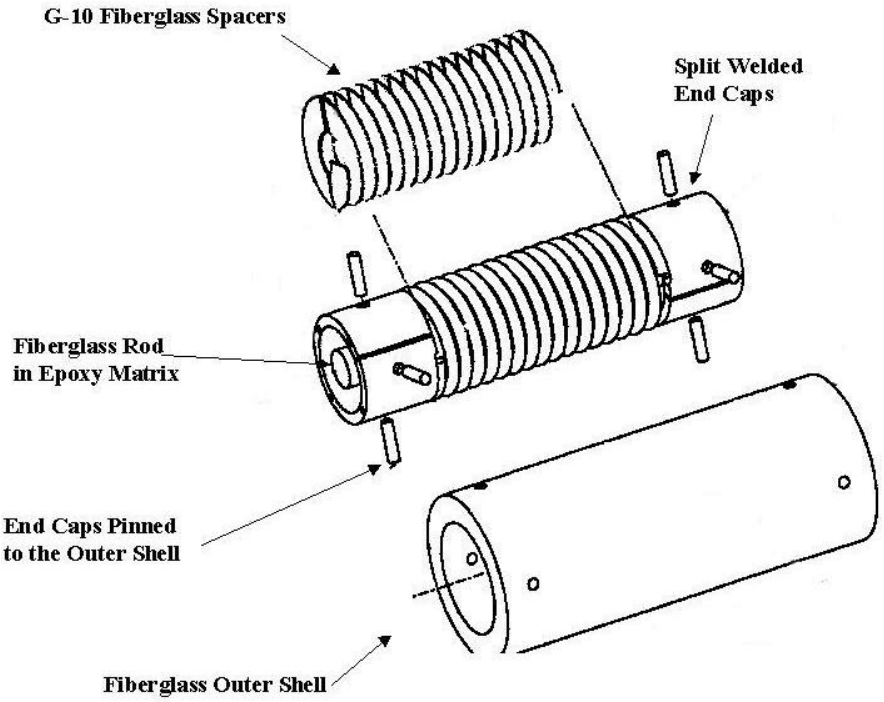


Figure 64. The essential elements of the improved damping inductor are shown. End caps were welded to the coil and pinned to the outer shell. G-10 fiberglass spacers were inserted between turns and fiberglass rods were added to the center of the coil.

[43] American Control Engineering, "Damping Element Tests of Split Sleeve Design," Feb. 3, 1999.

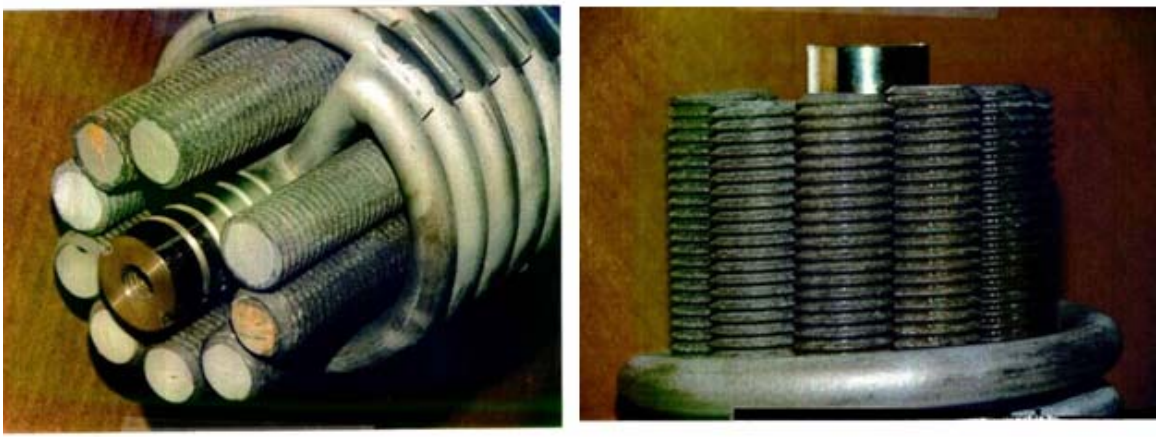

Figure 65. Threaded fiberglass rods are added to the center of the coil before epoxy encapsulation. These act to maintain the length of the coil in a fault situation even though the mechanical integrity of the outer sleeve may be significantly damaged, see Figure 66.

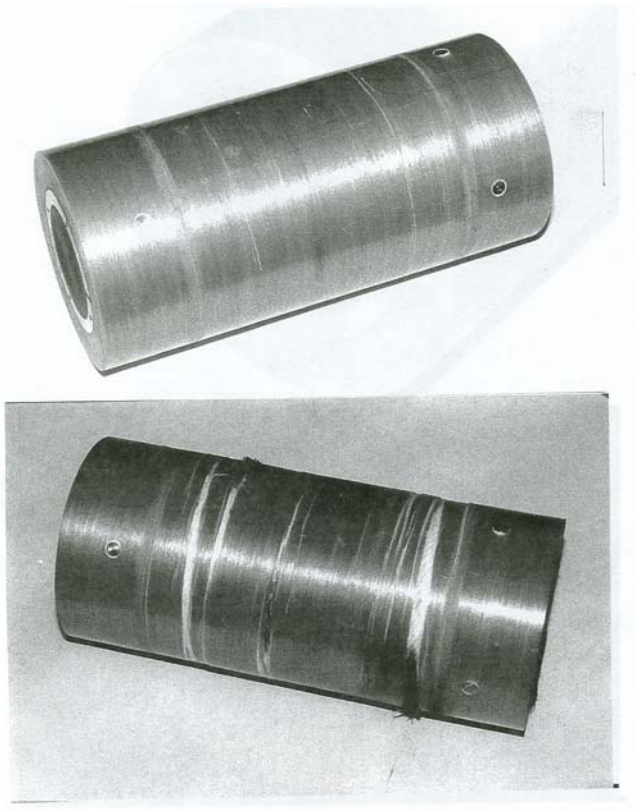

Figure 66. The modified damping before (top) and after (bottom) fault tests in excess of 400 kA. The coil is visibly damaged but holds together at this fault current level. Following this fault current in the system, the inductor would be replaced.

The description of these examples are intended to impart on the reader the level of understanding, testing, re-design, and re-testing and optimizing that is realistically required to create a genuinely reliable component for a large system. Since the data gathered are inevitably statistical, failures will occur nevertheless. However, they will now occur at a rate that is understood to be sufficiently low so that it can be accommodated by scheduled down times, and the failure will be sufficiently contained such that it is not a safety issue.

Clearly, to go through each component and subsystem contained in a pulsed power system of a large laser would turn this book on pulsed power design fundamentals into a book on pulsed power testing. We therefore refer the reader who wants to go deeper to start with the references listed at the end.

# CHAPTER 9

## SYSTEM GROUNDING OVERVIEW

Grounding of large laser systems is a critical part of the overall engineering design. If not carried out thoughtfully and correctly, it is likely that serious safety and operational issues will result. The normal grounding practices for industrial buildings are a base from which to begin, but they do not take into account the unique problems associated with very large pulsed power systems.

There is no single approach that works for all systems because each has different requirements. However, the fundamental considerations are common to all large systems of this type.

Glass laser systems such as the National Ignition Facility are, by necessity, very large and extend over a considerable physical area. There are numerous interfaces with control, diagnostic, utility and other supporting subsystems. Each of these interfaces represents a potential path for fault currents and/or high frequency "noise". The isolation of these subsystems from the pulsed power components is essential. This is true for normal operation of the system, but especially relevant in the event of a fault in the pulsed power system.

There are three major considerations driving the design. These are:

- Personnel Safety
- Effects of Noise and Transients
- Fault Isolation

Fault isolation is discussed in later sections.

**Personnel safety**

This is first and foremost. The hazards associated with multi-megajoule high-voltage capacitor banks are extreme and potentially lethal. It should be understood at the outset that the primary consideration is to avoid placing anyone in a hazardous situation.

Generally, a multi-tiered approach is taken:

- Design the system such that during both normal operation and fault conditions, hazardous situations are avoided, and in situations where faults cannot be avoided (for instance a capacitor short) the hazardous effects are mitigated.
- Give special attention to developing procedures for unexpected faults, as they are often difficult to plan for.
- Isolate and control access to areas of potential hazards with both fixed and interlocked barriers.

**Noise Reduction and Isolation**

When the capacitor banks are discharged into the flashlamps, peak power levels are extremely high. Consider, for example, the National Ignition Facility. There are 192 energy storage modules each storing 2.2 MJ and discharged in approximately 500 μsec. When this energy is delivered to the flashlamps, the peak power level is approximately:

$$192 \cdot 2.2 \cdot 10^6 \text{ Joules} / 500 \text{ μsec} = .85 \text{ Terrawatts}$$

This is about 100 to 1000 times the peak power in a lightning bolt with a time scale of roughly the same duration. As a result, energetic high-frequency transients are generated.[44] These can be either directly radiated or appear as the result of displacement currents. Transient-induced noise is especially significant factor because while the pulsed power system is delivering hundreds of megajoules to the flashlamps, the control, diagnostic and target systems are attempting to resolve a few hundred microvolts of signal.

**Building Grounding**

Ideally the pulsed power system and faults and noise generated within it should be totally isolated from the building in which it is located. This is always a consideration in the design. However, given the realities of these types of systems and the great number of connections that must be made, total isolation between the building and the pulsed power system isn't practical or achievable. It is likely that at some point in the operational life of the system, a fault will involve some part of the building and the building grounding system. It is therefore important that the impedance of these grounds be low enough such that fault current flowing through them will not generate hazardous potentials. If this is not possible or practical, then the system should be configured in such a way that fault currents are returned on a path that does not involve the building ground grid. Also, procedures and interlocks must be established to restrict access to any area where hazardous voltages might exist during a fault condition.

There exists an extensive amount of information regarding grounding practices in the literature.[45, 46, 47] For large solid-state laser systems, two aspects of the overall grounding system must be considered:

- The first is to incorporate a high degree of isolation between the pulsed power system and the building structure. There are numerous viable approaches to this problem. Some examples are given later in this chapter.
- The second is to insure that the impedance of the building ground system is as low as possible so as not to produce, during fault conditions, hazardous step or touch potentials.

---

[44] R. A. Anderson et al., "Measurements of the Radiated Fields and Conducted Current Leakage from the Pulsed Power Systems in the National Ignition Facility at LLNL," UCRL-JC-151432.

[45] R. Morrison and W. Lewis, "Grounding and Shielding in Facilities," John Wiley & Sons, ISBN 0-471-83807-1, 1990.

[46] Chien-Hsing Lee and P. Sakis Meliopouous, "A Comparison of IEC 479-1 and IEEE Std. 80 on Grounding Safety Criteria," Proc. National Science Council, Vol. 23, No. 5, 1999, Pgs. 612-621.

[47] Ralph Morrison, "Grounding and Shielding Techniques in Instrumentation," John Wiley and Sons, 1967.

Generally, buildings housing pulsed power systems are steel I-beam construction on cement pads. The cement pad contains steel reinforcing bar for structural strength. In addition, a 4/0 copper cable matrix is embedded in the pad. This arrangement is shown in Figure 67.

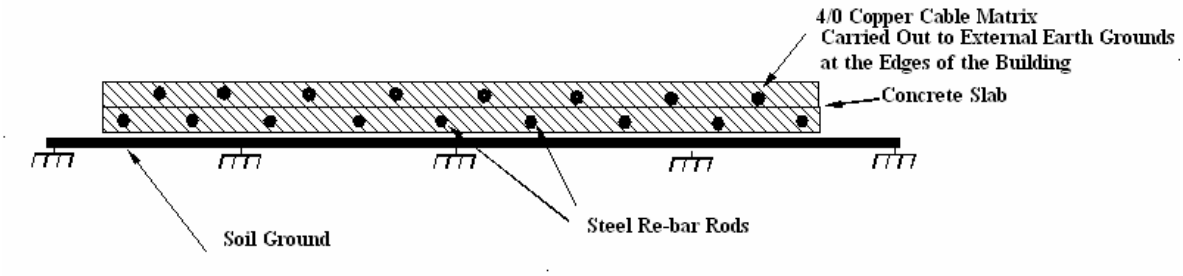


Figure 67. Example of Building Pad with the Associated Steel Rebar and 4/0 Copper Cable Matrix.

A picture of the rebar before concrete was poured is shown in Figure 68. These reinforcing bars must be electrically well-connected at their junctions to be a viable part of the grounding system. This configuration is enhanced by an effect known as the Ufer[48] ground, which relies upon certain properties of cement. These are:

- Cement absorbs moisture quickly and easily and releases it slowly.
- The mineral content of cement is such that ions are available to conduct current.
- The soil in contact with the cement becomes "doped" by the cement and alters favorably the pH of the soil. This lowers the resistivity of the soil.
- This combination makes the slab a good ground plane.

Figure 68. Re-bar for the National Ignition Facility before the cement pad was poured. Note that the junctions are welded. The re-bar matrix is carried out to the external ground rods. This constitutes a good ground plane.

[48] Named for the inventor, Mr. Ufer, a consultant to the U. S. Army during World War II.

A plan view is shown in Figure 69. The closer the spacing of the 4/0 cables, the lower the impedance of the ground plane. The 4/0 cables are:

- Connected at their intersections.
- Attached to the external ground grid array.
- Attached to the steel columns.

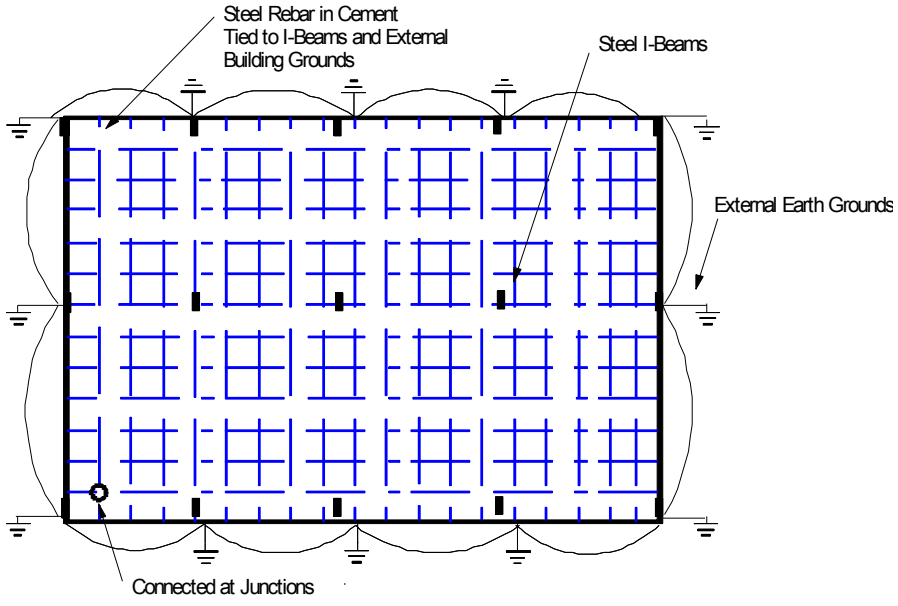


Figure 69. Plan view of a typical cement pad foundation for a large laser building. The steel rebar in the cement pad is tied to the steel I-beams (Figure 71) and the external grounding rods. The junctions of the rebar are connected to make good electrical contact.

In addition, the ground plane is carried by I-beams up above the slab floor for easy access. An example is shown in Figure 70.

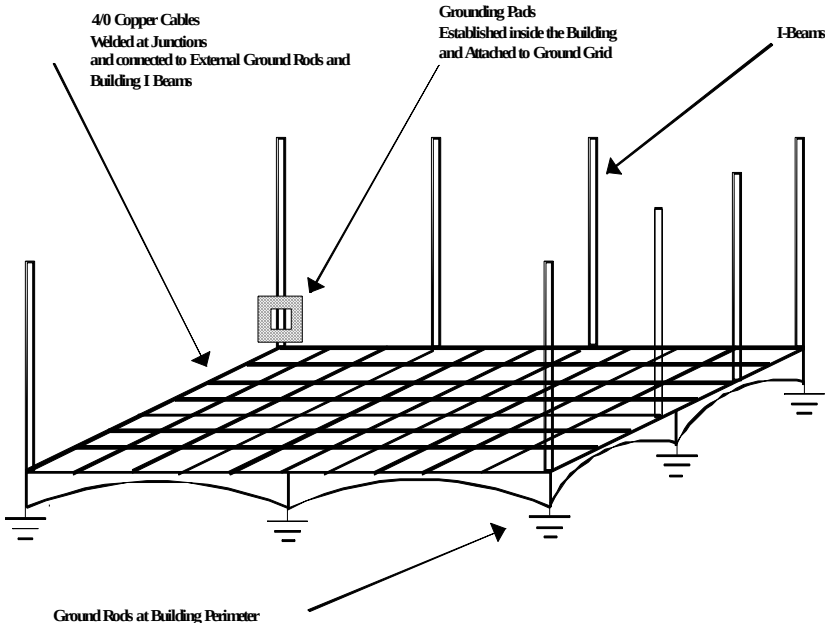


Figure 70. 4/0 copper cables in a rectangular array in the cement pad provide a uniform and predictable ground plane. A closer spacing produces a lower impedance.

Figure 71. The grounding grid is carried up to by I beams to an access point in the pulsed power bay.

**Ground Plane Impedance of 4/0 Cable Matrix**

As mentioned above, the spacing of the copper cables within the cement matrix will influence the impedance of the ground return path in the event of a fault. As an example, consider a grid of 4/0 copper cables spaced on 12-foot centers in the cement pad as shown in Figure 72. This can be modeled to estimate the distribution of voltages along the grid in the event of a fault. Note that under these conditions, the first peak of the fault transient can be as high as 5 kV.

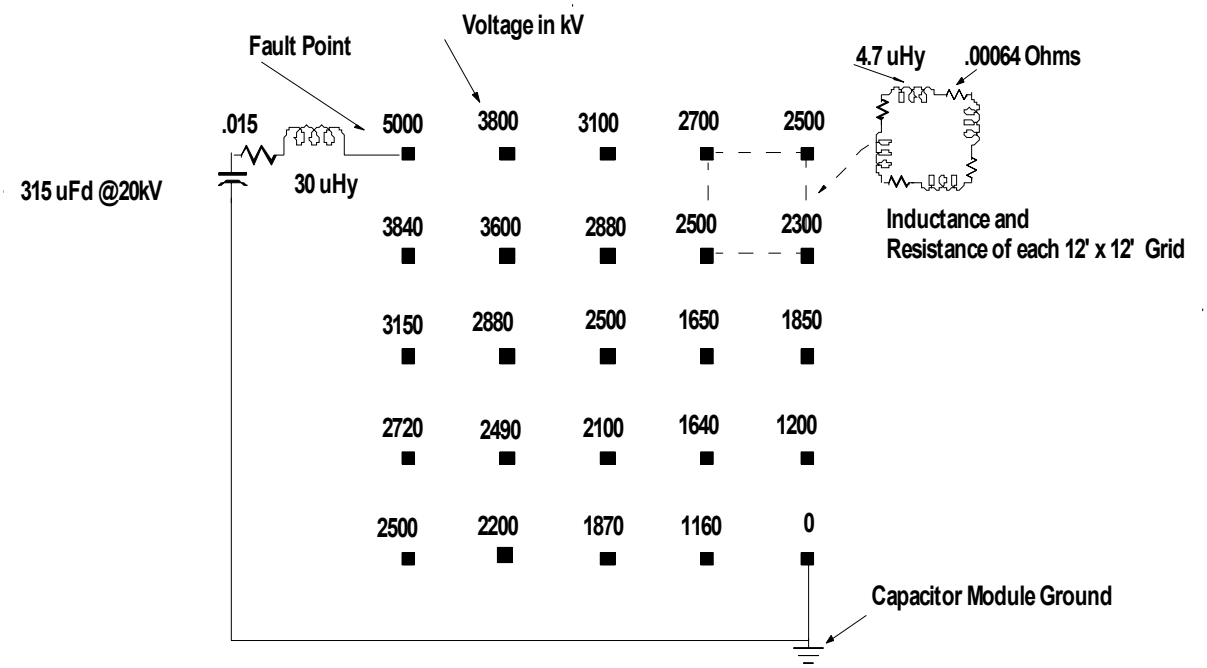


Figure 72. Simplified model of a 12' x 12' ground grid. Mutual inductance effects are ignored. It is assumed that a high voltage fault occurs to ground at the upper left corner of the slab. The numbers at the intersections of the 4/0 cables are the peak voltages generated as the fault current flows across the grid to ground.

If, however, the spacing of the 4/0 cables is reduced to 6’ x 6’, there is a corresponding reduction in the peak voltage. This is shown in Figure 73.

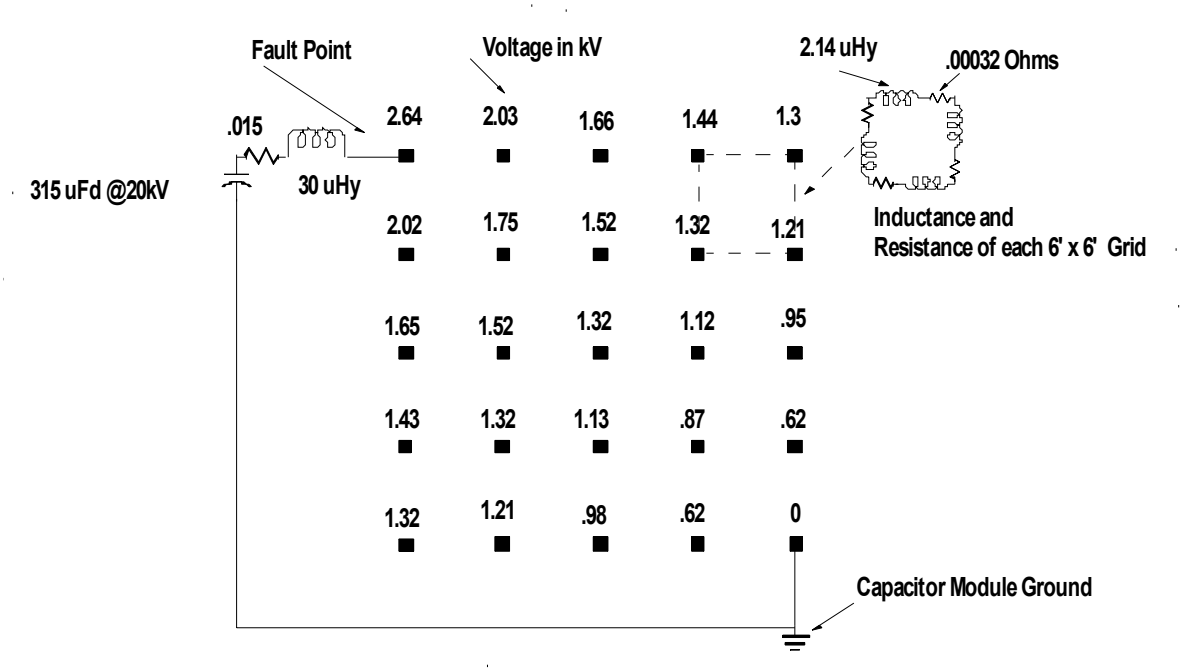


Figure 73. Same situation as Figure 73, but now the 4/0 copper cables are placed at 6’ centers. The peak voltages across the ground grid are reduced accordingly. For the sake of simplicity, mutual inductance effects are again ignored.

# CHAPTER 10

# ELECTRICAL FAULT SAFETY AND OPERATING PROCEDURES

There are two major areas of concern with regard to electrical safety in large laser systems. These are:

- Electrical shock hazards.
- Shrapnel or debris resulting from an explosive high-energy fault.

Shrapnel and debris are addressed by containing the energy storage modules with structures and barricades that prevent dispersal. Electrical shock hazards are more complicated in that personnel must have frequent and safe access to all parts of the facility. For this reason procedures are carefully developed for each step in the process of operating and maintaining the pulsed power system. Some examples are given below.

## Safety Procedures

A very important aspect of pulsed power engineering is that of planning for safe operation and repair of the system. Over the years, Laser Fusion research facilities have become quite large. Without carefully planned safeguards, it is entirely possible to have personnel in harm's way in a remote corner of the facility without operators being aware of the situation. This could lead to injury or death if personnel happened to be working on or near any of the high-voltage systems when they were activated. Also, after a system shot has been completed, engineers and technicians generally require access to various areas of the facility. Diagnostics and procedures need to be in place to insure safe access. These elements should be developed, documented and explained to all relevant personnel in advance of the first day of operation. An example of procedures developed at the National Ignition Facility for an "off-normal" event is described in Appendix D, Off-Normal Fault Event Safety Procedure.

## Electrical Shock Hazards

Solid-state laser pulsed power systems involve both high-voltage and high-energy circuits. If, during a fault, some of this energy is transferred to the building structure, personnel can be exposed to potentially lethal electric shocks. To avoid exposure of personnel during fault conditions, the following steps, as a minimum, should be taken.

- Configure the pulsed power circuitry such that fault currents are confined and returned by way of low impedance paths to single point grounds at the energy storage modules.
- Prevent access to the energy storage areas during operation with the use of interlocked doors and barriers.
- Create dielectric breaks to isolate the pulsed power areas from the remainder of the building.

- Establish and document procedures[49] for dealing with fault situations. In particular, establish procedures for dealing with "off-normal" faults.

**Effects of Electrical Shock on Human Physiology**

There exists in the literature a wealth of information on the effects of electrical shock on the human body. It is not the intent of this book to present any of this work in detail yet again. Rather, we include very useful, comprehensive references to this material in the bibliography. In particular, "*A Comparison of IEC 479.1 and IEEE Standard 89 Grounding Safety Criteria" (Chien-Hsing Lee and A.P. Sakis Meliopoulos)* is an excellent source.

Grounding designs are unique to each system, but the effects of electrical shock on the human body are system independent. In the literature, there is much analysis having to do with step voltage and touch voltage.[50] These simply describe the manner in which one is exposed to shock voltages,[51] *(e.g., walks in the vicinity of a ground system during a fault (step voltage), touches a grounded structure during a fault (touch voltage), etc.)* The important issue is to quantify the effect of electrical shocks on the human body. A concise summary is shown in Figure 74.[52]

The effects depend upon the following factors:

- The magnitude of the current
- The path–e.g., hand to foot, had to hand etc.
- The length of time one is in contact.
- The frequency of the current.

| **Current** | **Reaction** |
|---|---|
| Below 1 ma | Not perceptible |
| 1 ma | Faint tingle |
| 5 ma | Slight shock ( Not painful) |
| 6-25 ma | Painful shock, loss of muscle control |
| 9-30 ma | Individual cannot let go |
| 50-150 ma | Respiratory arrest |
| 1000-4300 ma | Rhythmic pumping |
| 10,000 ma | Cardiac arrest - burns |

Figure 74. Effects of electrical shocks on the human body. (L. Bruce McLong, "Common Sense and Knowledge Approach to Electrical Safety," IEEE-IAS/PES 2002-03.)

[49] M. Newto,n LLNL, W. Gagnon, Brookings Engineering, "NIF Amplifier Power Conditioning System (PCS) Hazards Analysis and Safety Implementation Plan." UCRL-MA- 150514. Oct. 2002.
[50] OSHA Standards-29 CFR, "Protection from Step and Touch Potentials," 1910.269 App C.
[51] Chien-Hsing Lee and A.P. Sakis Meliopoulos, "A Comparison of IEC 479.1 and IEEE Standard 89 Grounding Safety Criteria."
[52] L. Bruce McLong, "Common Sense and Knowledge Approach to Electrical Safety," IEEE-IAS/PES 2002-03.

In general, a maximum threshold energy of approximately 13 joules should be avoided.[53] This is driven by voltage, time and skin resistance. Typical values of skin resistance are in the range of 500 to 5000 ohms. However, if skin resistance is ignored, the internal resistance of the human body can approach 90 to 200 ohms. Therefore, given a 90-ohm path, 500-volt fault pulse and a 300-μsec pulse duration, the deposited energy would be 830 mJ.

[53] Bill Primex (DeHope), "Study of Touch Potential Standards for NIF Project," April 1998.

# APPENDIX A[54]--- Derivation of Emmett and Markiewicz lamp equations

Ignoring the plus/minus and the absolute sign, equation (5) is given as:

$$L\frac{di}{dt} + Ko\sqrt{i} + \frac{1}{C}\int_0^t i\, d\tau' = Vo \qquad [1]$$

The following substitutions are made:

$$Z_0 = \sqrt{\frac{L}{C}} \qquad i = I\frac{V_0}{Z_0} \qquad \tau = \frac{t}{T} \qquad T = \sqrt{LC}$$

$$\alpha = \frac{K_0}{\sqrt{V_0 Z_0}} = \text{Nonlinear damping factor}. \qquad [2]$$

This yields the normalized equation: $\frac{dI}{d\tau} \pm \alpha\sqrt{I} + \int_0^\tau I\, d\tau = 1$ [3]

This is derived as follows:

1. First dividing (1) by Vo:

$$\frac{L}{Vo}\frac{di}{dt} + \frac{Ko}{Vo}\sqrt{i} + \frac{1}{CVo}\int_0^t i\, d\tau' = 1 \qquad [4]$$

2. Then, Changing the variable from t to τ using τ=t/T :

$$\frac{d}{dt} = \frac{d}{d\tau}\frac{d\tau}{dt} = \frac{1}{T}\frac{d}{d\tau} = \frac{1}{\sqrt{LC}}\frac{d}{d\tau} \qquad [5]$$

3. Treating each term in [4] separately. First, we introduce τ:

$$\frac{L}{Vo}\frac{di}{dt} = \frac{L}{Vo}\frac{1}{\sqrt{LC}}\frac{di}{d\tau} = \sqrt{\frac{L}{C}}\frac{1}{Vo}\frac{di}{d\tau}$$

4. Then we change i to I:

[54] Georg Albrecht, Internal LLNL Technical Note, Sept. 2004.

$$\sqrt{\frac{L}{C}}\frac{1}{Vo}\frac{di}{d\tau}=\frac{1}{Vo}\sqrt{\frac{L}{C}}\frac{Vo}{Zo}\frac{dI}{d\tau}=\sqrt{\frac{L}{C}}\frac{1}{Zo}\frac{dI}{d\tau}$$ and introducing $Zo=\sqrt{L/C}$ this becomes:

$$\sqrt{\frac{L}{C}}\frac{1}{Zo}\frac{dI}{d\tau}=\sqrt{\frac{L}{C}}\sqrt{\frac{C}{L}}\frac{dI}{d\tau}=\frac{dI}{d\tau}$$, and this is the first expression in [3].

5. For the next term in (3):

Introduce I instead of i, and then use the definition of α as given in [2]:

$$\frac{Ko}{Vo}\sqrt{i}=\frac{Ko}{Vo}\sqrt{\frac{Vo}{Zo}}\sqrt{I}=\frac{Ko}{\sqrt{VoZo}}\sqrt{I}=\alpha\sqrt{I}$$

This is the second expression in [3].

On to the last expression:

$$\frac{1}{CVo}\int_0^t i\,d\tau'$$

6. First, we change i into I.

$$\frac{1}{CVo}\int_0^t i\,d\tau'=\frac{1}{CVo}\frac{Vo}{Zo}\int_0^t I\,d\tau'=\frac{1}{CZo}\int_0^t I\,d\tau'$$

7. Then, we also need to change the upper limit of the integration from t to τ. To not make this too complicated, note that an integration in t (=time) simply results in multiplying with the time dimension. With that we get:

$$\frac{1}{CZo}\int_0^t I\,d\tau'=\frac{1}{CZo}\sqrt{LC}\int_0^\tau I\,d\tau'$$

8. Now we use the explicit form of $Zo=\sqrt{L/C}$ and get:

$$\frac{1}{CZo}\sqrt{LC}\int_0^\tau I\,d\tau'=\frac{1}{C\sqrt{\frac{L}{C}}}\sqrt{LC}\int_0^\tau I\,d\tau'=\int_0^\tau I\,d\tau'$$

9. And with that, we have arrived at the last expression of [3].

# APPENDIX B – EXCEL spreadsheet for lamp equations

## Single-Mesh Flashlamp Circuit

**John Trenholme - 19 Jun 2003**
Now: 1 Sep 2003 10:07 AM

**Input Parameters:**

| | | | MKS Units |
|---|---|---|---|
| Initial voltage $V_0$ | 15 | kilovolts | 1.5000E+04 |
| Capacitance | 315 | microfarads | 3.1500E-04 |
| Inductance | 40 | microhenries | 4.0000E-05 |
| Resistance | 50 | milliohms | 5.0000E-02 |
| Lamp K factor | 54.4 | volts per amp$^p$ | |
| Lamp V-I exponent P | 0.5 | | |

**Calculated quantities:**

| | | | MKS Units |
|---|---|---|---|
| Impedance Z | 356.348323 | milliohms | 0.35634832 |
| 3*v(L*C) | 336.749165 | microseconds | 3.3675E-04 |
| Stored energy | 35.4375 | kilojoules | 3.5438E+04 |
| | | | |
| Alpha | 0.74407363 | [nonlinear damping: K / ( V$^{1-P}$ * | |
| Beta | 0.14031215 | [linear damping: R / Z] | |
| | | | |
| Peak current | 20246.3859 | amps | |
| Peak time | 140.312152 | microseconds | |
| Lowest current | -4.37669773 | amps | |
| | | | |
| Maximum time | 561.248608 | microseconds | |
| Reference current | 42.0936456 | kiloamps | 4.2094E+04 |

This spreadsheet solves the differential equations:

$$\frac{dI}{dt} = \frac{1}{L}\left[ V - \left( \frac{K}{\left(I^2 + \delta^2\right)^{\frac{1-P}{2}}} + R \right) I \right] \qquad I(0) = 0 \qquad \delta = 10^{-15}\,\frac{V_0}{Z}$$

$$\frac{dV}{dt} = -\frac{I}{C} \qquad V(0) = V_0$$

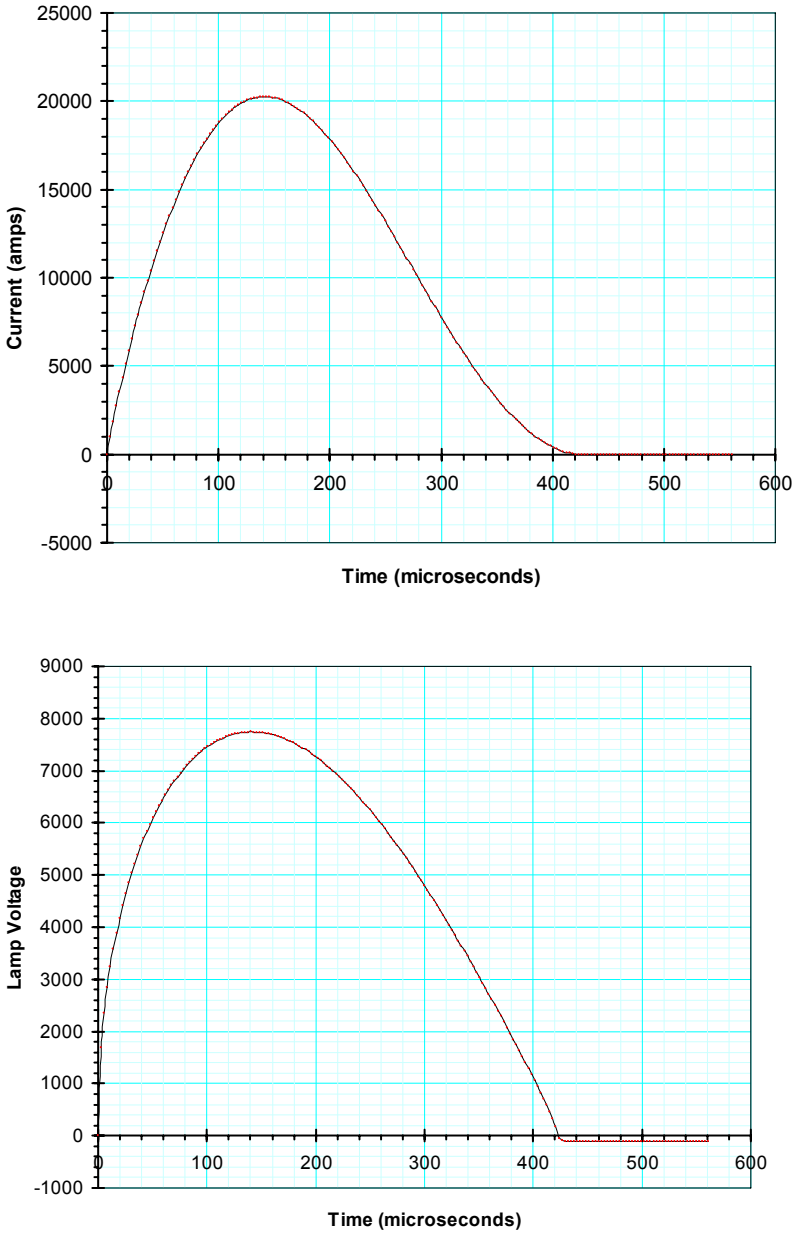


Figure B1. The figures above show calculated current and voltage waveforms.

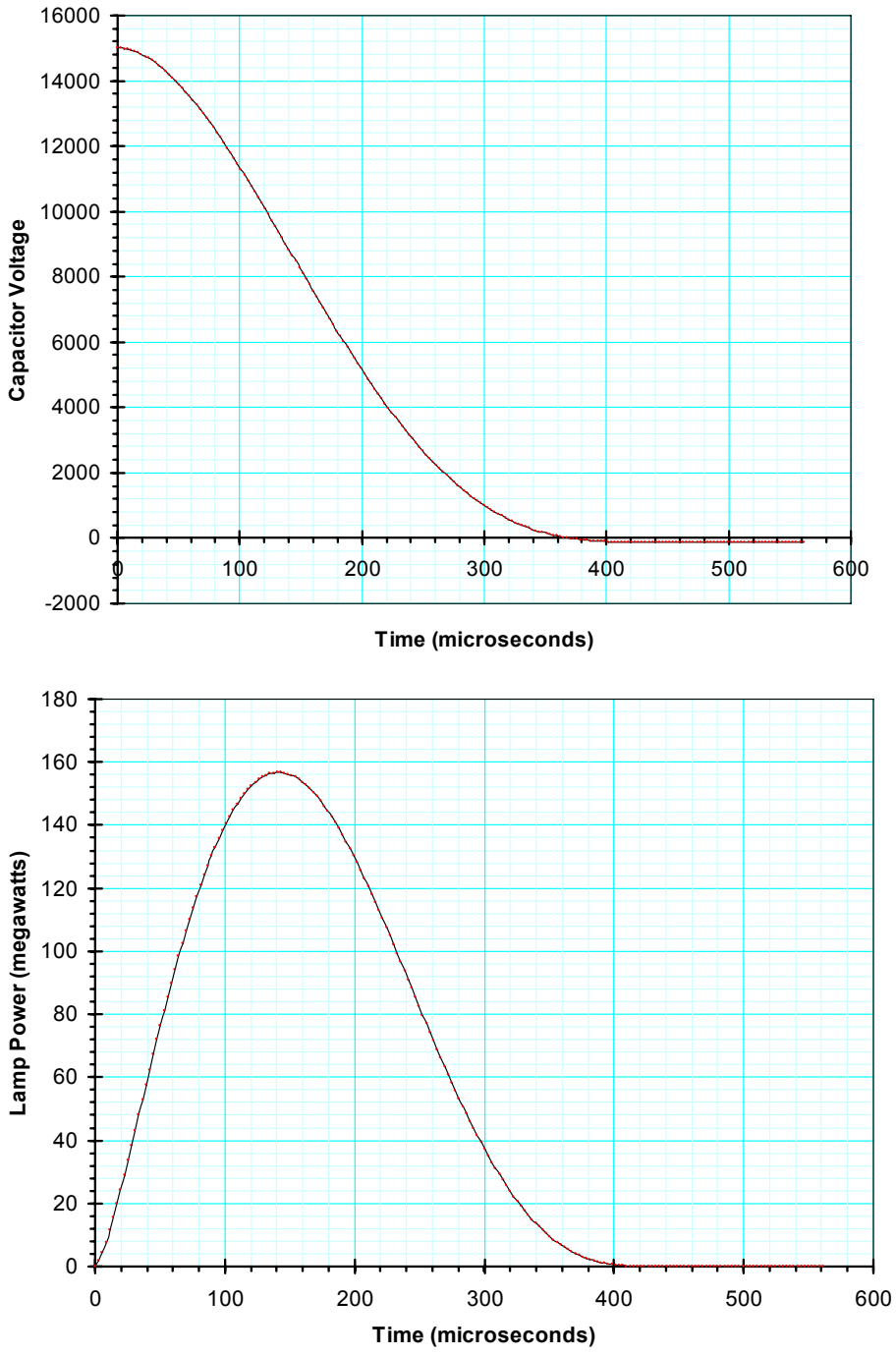


Figure B2. The two figures above show the calculated capacitor voltage and flashlamp power waveforms.

## Sanity Checks on the Spreadsheet Algorithms

**1) Can we do a linear damped circuit?**

| | | |
|---|---|---|
| Voltage | 15 | kilovolts |
| Capacitance | 200 | microfarads |
| Inductance | 50 | microhenries |
| Resistance | 500 | milliohms |
| Lamp K factor | 0 | volts per amp$^p$ |
| Lamp V-I exponent P | 0.5 | |
| N = | 120 | steps in time 3*v(L*C) |

This gives an underdamped waveform

Decay time = 0.0002 seconds

Frequency = 8660.254038 radians/sec

Coefficient = 34641.01615 amps

| Time: | 0.00025 | 0.0005 |
|---|---|---|
| Exact current: | 8223.296961 | -2638.272622 |
| Spreadsheet: | 8223.296957 | -2638.272659 |
| Relative Error: | -5.22E-10 | 1.41E-08 ✓ |

**2) Will a "lamp" with P = 1 do the same?**

| | | |
|---|---|---|
| Resistance | 0 | milliohms |
| Lamp K factor | 0.5 | volts per amp$^p$ |
| Lamp V-I exponent P | 1 | |

| Time: | 0.00025 | 0.0005 |
|---|---|---|
| Exact current: | 8223.296961 | -2638.272622 |
| Spreadsheet: | 8223.296957 | -2638.272659 |
| Relative Error: | -5.22E-10 | 1.41E-08 ✓ |

**3) Does lossless circuit ring to "reference current"?**

| | | |
|---|---|---|
| Resistance | 0 | milliohms |
| Lamp K factor | 0 | volts per amp$^p$ |

| Reference: | 30000 |
|---|---|
| Peak: | 29999.73493 |
| Relative Error: | -8.84E-06 ✓ |

**4) Does Runge-Kutta converge "properly" (slope around 4 on log-log) as step size changes?**

Do same case as 1) above, so exact result is available

Time: 0.00025

Exact current: 8223.296961

| Step size | Calculated | Rel. Error | Abs( Rel. Err.) |
|---|---|---|---|
| 0.00000125 | 8223.296961 | -3.80154E-11 | 3.80154E-11 |
| 0.0000025 | 8223.296957 | -5.22006E-10 | 5.22006E-10 |
| 0.000005 | 8223.296916 | -5.54469E-09 | 5.54469E-09 |
| 0.00001 | 8223.296995 | 4.15581E-09 | 4.15581E-09 |
| 0.000025 | 8223.395566 | 1.19909E-05 | 1.19909E-05 |
| 0.00005 | 8227.874375 | 0.00055664 | 0.00055664 |

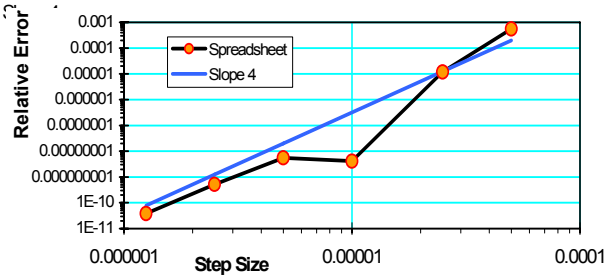

# APPENDIX C – Spreadsheet solutions for flashlamp equations

## Definition of terms

$\tau = \sqrt{LC}$ Approximate time for the current pulse to reach 80% of the peak value, assuming a pulse shape close to critical damping.

$T = 3\sqrt{LC} =$ Approximate time from 15% point to 15% point on the current waveform assuming a pulse shape close to critical damping.

This is shown in the simulation below of a typical flashlamp current waveform.

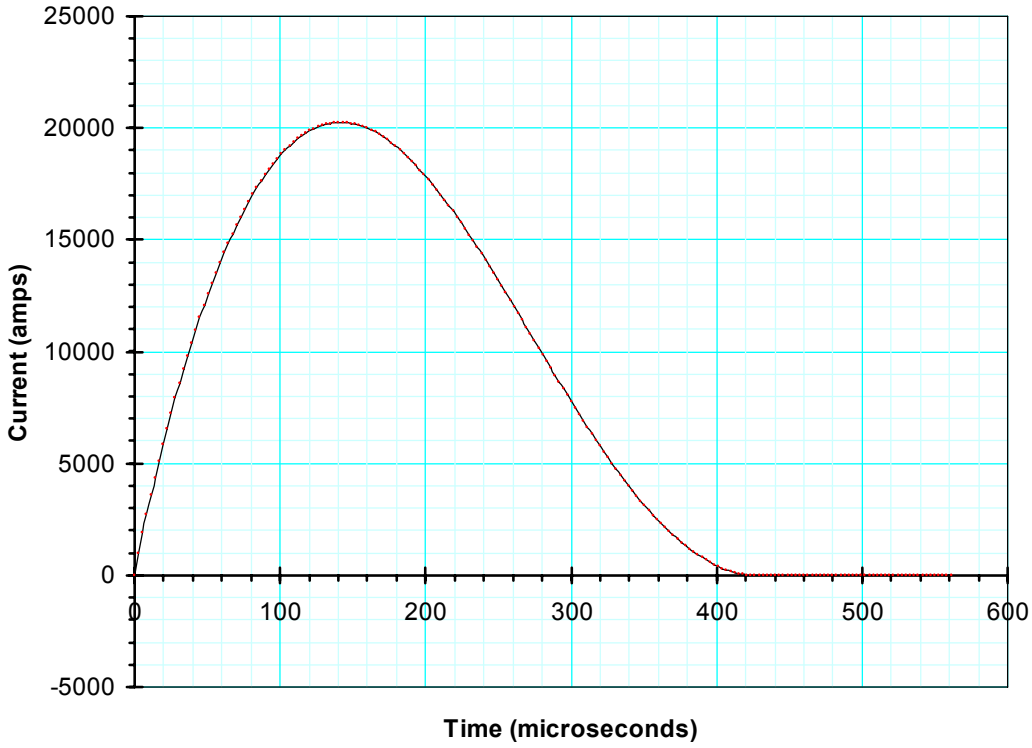


Figure C1. Typical flashlamp current waveform calculated from a spreadsheet.

### (1) Single Shot Explosion Energy—$E_{exp}$

$$E_{\exp} = 2\times10^{4} l d \tau^{1/2}$$

*Where*:

$\tau = \sqrt{LC}$

$l$ = Lamp Length in cm

d= Lamp Diameter in cm

C= Circuit Capacitance in Fd

$E_{exp}$ = Single Shot Explosion Energy in Joules

### (2) K for a Single Lamp

$$K = \frac{4}{3}\times\frac{l}{d}\times\left(\frac{P}{450}\right)^{2} = \sqrt{V\times I}$$

**Where,**

$l$ = Lamp Length in cm

d=Lamp Diameter in cm

P=Gas pressure in Torr

### (3) K for Multiple Lamps

$$K_0\ combination = K_{(0)}\times\frac{n_{(series)}}{\left(n(_{parallel})\right)^{(m)}}$$ where;

$K_0 = K\ for\ a$ single lamp,

$n_{(series)}$ = number of lamps in series

$n_{(parallel)}$ = number of lamps in parallel

and $m$ = the exponent the current is raised to in order to fit a particular lamp

**(4) Input Circuit Energy**

$E_0 = \frac{CV_0^2}{2} =$ Input Energy in Joules

Where C = Circuit Capacitance Farads
Vo = Circuit Voltage

**(5) Circuit Capacitance --- C**

$C = \left[ \frac{2E_0 \alpha^4 \tau^2}{K} \right]^{1/3}$ = Circuit Capacitance Fd

**Where**

$\alpha$ = Nonlinear Loss : .75 for Critical Damping $= \frac{K}{\sqrt{V_0 Z_0}}$

$E_0$ = Circuit Energy in Joules

$\tau = \sqrt{LC} =$ Approximate Current Rise Time to 80% of Maximum

K= Lamp Constant

**(6) Circuit Driving Voltage --- V(o)**

$V_0 = \sqrt{\frac{2E_0}{C}}$ *Where*;

C=Circuit Capacitance Farads

$E_0$ = Energy Joules

**(7) Circuit Inductance --- L**

$L = \frac{\tau^2}{C}$ Where;

$\tau^2 = LC$

$L =$ Circuit Inductance Hy

C = Circuit Capacitance Fd

**(8) Linear Loss Factor --- Beta (β)**

$\beta = \frac{R}{Z_0}$ Where;

R = Linear Circuit Resistance

$Z_0 = \sqrt{\frac{L}{C}}$

# APPENDIX D – Off-Normal Fault Event Safety Procedure

**Equipment Required**
None

**Definitions**

| | |
|---|---|
| ***Power Conditioning System (PCS)*** | An energy storage system that is primarily located in the capacitor bays, which consist of the following: Main Module, PILC Module, Main Module Trigger (TG-803), Control system. Rack, Transmission Lines and Grounding system. |
| ***PCS Main Energy Storage Module (Main Module)*** | One of 192 circuits that consist of a trigger unit, a switch, 20 to 24 high-energy capacitors and inductors, and their associated hardware. Each module is fully contained in a metal enclosure. |
| ***PILC Module*** | Pulsed Ionization Lamp Check module; each Main Module has a PILC Module associated with it. The PILC Module consists of two high voltage capacitors, a switch, and their associated hardware. Each PILC is contained a metal cabinet. |
| ***GUI*** | Graphical User Interface. |
| ***DAS*** | Data Acquisition System |
| ***SIS*** | Safety Interlock System |

**PCMS Off-Normal Events Procedure**

**Overview**
The definition of an Off-Normal Event as used in this procedure: is any abnormality observed in the function or performance of individual modules or systems of modules. The failure may be caused by PCS Module Subsystem components, transmission lines or the flashlamp load.

Off-Normal Events range in their severity from catastrophic explosions to the barely detectable loss of current transferred to the load.

This procedure will not try to address the action required for all Off-Normal Events. This procedure provides a checklist of required actions that will:

- Ensure the facility is safe for personnel
- Protect the facility equipment and property
- Capture as much information as possible to help determine the cause of the event
- Notify the Responsible Individuals

**Off-Normal Event Categories**
This procedure must be implemented if any of the following occur:

*Explosions or destructive events*
These events may be heard by the control room operators or observed on the video monitors and are probably caused by:

- Capacitor failures
- High-voltage bus/connection failures,
- Resistor failures
- PILC failures
- Top Hat/cable failures

*Other (must be corrected before the next shot)*
These events may be detected with the system software or through observation of the diagnostic signals. (Early release of multi-module software does not include automated detection of abnormal conditions)

- Power supply, abnormal charge voltage rate (PILC or Main)
- PILC or PCS Main Energy Storage Module no fire
- PILC or PCS Main Energy Storage Module pre-fire
- PILC or PCS Main Energy Storage Module output current decreases by more than 5%
- Abnormal discharge current shape
- Flashlamp failure

*These events are detected by the DAS*

- Cable current fault (in excess of 30 kA)
- Reflector current fault
- Ground current fault
- No current on one or more of the output current monitors

**Procedure**
When an Off-Normal Event occurs, the operator must ensure the facility is safe and remains safe for personnel. The first action by the operator is to retrieve shot data and then to abort the charge sequence and discharge the capacitor banks if not already accomplished by the software/control system. The operator must maintain facility access control by taking possession of the capacitor bay key in the SIS panel in the control room.

In the case of an explosive event, the operator must execute the checklist in Appendix A. If the off-normal event does not require an immediate response, the operator should execute the checklist in Appendix B. See Appendix C for Fire Department Response to NIF Capacitor Bays.

## Appendix A – PCS Off-Normal Events Checklist

### Explosions

| | | |
|---|---|---|
| 1 | Download waveform data by pressing the "Retrieve Data" button on the "Bank Participation" GUI. | ☐ |
| 2 | Activate the Abort Button on the shot sequence GUI. This will abort the charge cycle and discharge the capacitor banks, i.e., close the dump switches and turn off the power supplies. | ☐ |
| 3 | Note the time _____ | ☐ |
| 4 | Verify that all access doors to the capacitor bays are closed using the SIS display system. Maintain access control of the affected capacitor bay. | ☐ |
| 5 | Observe the capacitor bays with the closed-circuit television, checking for fires, electrical discharges, oil vapor, component dust and/or debris. | ☐ |
| 6 | Identify failed module from control system diagnostics from video images | ☐ |
| 7 | Using the attached "Capacitor Bay Module Status Checklist" and control GUIs, verify all Main Modules and PILCs are discharged. | ☐ |
| 8 | If sustained fire is present in capacitor bay, call fire department (911). Fire department shall be advised to only fight fire if it is increasing in intensity or spreading. The preferred method is to let fire burn itself out due to the limited supply of burnable material in the module. If fire sprinklers have been activated, fire department personnel should not enter capacitor bay. | ☐ |
| 9 | Identify number of 800A, 480 VAC breaker feeding the failed module. | ☐ |
| 10 | If no heavy smoke is present, PCS personnel shall enter the capacitor bay and turn off the 800 A breaker identified in the previous step. If heavy smoke is present, fire department personnel shall enter the capacitor bay and turn off all 800 A breakers specified by PCS personnel. Fire department personnel shall be informed that modules may contain lethal amounts of stored electrical energy. Fire department personnel shall be advised not to remove module doors or insert conducting objects or liquids through door vents. | ☐ |
| 11 | If sustained fire is present in a PCS module, fire department personnel shall discharge CO2 fire extinguisher through door vent in module. | ☐ |
| 12 | Do not enter module. | ☐ |
| 13 | Notify the Responsible Individual. | ☐ |

## Appendix B – PCS Off-Normal Events Checklist

**Other**

1 Continue through the shot sequence to "retrieve data" step if not already completed. This will acquired all available shot data. ☐

2 Activate the "Abort Button" on the "Shot Sequence" GUI. This will abort the charge cycle and discharge the capacitor banks. ☐

3 Note the time _____ ☐

4 Verify that all access doors to the capacitor bays are closed using the SIS display system. Maintain access control of the affected capacitor bay. ☐

5 Using the "Capacitor Bay Module Status Checklist" and control GUIs, verify all Main Modules and PILCs are discharged. ☐

6 Notify the Responsible Individual. ☐

## Appendix C – Fire Department Response to NIF Capacitor Bay 3

Contact Main Control Room at xxx-xxxx

Do not enter any Capacitor Bay when its external status panel indicator is RED "Keep Out"

Capacitor bay may be entered using the key located in the Knox Box when the external status panel indicator is YELLOW or GREEN

Do not enter the main module enclosures or spray any conductive material into module enclosures because they may contain stored electrical energy.

$CO_2$ may be sprayed into the module enclosures through the "louvers" on the main module doors.

If smoke or flames are coming from a capacitor module, turn off all main breakers (Breaker # 1834A1, 1834A2, 1834A3, 1834A4. 1834A5, 1834A6, 1834A7, 1834A8) located in the power panel shown below.

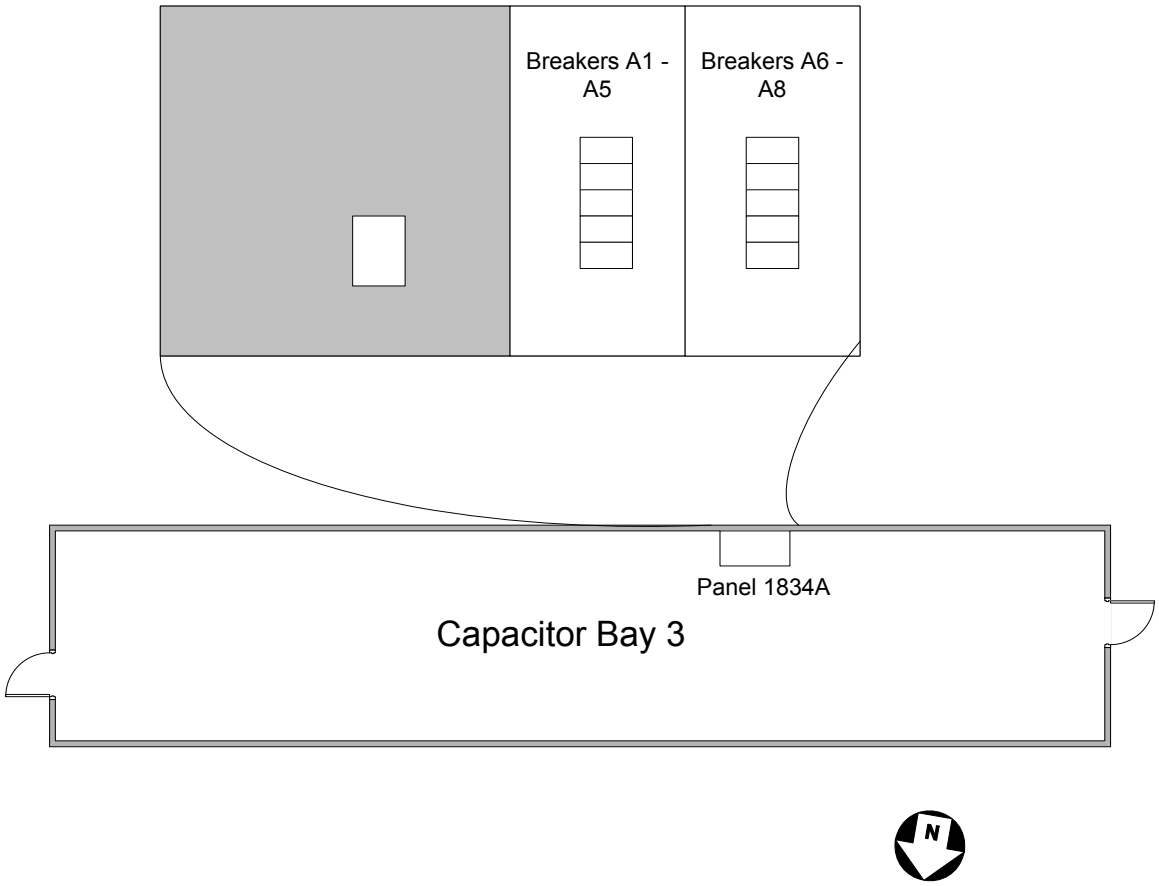


Figure D1. Location of the main breakers in Capacitor Bay 3 power panel 1834A.

# List of Figures

# References and Footnotes

[1] "To Engineer is Human, The Role of Failure in Successful Design", Henry Petroski, Vintage Books, 1992, ISBN 0-679-73416-3.

[2] "Lost at Sea", Patrick Dillon, Simon and Schuster, 2000, ISBN 0-684-6909-8

[3] Pictures from this section have been taken from the many NIF websites and from old archival materials

[4] In that case, we have a so-called three-level laser, whereas $Nd^{3+}$ is a four-level laser. The first laser ever built, the ruby laser, is such a three-level laser, and it takes comparatively enormous pump powers to generate an inversion.

[5] Especially so-called zigzag lasers need to be designed with great care to avoid this problem.

[6] Named after F.C. A. Pockels, 1865-1913, who discovered electric field-induced birefringence. His sister, A. Pockels, corresponded with Lord Rayleigh on issues of surface tension of water. The often-found genitive "Pockel's cell" is wrong.

[7] The effect of polarization rotation in certain materials of a beam traveling along a magnetic field is named after Emile Verdet, French physicist (1824-1866).

[8] The units of irradiance are $W/m^2$. Almost everywhere this is incorrectly called intensity. The actual units of intensity are W/sterad. See OSA Handbook of Optics, Radiometry and Photometry, or Hecht Zajak: "Optics".

[9] An excellent treatment of this effect is given in an article by J. Trenholme, 1974 Laser Program Annual Report.

[10] Note its dimension is $Joules/m^2$. This is an aerial energy density, also called fluence.

[11] The KDP in KD*P stands for potassium (=**K** in the periodic table) **D**i-hydrogen **P**hosphate. The star stands for the hydrogen having been largely replaced by deuterium. This shifts an absorption feature in the pure KDP crystal out of the 1.05 μm band and thus make the crystal more transparent to laser light.

[12] Blessed the professional who works within a team in which the decision maker is also an experienced designer. The inverse is true as well and the consequences are disastrous for almost everyone.

[13] S.Atzeni, J.Meyer-Ter-Vehn:"The Physics of Inertial Fusion," Clarendon, 2004

[14] G. Albrecht, S. Payne, "Solid-state Lasers," Electro-Optics Handbook, Waynant Ediger, Editor.

[15] LRC stands for the inductance (L), resistance (R) and capacitance (C) of the circuit. Footnote list

[16] Bruce Carder, Bill Gagnon, "Energy Storage Options for SHIVA Upgrade," IIB-91st IEEE International Pulsed Power Conference, Lubbock, Texas, 1976, T. R. Burkes and M. Kristiansen, Editors, IEEE Catalog Number 76CH1147-8.

[17] E. L. Kemp: "Principal Considerations in Large Energy-Storage Capacitor Banks," IIC-11th IEEE International Pulsed Power Conference, Lubbock, Texas, 1976, T. R. Burkes and M. Kristiansen, Editors, IEEE Catalog Number 76CH1147-8.

[18] W.L. Gagnon, G. Allen, A. Pemberton, R. Holloway, J. Vieira, H. Lane, K. Snyder, S, Hawlery, D. Matoon, C. Nelson, D. Padilla, R. Parker, T. Pelley, "Glass Laser Power Conditioning," Lawrence Livermore National Laboratory, 1975.

[19] "Design of the 40 MJ Turnkey Power Conditioning System for 60 Beam Omega Laser E-Stage and F-Stage Single Segmented Amplifiers." N.C. Jaitly et al., Maxwell Laboratories and L. Folnsbee et al, Laboratory for Laser Energetics, U of Rochester. 1994 Pulsed Power Conference, pp. 164-169.

[20] N. C. Jaitly et al., "Pulsed Discharge Fuses for Capacitor Bank Protection" Maxwell Laboratories.

[21] American Control Engineering, "Final Report for fabrication and testing of a 2-MJ capacitor bank," LLNL Subcontract BC 39943.

[22] M.A. Newton, R.E. Kamm, E.S. Fulkerson, S.D. Hulsey, D.L. Pendleton, D.E. Petersen, M. Polk, M. Tuck, G.T. Ullery,M3-2 Initial Activation and Operation of the Power Conditioning System for the National Ignition Facility, Lawrence Livermore National Laboratory, W.B. Moore, Sandia National Laboratory

[23] N.C. Jaitly et al, Maxwell Laboratories and L. Folnsbee et al., "Design of the 40 MJ Turnkey Power Conditioning System for 60 Beam Omega Laser E-Stage and F-Stage Single Segmented Amplifiers," Laboratory for Laser Energetics, University of Rochester, 1994, Pulsed Power Conference, Pgs. 164 to 169.

[24] EG&G Electro-Optics, "Flashlamp Application Manual."

[25] W. Koechner, "Solid-State Laser Engineering," Springer Series in Optical Sciences, 5th edition, 1999.

[26] J.P. Markiewicz and J.L. Emmett, "Design of Flashlamp Driving CircuitsJournal of Quantum Electronics," Vol. QE2, No. 11, 1966.

[27] See Appendix C, Internal LLNL Note, John Trenholme, July 2004.

[28] John Trenholme, LLNL Internal Note, 26 Jan. 2005.

[29] A. E. Orel and H.T. Powell, "Transient Response of Flashlamps," LLNL Laser Program Annual Report, 1983.

[30] John Trenholme, LLNL Laser Program Internal Memo, July 2003.

[31] A better approach would be to shape the drive pulse such that it is terminated shortly after the energy is extracted from the laser media. This would result in more efficient energy use by saving the energy supplied to the lamp following the laser pulse extraction. This would also result in less energy absorption in the laser disks and therefore less optical distortion.

[32] See Appendix A for derivation. G. Albrecht, LLNL Internal Memo, July 2003.

[33] John Trenholme, LLNL Laser Program Internal Note, Aug. 2003.

[34] American Control Engineering, "Preliminary Pre-ionization Circuit Notes," LLNL Subcontract B313903, Sept. 20, 1996.

[35] American Control Engineering, "Trigger Latitude Testing of NIF Production Flashlamps," April 6, 2000, LLNL Subcontract B348073.

[36] Mark A Newton, LLNL, and William Gagnon, Brookings Engineering, NIF Amplifier Power Conditioning System Hazard Analysis and Safety Implementation Plan, UCRL-MA-150514, Oct. 2002.

[37] Russel Greenlaw, Revised Draft Report, Jan. 2001, Lawrence Livermore National Laboratory Structural and Applied Mechanics Group.

[38] Sandra Brereton et al., LLNL Mechanical Engineering Safety Note MESN99-066-0A. "Analysis and Control of Hazards Associated with NIF Capacitor Module Events," Sept. 1999.

[39] Russel Greenlaw, Revised Draft Report, Jan. 2001, Lawrence Livermore National Laboratory Structural and Applied Mechanics Group.

[40] Sandra Brereton et al., LLNL Mechanical Engineering Safety Note MESN99-066-0A. "Analysis and Control of Hazards Associated with NIF Capacitor Module Events," Sept. 1999.

[41] William B. Moore, "Wrench Incident In the Prototype Module Test Facility," Internal Note, NIF Power Conditioning (SNL).

[42] John Emmett, July 2006. Note to Bill Gagnon

[43] mil = 1/1000 inch.

[44] American Control Engineering, "Capacitor Fault Damping Element Status," LLNL Subcontract B313903, Oct, 1996.

[45] American Control Engineering, "Damping Element Tests of Split Sleeve Design," Feb. 3, 1999.

[46] R. A. Anderson et al., "Measurements of the Radiated Fields and Conducted Current Leakage from the Pulsed Power Systems in the National Ignition Facility at LLNL," UCRL-JC-151432.

[47]R. Morrison and W. Lewis, "Grounding and Shielding in Facilities," John Wiley & Sons, ISBN 0- 471-83807-1, 1990.

[48] Chien-Hsing Lee and P. Sakis Meliopouous, "A Comparison of IEC 479-1 and IEEE Std. 80 on Grounding Safety Criteria," Proc. National Science Council, Vol. 23, No. 5, 1999, Pgs. 612-621.

[49] Ralph Morrison, "Grounding and Shielding Techniques in Instrumentation," John Wiley and Sons, 1967.

[50] Named for the inventor, Mr. Ufer, a consultant to the U. S. Army during World War II.

[51]M. Newto,n LLNL, W. Gagnon, Brookings Engineering, "NIF Amplifier Power Conditioning System (PCS) Hazards Analysis and Safety Implementation Plan." UCRL-MA- 150514. Oct. 2002.

[52] OSHA Standards-29 CFR, "Protection from Step and Touch Potentials," 1910.269 Appendix C

[53] Chien-Hsing Lee and A.P. Sakis Meliopoulos, "A Comparison of IEC 479.1 and IEEE Standard 89 Grounding Safety Criteria."

[54] L. Bruce McLong, "Common Sense and Knowledge Approach to Electrical Safety," IEEE-IAS/PES 2002-03.

[55] Bill Primex (DeHope), "Study of Touch Potential Standards for NIF Project," April 1998.

[56] Georg Albrecht, Internal LLNL Technical Note, Sept. 2004.

# Index